

VYSOKÉ UČENÍ TECHNICKÉ V BRNĚ

BRNO UNIVERSITY OF TECHNOLOGY

FAKULTA CHEMICKÁ
ÚSTAV CHEMIE MATERIÁLŮ

FACULTY OF CHEMISTRY
INSTITUTE OF MATERIALS SCIENCE

RING-OPENING POLYMERIZATION OF LACTONES AND LACTIDES

DIZERTAČNÍ PRÁCE
DOCTORAL THESIS

AUTOR PRÁCE
AUTHOR

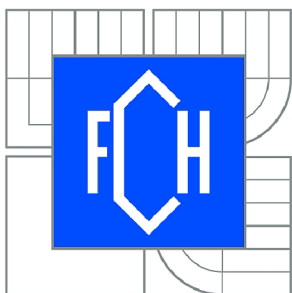
Ing. ZDEŇKA BOHÁČOVÁ

BRNO 2015



VYSOKÉ UČENÍ TECHNICKÉ V BRNĚ

BRNO UNIVERSITY OF TECHNOLOGY



FAKULTA CHEMICKÁ
ÚSTAV CHEMIE MATERIÁLŮ

FACULTY OF CHEMISTRY
INSTITUTE OF MATERIALS SCIENCE

RING-OPENING POLYMERIZATION OF LACTONES AND LACTIDES

POLYMERACE ZA OTEVŘENÍ KRUHU LAKTONŮ A LAKTIDŮ

DIZERTAČNÍ PRÁCE

DOCTORAL THESIS

AUTOR PRÁCE

AUTHOR

Ing. ZDEŇKA BOHÁČOVÁ

VEDOUCÍ PRÁCE

SUPERVISOR

doc. Ing. LUCY VOJTOVÁ, Ph.D.

BRNO 2015



Vysoké učení technické v Brně
Fakulta chemická
Purkyňova 464/118, 61200 Brno 12

Zadání dizertační práce

Číslo dizertační práce:	FCH-DIZ0106/2014	Akademický rok: 2014/2015
Ústav:	Ústav chemie materiálů	
Student(ka):	Ing. Zdeňka Boháčová	
Studijní program:	Makromolekulární chemie (P1422)	
Studijní obor:	Chemie makromolekulárních materiálů (1405V003)	
Vedoucí práce	doc. Ing. Lucy Vojtová, Ph.D.	
Konzultanti:		

Název dizertační práce:

Polymerace za otevření kruhu laktonů a laktidů

Zadání dizertační práce:

- 1) Vypracování literární rešerše na téma polymerace cyklických esterů pomocí N-heterocyklických karboenových katalyzátorů
- 2) Příprava a charakterizace "free" karboenového katalyzátoru různými metodami a ověření jejich účinnosti pro polymeraci cyklických esterů
- 3) Polymerace za otevření kruhu termocitlivého kopolymeru vybraným "free" karbenem a charakterizace chemické struktury
- 4) Evaluace viskoelastických vlastností připraveného kopolymeru pro injektovatelné aplikace v medicíně
- 5) Shrnutí výsledků a závěr

Termín odevzdání dizertační práce: 20.7.2015

Dizertační práce se odevzdává v děkanem stanoveném počtu exemplářů na sekretariát ústavu a v elektronické formě vedoucímu dizertační práce. Toto zadání je přílohou dizertační práce.

Ing. Zdeňka Boháčová
Student(ka)

doc. Ing. Lucy Vojtová, Ph.D.
Vedoucí práce

prof. RNDr. Josef Jančář, CSc.
Ředitel ústavu

V Brně, dne 1.9.2014

prof. Ing. Jaromír Havlica, DrSc.
Děkan fakulty

Abstract

Biodegradable aliphatic polyesters based on polylactones, polylactides and their copolymers are particularly interesting for their applications in the medical field. The major polymerization method used to synthesize these polymers has been the ring-opening polymerization (ROP) of lactones or lactides. Many organometallic compounds are effective initiators for the controlled ROP synthesis of polyesters but heavy metals derivatives are harmful for the human organisms. There has been an increasing interest in the development of efficient "green" catalytic systems for the synthesis of biodegradable aliphatic polyesters.

This thesis is dedicated to the synthesis of aliphatic polyesters based on polycaprolactone, polylactide and polyglycolide and especially their copolymers using organic catalyst from the group of free N-heterocyclic carbenes (NHC) without the central heavy metal atom.

A literature review is focused on the recent advances in the ROP of lactones and lactides using organic metal-free catalysts. However, there is no evidence of using carbenes for ROP synthesis of polyglycolide or its copolymers.

An experimental part of this work briefly describes the preparation and properties of 1,3-di-*tert*-butylimidazol-2-ylidene (NHC-*t*Bu) free carbene from its stable chloride salt. The next section is focused on the preparation of polyesters from cyclic ester monomers, namely L-lactide, D,L-lactide, glycolide and ϵ -caprolactone using NHC-*t*Bu catalyst. In particular, novel synthesis of thermosensitive amphiphilic triblock copolymers based on hydrophobic biodegradable polylactide, polyglycolide and biocompatible hydrophilic polyethylene glycol (PLGA-PEG-PLGA) using prepared NHC-*t*Bu has been investigated. Consequently, influences of reaction conditions (*i.e.* monomers purification, reaction temperature, type of solvent, solvent to monomer ratio and initiator to catalyst ratio) have been evaluated. Finally, the comparison of PLGA-PEG-PLGA copolymers prepared using NHC-*t*Bu and Sn(II)2-ethylhexanoate catalysts has been performed.

It was demonstrated that combination of NHC-*t*Bu with PEG creates the effective catalytic system for ring opening polymerization of lactone or lactides. Polymers were prepared with the high conversion of monomer (70 - 85%) and low polydispersity index (M_w/M_n at around 1.2). PLGA-PEG-PLGA copolymer with two phase transitions (sol-gel and gel-suspension) and gelation temperature between 35 – 43 °C was obtained. In most cases, changes in the reaction conditions did not have significant influence on chemical properties such as molecular weight or polydispersity index, however essentially affected the physical properties such as visco-elastic behaviors.

Keywords

Ring-opening polymerization, N-heterocyclic carbenes, aliphatic polyesters, thermosensitive copolymers, sol-gel phase transition.

Abstrakt

Medicínské aplikace tvoří z biodegradabilních alifatických polyesterů na bázi polylaktonů, polylaktidů a jejich kopolymerů velmi atraktivní skupinu materiálů. Metody přípravy těchto polymerů jsou založeny na polymeraci za otevření kruhu laktonů a laktidů. Mnoho organokovových sloučenin se vyznačují jako účinné a vysoce selektivní katalyzátory těchto polymerací, avšak je známo, že deriváty těžkých kovů jsou škodlivé pro lidský organismus. Z tohoto důvodu je v dnešní době rostoucí zájem o vývoj účinných „green“ polymeračních systémů pro syntézu biodegradabilních alifatických polyesterů.

Předložená disertační práce se věnuje přípravě alifatických polyesterů založených na polykaprolaktonu, polylaktidu, polyglykolidu a zejména jejich kopolymeru pomocí organického katalyzátoru náležícího do skupiny N-heterocyklických karbenů (NHC) bez přítomnosti centrálního atomu těžkého kovu.

Literární rešerše je zaměřená na pokroky v polymeraci za otevření kruhu (ROP) cyklických esterů (laktonů a laktidů) pomocí organických "metal-free" katalyzátorů. Nicméně, nebyly nalezeny žádné studie, kde se pro přípravu polyglykolidu nebo jeho kopolymerů využívá polymerace za otevření kruhu pomocí karbenových katalyzátorů.

Experimentální část práce popisuje přípravu a vlastnosti 1,3-di-*tert*-butylimidazol-2-ylidenu (NHC-*t*Bu) karbenu připraveného z jeho stabilní chloridové soli. Další část je zaměřena na přípravu polyesterů z cyklických monomerů, jmenovitě L-laktidu, D, L-laktidu, glykolidu a ϵ -kaprolaktonu pomocí NHC-*t*Bu jako katalyzátoru. Byla zkoumána nová metoda přípravy termosenzitivního amfifilního triblokového kopolymeru na bázi biodegradabilního hydrofobního polylaktidu, polyglykolidu a biokompatibilního hydrofilního polyethylenglykolu (PLGA-PEG-PLGA) pomocí připraveného NHC-*t*Bu. Dále byly studovány podmínky polymerace (například: přečištění monomeru, teploty polymerace, různé typy rozpouštědel, poměry rozpouštědla ku monomeru a nebo různé poměry iniciátoru ku katalyzátoru). Na závěr byl připravený PLGA-PEG-PLGA kopolymer srovnán s kopolymerem připraveným pomocí Sn(II)2-ethylhexanoátu.

NHC-*t*Bu se v přítomnosti PEG projevil jako účinný katalyzátor polymerace za otevření kruhu laktonu a laktidů. Připravené kopolymery dosahovaly vysoké konverze monomeru (70 – 85 %) s polydisperzitou (M_w/M_n okolo 1.2). Byl připraven PLGA-PEG-PLGA kopolymer se dvěma fázovými přechody (sol-gel a gel-suspenze) a gelační teplotou v rozmezí 35 – 43 °C. Změny polymeračních podmínek neměly ve většině případů zásadní vliv na chemické vlastnosti kopolymeru, jako jsou molekulová hmotnost nebo polydisperzita, ale měly významný vliv na viskoelastické vlastnosti.

Klíčová slova

Polymerace za otevření kruhu, N-heterocyklické karbeny, alifatické polyesterly, termocitlivé kopolymery, sol-gel fázový přechod.

BOHÁČOVÁ, Z. *Ring-opening polymerization of lactones and lactides*. Brno: Brno University of Technology, Faculty of Chemistry, Institute of Materials Science, 2015. p. 89. Supervisor: doc. Ing. Lucy Vojtová, Ph.D.

Declaration

I declare that the doctoral thesis has been worked out by myself and that all the quotations from the used literary sources are accurate and complete.

.....
student's signature

Acknowledgements

I wish to express my sincere gratitude to my supervisor Doc. Ing. Lucy Vojtová, Ph.D., for accepting me as her Ph. D. student and for her encouragement and scientific support throughout this work and the writing of this thesis. As well as, I would like to express my gratitude to prof. RNDr. Josef Jančář, CSc. for creation of working conditions.

I would also like to thank RNDr. Otakar Humpa for measurement of ^1H NMR spectra, Ing. Jana Oborná for the measurement and evaluation of the GPC chromatograms, Ing. Ivana Chamradová for rheological analyses and Ing. Lenka Michlovská, Ph.D. for cooperation in laboratory and interpretation of ^1H NMR spectra. I wish to thank all my research colleagues and friends at BUT Faculty of Chemistry and also at CEITEC BUT.

I am forever indebted to my parents Alena and Zdeněk for everything they have done for me. I thank you both for all the sacrifices since. Thanks to my sisters for the support.

Last, but certainly not the least, with great pleasure I would like to express my thanks to my husband for his love, support and encouragement in my life.

Table of Content

1.	Introduction	7
2.	Literature Review	8
2.1	Cyclic Esters.....	8
2.2	Biodegradable Aliphatic Polyesters.....	9
	2.2.1 Poly(ϵ -caprolactone) (PCL).....	10
	2.2.2 Polylactide (PLA)	11
	2.2.3 Polyglycolide (PGA).....	11
2.3	Synthesis of Aliphatic Polyesters	12
	2.3.1 Polycondensation.....	12
	2.3.2 Ring Opening Polymerization	13
2.4	Significant Catalytic/initiation Systems for the Polymerization of Lactones and Lactide.....	16
	2.4.1 Organometallic Compounds.....	16
	2.4.2 Organocatalysts	17
2.4	Smart Hydrogels	33
	2.4.1 Phase Diagrams	33
	2.4.2 Mechanism of Gelation	34
3.	Main Goal of the Thesis	37
4.	Experimental Part	38
4.1	Chemicals	38
4.2	Equipment	39
4.3	Methods.....	40
	4.3.1 Characterization of Polymers	40
	4.3.2 Preparation of Free Carbene.....	42
	4.3.3 Polymerization of L-lactide.....	42
	4.3.4 Synthesis of PLGA-PEG-PLGA Copolymers	43
5.	Results and Discussion	44
5.1	Synthesis and Polymerization Behavior of 1,3-di- <i>tert</i> -butylimidazol-2-ylidene	44
5.2	Polymerization of Cyclic Esters Using NHC/PEG Catalytic System	47
5.3	Synthesis of PLGA-PEG-PLGA Copolymers	51
	5.3.1 Optimization of Copolymerization Conditions	59
	5.3.2 Comparison of the Copolymers Prepared by the Organic Catalyst and Organometallic Catalyst	72
6.	CONCLUSION	76
	References	78
	List of Abbreviations	85
	List of Figures	87
	List of Tables.....	89

1. Introduction

Synthetic petrochemical-based polymers have had a tremendous industrial impact since the 1940s. Despite the numerous advantages of these polymers two drawbacks remains to be solved, namely the use of non-renewable resources in their production and the ultimate fate of these large scale commodity polymers. Biodegradable polymers are a more environmentally friendly alternative to petrochemical-based polymers. The advantage of these polymers is that they are in a suitable environment completely degradable within a short time. This means that the potential waste would be several times smaller than synthetic polymers. Processing of these materials has given rise to a broad range of applications from packing to more sophisticated biomedical devices [1].

Aliphatic polyesters such as hydrophobic polylactide (PLA), polyglycolide (PGA) and poly(ϵ -caprolactone) (PCL) represent an important class of biodegradable and biocompatible macromolecules. They offer a number of advantages for developing biomedical materials. The key advantages include the ability to tailor mechanical properties and degradation kinetics to suit various applications. These polymers are also attractive because they can be fabricated into various shapes with desired pore morphologic features. Furthermore, polyesters can be designed with chemical functional groups [2].

Ring-opening polymerization (ROP) of cyclic esters is one of the most important methods in the synthesis of aliphatic polyester. Catalysts used in ROP are mainly metal-containing compounds, which residues contaminate the polyesters make them inappropriate for bio-applications. Therefore, research and development of metal-free catalysts draw more attention in the synthesis of aliphatic polyesters in recent years. The application of organic nucleophilic N-heterocyclic carbenes (NHCs) as a “green“ catalysts has resulted in a highly active and versatile route for the metal-free polymerization of cyclic esters.

2. Literature Review

2.1 Cyclic Esters

Cyclic ester can be seen as the condensation product of an alcohol group –OH and a carboxylic acid group –COOH in the same molecule (Figure 1). Locant indicating the position of the hydroxyl functional group in the acid molecule is given in the name of the cyclic monomer (for example ϵ -caprolactone) [3].

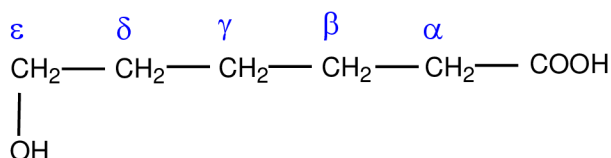
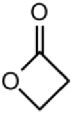
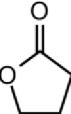
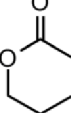
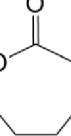
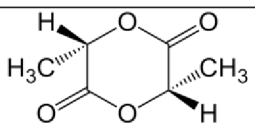
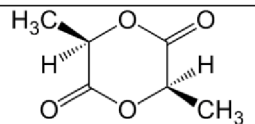
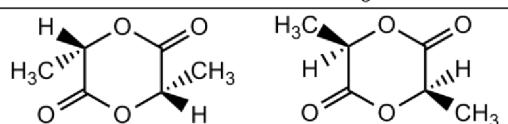
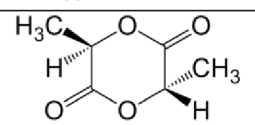
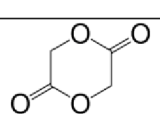


Figure 1 The order of locants on C atoms adjacent to carboxyl group in the hydroxy acid.

The ability of cyclic monomers to open the ring during ROP is affected by their thermodynamic stability. In general, thermodynamic stability of cyclic monomer decreases with increasing ring strain. The strain is relatively high for the 3- and 4-membered rings, decreases sharply for 5-, 6-, and 7-membered rings, increases for 8 – 13-membered rings, and then decreases again for larger rings [4]. The thermodynamic data for small and medium – sized cyclic esters show that the entropy change during polymerization is negative; thus, the driving force for the polymerization of these cyclic esters is the negative change of enthalpy [5]. In addition, the ability to polymerize is also influenced by polymerization conditions, stiffness of molecules and structure of monomers, such as substituents on a ring structure generally increase its stability [4]. Table 1 presents the cyclic monomer structures and their abbreviations.

Table 1 Overview of the most common cyclic ester monomers.

Monomer	Structure
β -propiolactone β -PL	
γ -butyrolactone γ -BL	
δ -valerolactone δ -VL	
ϵ -caprolactone ϵ -CL	

Monomer	Structure
L-lactide L-LA	
D-lactide D-LA	
D,L-lactide D,L-LA	
Meso-lactide Meso-LA	
Glycolide GA	

2.2 Biodegradable Aliphatic Polyesters

Biodegradable polymers have gained increasing interest over the past two decades in the fundamental research as well as in the chemical industry. Degradable plastics as defined by the American Society for Testing of Materials and the International Standards Organization are those which can go through a significant change in the chemical structure under specific environmental conditions [5]. Biodegradable plastics go through the process of degradation with the help of naturally occurring microorganisms such as bacteria, fungi, and algae [6].

A number of polymers have been developed as potential biodegradable materials due to their various compositions, special structures, and excellent properties that cover a wide range of applications (Figure 2). The most commonly used synthetic biodegradable polymers are polycaprolactone (PCL), polylactide (PLA), polyglycolide (PGA) and their corresponding copolymers. These polymers are widely used in the medical and packaging engineering fields. In the human body, these polymers degrade through hydrolysis into nontoxic components that are eliminated via the Krebs cycle as water and carbon dioxide [7], which makes the polymers suitable as resorbable medical materials. The major applications include resorbable sutures, drug delivery systems and orthopaedic fixation devices such as pins, rods and screws [1, 8]. Polyesters have also been considered for development of tissue engineering applications [8].

These biodegradable polymers may provide a practical solution to the ecological problems associated with bioresistant wastes. Flexible films, rigid containers, drink cups and bottles are products already available in the marketplace [7].

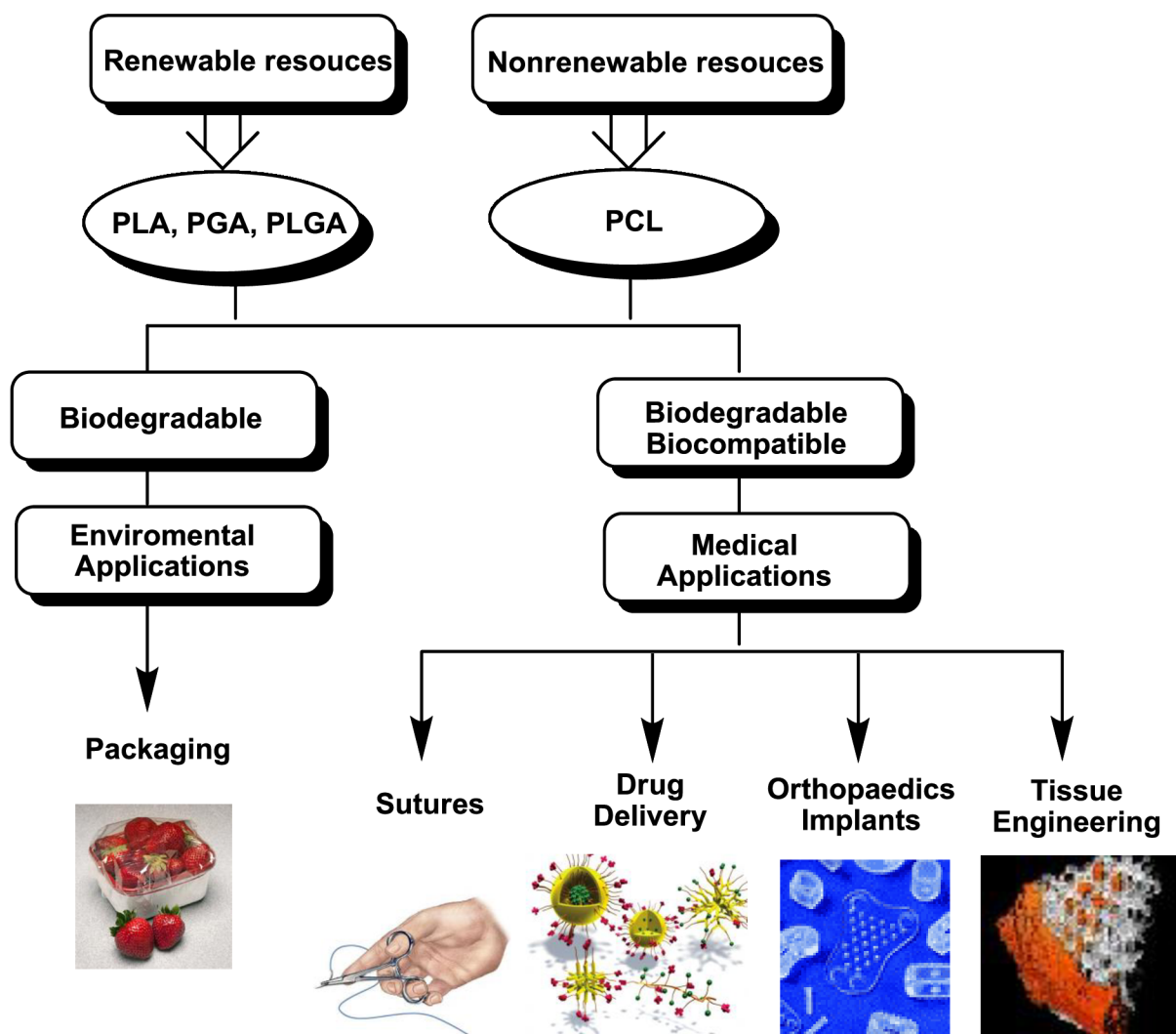


Figure 2 Practical applications of the biodegradable polyesters [7, 9 – 13].

2.2.1 Poly(ϵ -caprolactone) (PCL)

Poly(ϵ -caprolactone) derived from ϵ -caprolactone (Figure 3) belongs to the most attractive and commonly used biodegradable polyesters [14].

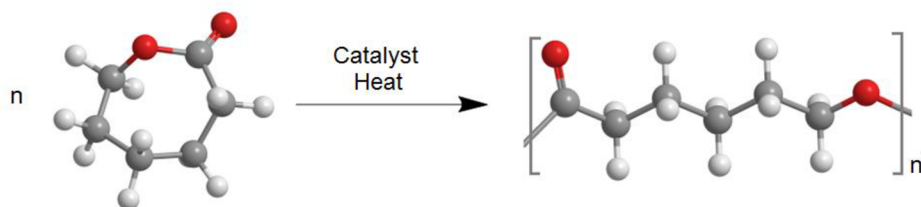


Figure 3 Scheme of the ROP of ϵ -caprolactone to poly(ϵ -caprolactone).

PCL is polyester with a valuable set of properties such as high permeability, biodegradability and compatibility and thus is blended with various commercial polymers or biopolymers [15]. PCL is a

hydrophobic, tough, crystalline thermoplastic material with a melting point (T_m) of about 61 °C and glass transition temperature (T_g) of -60 °C. In general, PCL crystallizes readily to an approximate degree of crystallinity of 40 – 50 % [16, 17]. The relative high degree of crystallinity is related to regular structure of PCL chains. One of its most attractive qualities for the use in specific biomedical applications is its slow degradation. The degradation time depends on its initial molecular weight and usually is in the order of 2 years [14, 18].

2.2.2 Polylactide (PLA)

Poly lactide is perhaps the most frequently used polyester in biomedical applications due to its many favorable characteristics, such as high strength and biocompatibility. PLA is synthesized either from lactic acid by a condensation reaction or more commonly by the ring-opening polymerization of cyclic lactide dimer (Figure 4) [19].

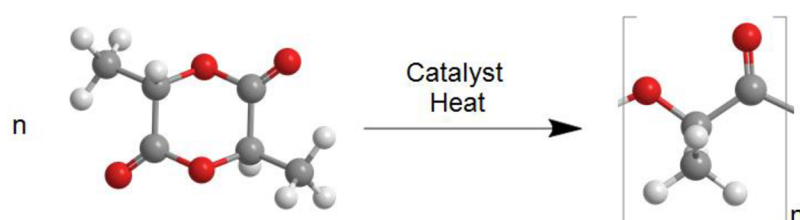


Figure 4 Scheme ROP of lactide to polylactide.

The lactide monomer exists in four different isomers (Table 1) which polymerizations lead to structurally and morphologically distinct polymers. The chirality of LA units provides a means to adjust degradation rates, as well as physical and mechanical properties [20, 21]. L-PLA is a highly crystalline isotactic polymer ($T_g = 55 - 60$ °C, $T_m = 180$ °C) and is preferred in application where high mechanical strength and toughness are required such as sutures, staples and orthopedic devices. D,L-PLA is generally amorphous ($T_g = 45 - 50$ °C) and is usually considered in application such as controlled drug release [21].

2.2.3 Polyglycolide (PGA)

Polyglycolide or polyglycolic acid is a biodegradable, thermoplastic polymer and also the simplest linear, aliphatic polyester. It can be prepared from glycolic acid by polycondensation or from glycolide by the ring-opening polymerization (Figure 5) [22].

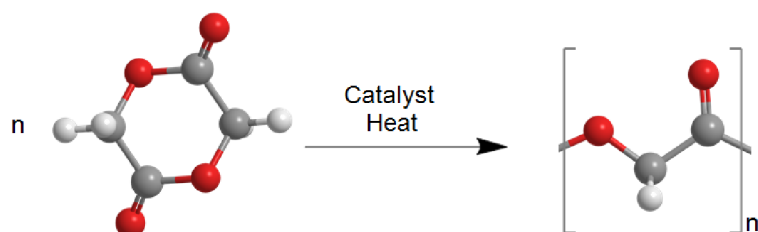


Figure 5 Scheme ROP of glycolide to polyglycolide.

Polyglycolide with a high molecular weight is a hard, tough, crystalline polymer (around 45 – 55 %) with a melting point between 225 – 230 °C, glass transition temperature around 35 – 40 °C and very high tensile strength (12.5 GPa) [23 – 25]. Its high crystallinity results in insolubility in most organic solvents; the exceptions are highly fluorinated organic solvents such as 1,1,1,3,3,3-hexafluoro-2-propanol [8].

2.3 Synthesis of Aliphatic Polyesters

As mentioned previously, aliphatic polyesters such as poly(ϵ -caprolactone), polylactide, and polyglycolide can be generally prepared by two methods: the step-growth polymerization (polycondensation) and by the ring opening polymerization (ROP) methods.

2.3.1 Polycondensation

A well-known method to synthesize linear and branched polyesters is step-growth polymerization. Polycondensation relies on the condensation of hydroxy acids (or a mixture of diacids and diols) either in the melt or in solution at high temperatures, often in the presence of a Lewis acid catalyst (Figure 6) [18].

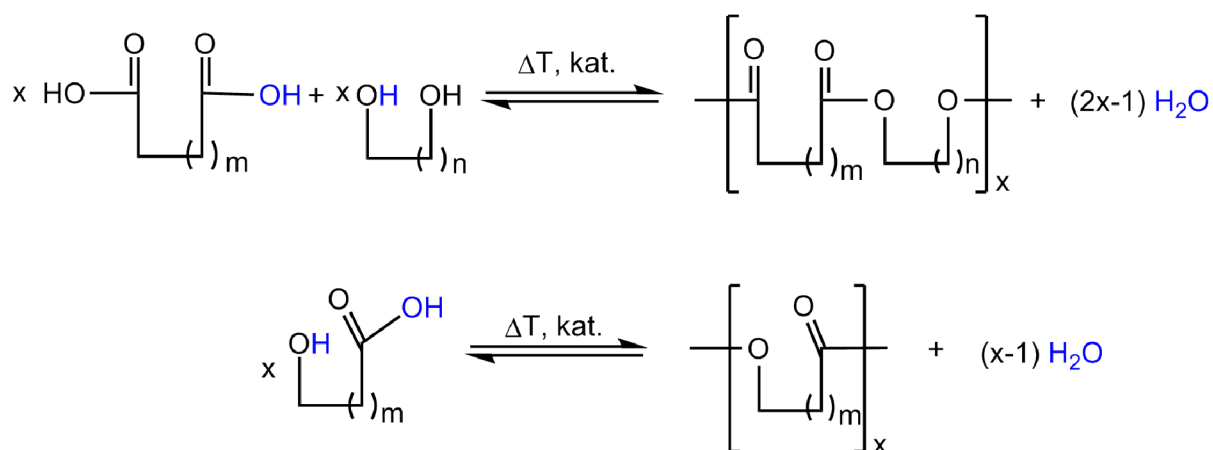


Figure 6 A schematic representation of the polycondensation.

Such reaction is also limited to equilibrium; thus water must be removed from the polymerization medium to increase the conversion and the molecular weight. The major drawbacks of this polycondensation mechanism are not very high yields and relatively low molecular weight products ($M_n < 30\,000 \text{ g}\cdot\text{mol}^{-1}$) with broad molecular weight distribution and previously difficult controllable structure. Moreover, the stereoregularity cannot be controlled during the course of polymerization [26].

Therefore, other routes such as ring opening polymerization of cyclic esters were developed to synthesize aliphatic polyesters. This class of polymerization method will be discussed in more detail in the next section.

2.3.2 Ring Opening Polymerization

The most common method to obtain high-molecular-weight aliphatic polyesters is the ROP of lactones or lactides. This method was developed by Carothers et al. in 1930s [28]. Many research laboratories have been involved in this research area and many different initiators and catalysts have been developed since then. By ROP it is possible to control properties such as molecular weight, molecular weight distribution and the architecture of the polymer. The method also provides the possibility to achieve desired chain end groups and copolymerization of various monomers [29]. Depending on the initiator, the polymerization proceeds according to different reaction mechanisms, *i.e.* anionic, cationic, or coordination-insertion mechanism. In addition, radical, zwitterionic, or active hydrogen initiations are also possible but are not used to any great extent [30].

2.3.2.1 Anionic Ring Opening Polymerization

Ring-opening polymerizations using nucleophilic reagents as initiators can be categorized into anionic ROP [5]. The reaction is initiated by the attack of a negatively charged initiator on the carbon of the carbonyl group or on the alkyl-oxygen, resulting in formation of linear polyester (Figure 7). Depending upon the reaction conditions, the type of initiators and the monomers, the polymerization may proceed either by a living or a nonliving mechanism [31].

The anionic ROP of four-membered rings (β -lactones) occurs through alkyl-oxygen or acyl-oxygen cleavage giving a carboxylate or alkoxide active chain end. Larger lactones, such as ϵ -caprolactone or lactide, react only by an attack of the anion on the carbonyl carbon atom with acyl-oxygen scission and the formation of an alkoxide as the growing species [32].

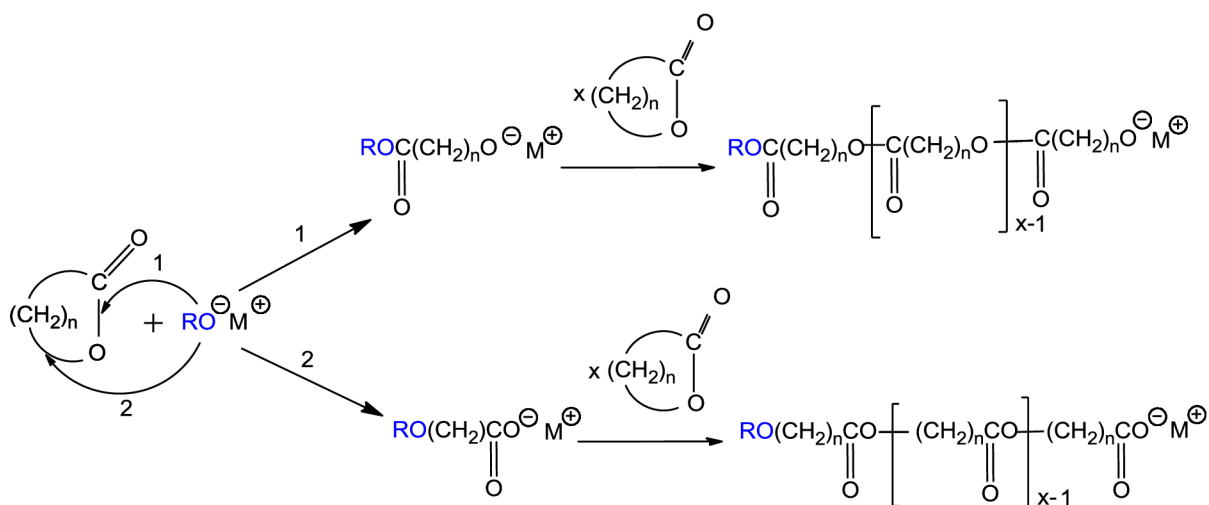


Figure 7 ROP of lactones via anionic mechanism; (1) acyl-oxygen scission (2) alkyl-oxygen scission.

The effective initiators for anionic polymerization of lactones are alkali metals, alkali metal oxides, alkali metal naphthalenide complexes with crown ethers, etc. [31].

2.3.2.2 Cationic Ring Opening Polymerization

In contrast to anionic ROP, cationic ROP represents another class of polymerization where electrophilic reagents are used as initiators. The cationic polymerization initiated by alkylating or acylating initiators is generally believed to proceed via alkyl–oxygen bond cleavage of the monomer, with the initiator being incorporated into the growing polymer chains (Figure 8) [5]. These type of polymerization is difficult to control and often only low molecular weight polymers are formed, due to the occurrence of intramolecular transesterification (cyclization) or other chain transfers within polymer reaction (including proton and hydride transfer reactions) [32].

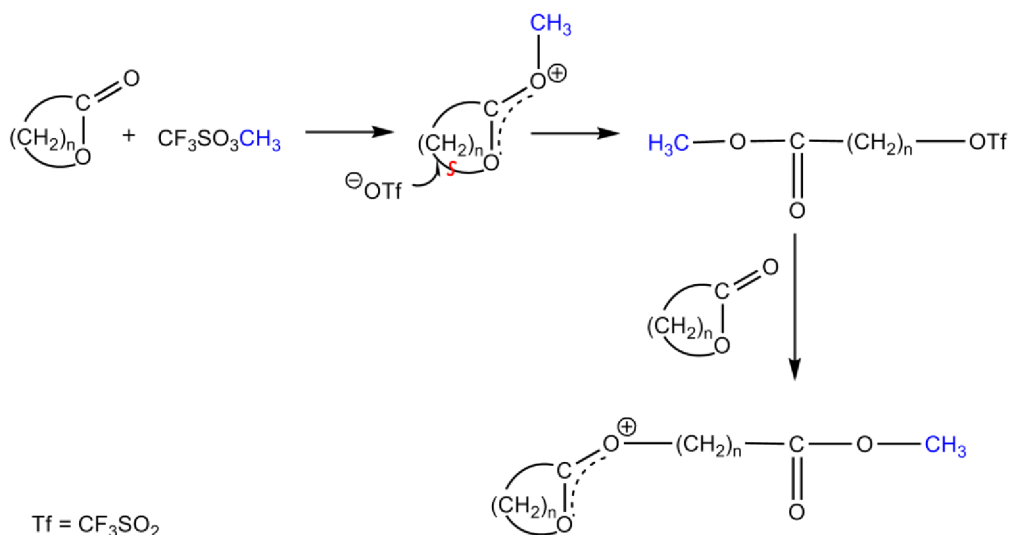


Figure 8 Proposed pathway for cationic ROP of cyclic esters.

Initiators for the cationic ROP of lactones include protonic acids (HCl, RCOOH, RSO₃H, etc.), Lewis acids (AlCl₃, BF₃, FeCl₃, ZnCl₂, etc.), stabilized carbocations (ET₃O⁺BF₄⁻) and acylating agents (CH₃CO)⁽⁺⁾(⁻)OCl₄ [32].

2.3.2.3 Coordination-insertion Ring Opening Polymerization

Coordination insertion polymerization has been extensively used for the preparation of aliphatic polyesters with well-defined structure and architecture. The ROP proceeds mainly via two major polymerization mechanisms depending on the used organometallics. In the first type of mechanism the organometallic compound (e.g. metal oxides and carboxylates) acts as catalysts, and activate the monomer by complexation with the carbonyl group (Figure 9). Polymerization is then initiated by any nucleophile, such as water or alcohol, present in the polymerization medium as impurities or as compound added on purpose.

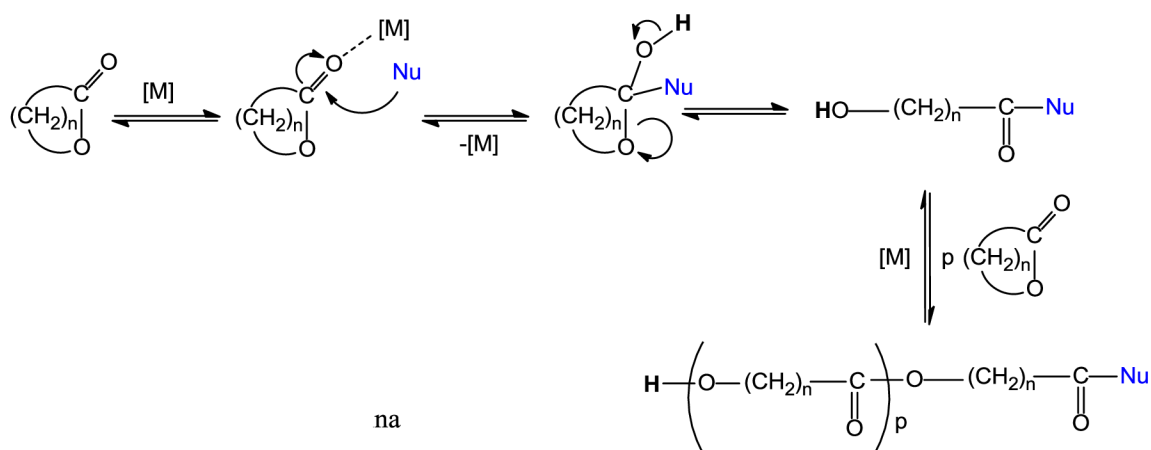


Figure 9 ROP of lactones catalyzed by organometallic species $[M]$ in the presence of nucleophiles (Nu).

The metals with free p-, d-, or f- orbitals of a favorable energy (Mg-, Sn-, Ti-, Zr-, Fe-, Al-, Y-, Sm-, Zn-alkoxides) are known to initiate the polymerization of various lactides and lactones through the coordination-insertion route [34]. The mechanism involves acyl-oxygen bond cleavage of the monomer and insertion into the metal-oxygen bond of the initiator. The coordination of the ring oxygen to the metal results in polarization and this makes the carbonyl carbon of the monomer more susceptible to nucleophilic attack. Figure 10 shows a schematic presentation of the coordination-insertion mechanism. The growing chain - "living end" remains attached to the metal through an alkoxide bond during the propagation [35, 36]. The reaction is terminated by hydrolysis forming a hydroxy end group. On the other hand, the alkoxide group of the initiator forms the "dead end" of the growing chain end [36].

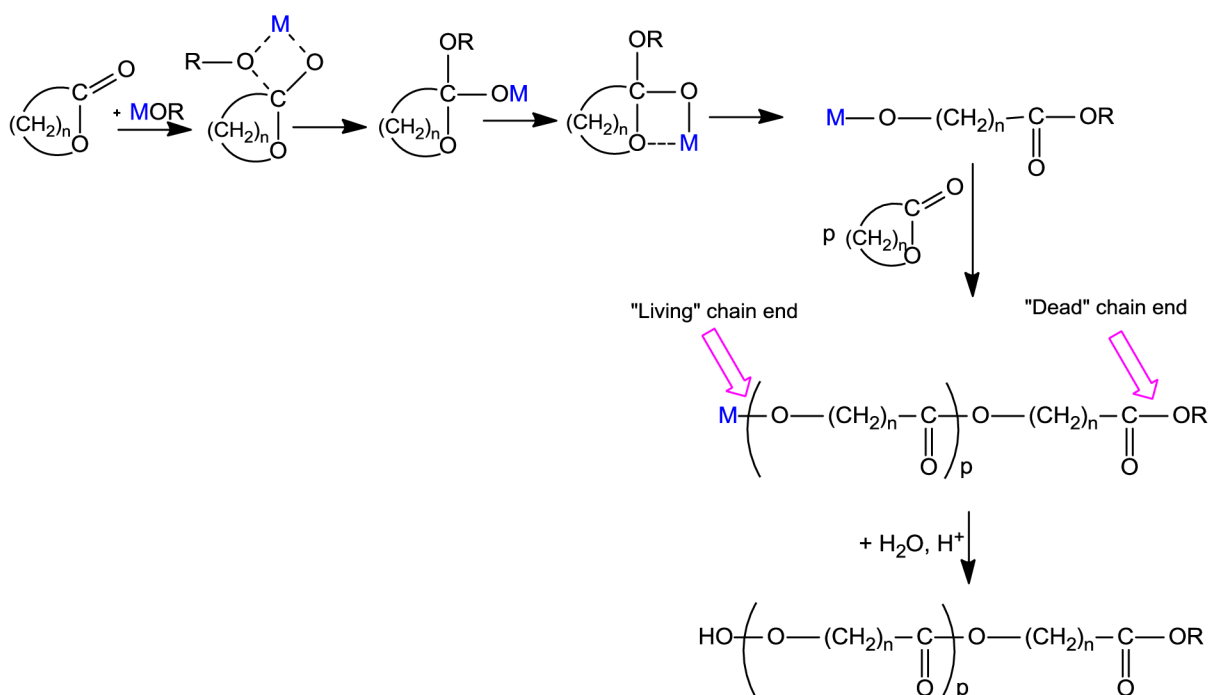


Figure 10 ROP of lactones by the coordination-insertion mechanism.

It is well known that ROP of lactones and lactides at high temperatures or long reaction times is accompanied by both inter- as well as intramolecular transesterification reactions (Figure 11) [35]. Intramolecular transesterification is a unimolecular back-biting reaction, releasing a fragment of a macromolecule in the cyclic form and leaving a shorter but still active macromolecule. The cyclic product can further react with growing species in the propagation step. Intermolecular transesterification takes place between two growing macromolecules as the cross-reaction without losing the activity of the chain end groups [32].

Both types of transesterification reactions lead to an increase of polydispersity of the polyester [31]. The reaction parameters that influence the extent of the transesterifications are temperature, reaction time, the type and concentration of catalyst or initiator, and the nature of the lactone or lactide [37].

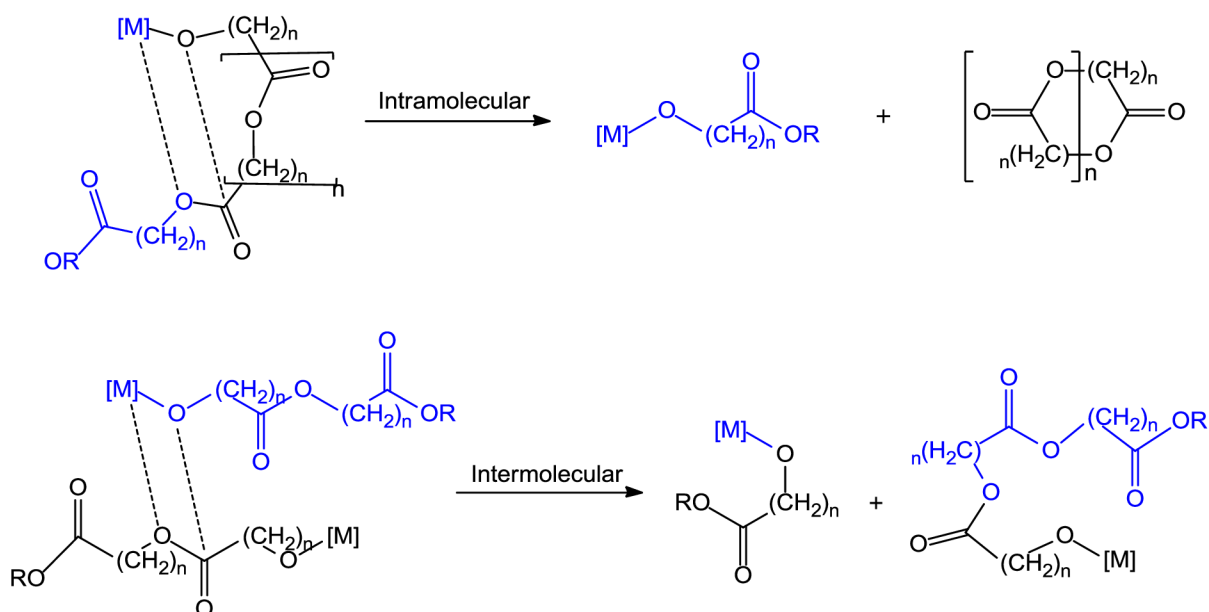


Figure 11 Scheme of intermolecular and intramolecular transesterification.

2.4 Significant Catalytic/initiation Systems for the Polymerization of Lactones and Lactides

The synthesis of novel catalysts or initiators for the ROP of existing or new monomers and macromers substituted with functional groups provide a very interesting and promising strategy for producing structurally advanced macromolecules.

2.4.1 Organometallic Compounds

A number of organometallic compounds, *i.e.* metal-oxides, carboxylates and alkoxides have been studied in order to achieve effective polyester synthesis via ROP of lactones or lactides. Several reactions catalyzed by metal complexes are highly specific, and reactions can be generated to form a desired polymer structure. Catalysts based on tin (Sn) and aluminum (Al), in particular Tin(II)-2-ethylhexanoate ($Sn(Oct)_2$) and aluminum tris-(isopropoxide) ($Al(iPr)_3$) (Figure 12), have been researched extensively for ROP of lactones or lactides [34].

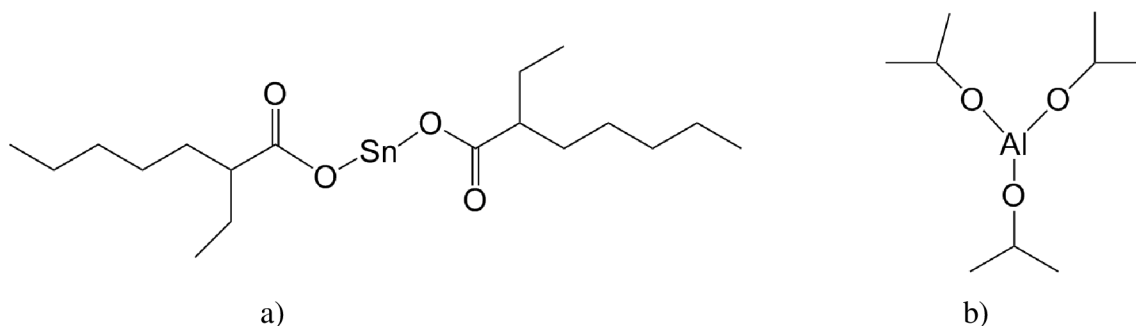


Figure 12 Structures of a) $\text{Sn}(\text{Oct})_2$ and b) $\text{Al}(\text{iPr})_3$.

Tin(II)-2-ethylhexanoate (SnOct_2), is the most widely used catalyst for the synthesis of polylactides and polylactones both in technical production and for research purposes. Reasons include a high efficiency and versatility, easy handling and its solubility in most common solvents and cyclic ester monomers. SnOct_2 have been approved by Food and Drug Administration for the use in food additive but it still possesses toxicity [31]. It has been reported that $\text{Sn}(\text{Oct})_2$ is not removed completely by a purification method involving dissolution and precipitation below a residual level of 306 ppm in PLA [38]. In this preview there is the major reason to search for effective and above all "green" polymerization systems for the synthesis of biocompatible polyesters.

2.4.2 Organocatalysts

An important consideration in the polymerization of lactone and lactide is the removal of metal contaminants, bound to the chain end before application in resorbable biomaterials. The application of organocatalysts to controlled polymerization would be a highly viable alternative to organometallic approaches. Several organic compounds have demonstrated high activity and enantioselectivity in a number of common organic transformations.

2.4.2.1 Pyridine-Based Organocatalysts

A decade ago, Hedrick and co-workers were the first who reported the use of nucleophilic organic catalyst 4-aminopyridines in the ROP of lactide. 4-(dimethylamino)pyridine (DMAP) and related bases such as 4-pyrrolidinopyridine (PPY) (Figure 13) used in equal quantities to that of the initiator were found to be highly active [39].

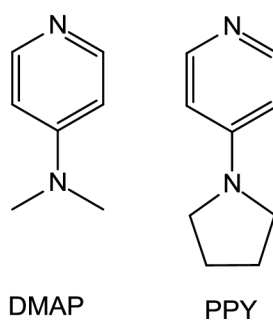


Figure 13 Structure 4-(dimethylamino)pyridine (DMAP) and 4-pyrrolidinopyridine (PPY).

The DMAP and PPY amines showed in the presence of ethanol as an initiators catalytic activity for the ROP of LA at 35 °C in CH₂Cl₂ with reaction times ranging from 20 to 96 hrs. PLAs with narrow polydispersity index (M_w/M_n) and with degrees of polymerization (DPs) ranging from 17 to 100 were prepared. Bulk polymerizations of D,L- and L-lactide were also investigated at 135 and 185 °C using benzyl alcohol as the initiator. Narrowly dispersed polylactides were obtained in about 5 to 20 minutes, depending on the targeted molecular weight. No polymerization was detectable in the absence of the initiator. The living character of the polymerization was demonstrated by the linear relationship of molecular weight and monomer conversion in addition to the resulting narrow M_w/M_n and predicted molecular weights based on monomer-to-initiator ratios. Polymerization was proposed to occur through a monomer-activated mechanism, as shown in Figure 14 [39, 40].

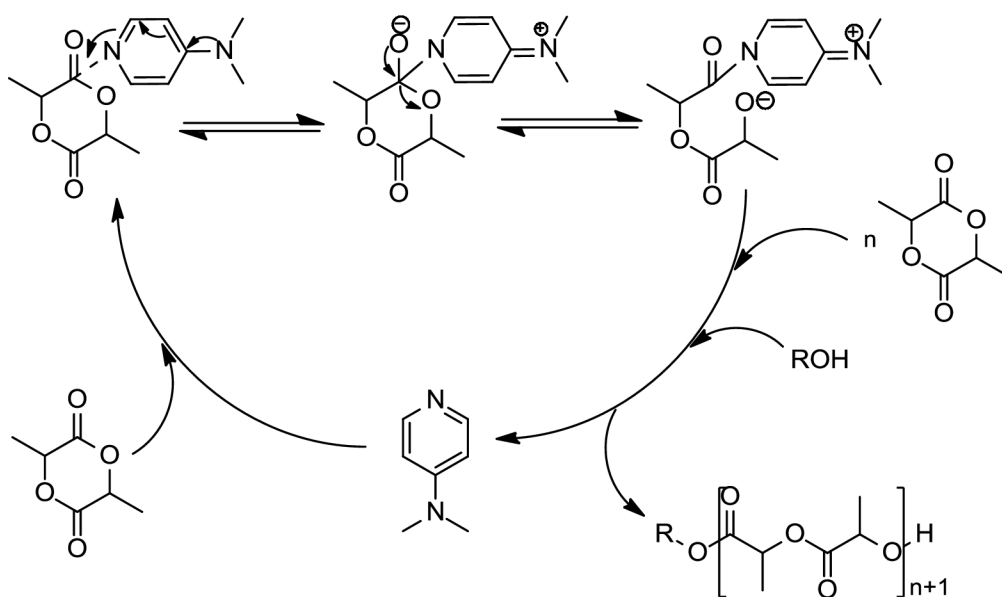


Figure 14 Proposed mechanism for the ROP of LA using DMAP catalyst.

Li and co-workers applied DMAP to catalyze the ring-opening copolymerization of linear L-LA in the presence of poly(L-lysine) dendron as initiator to produce linear-dendritic poly(L-lactide)-b-dendritic(L-lysine)s. High conversion (close to 85 %) was observed at 55 °C in chloroform after 20 — 80 hrs [41].

2.4.2.2 Phosphine Catalysts

Myers and co-workers investigated a number of phosphines (Figure 15) as catalysts for the ROP of L-LA in bulk at 135 and 180 °C and in solution of variety polymerization media, including tetrahydrofuran (THF), and toluene at 50 and 94 °C with benzyl alcohol as the initiator. Phosphines were proved to be much less active than 4-aminopyridines [42].

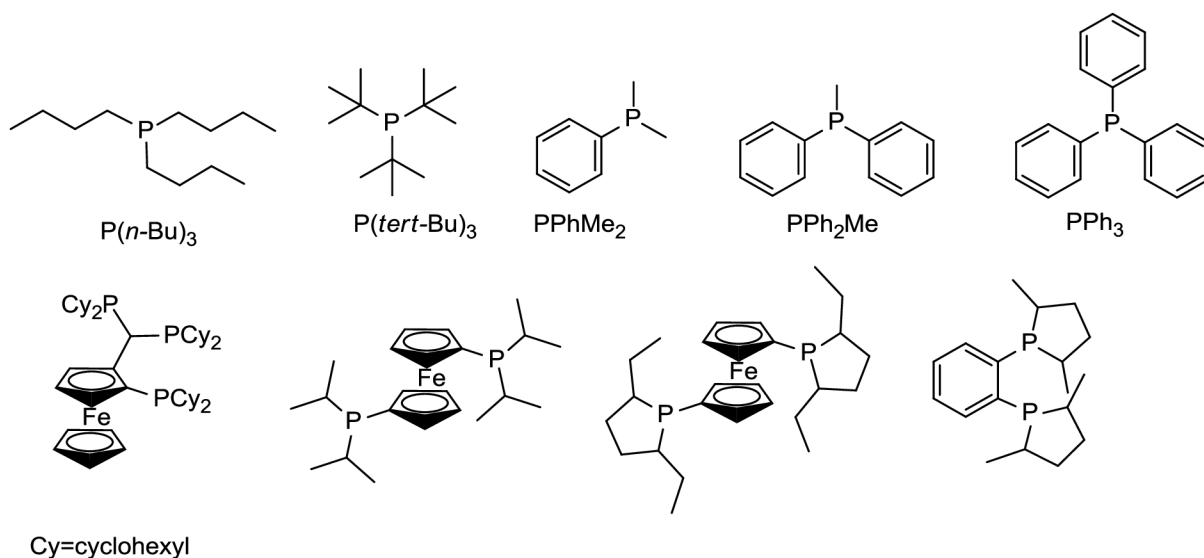


Figure 15 Phosphine catalysts for the ROP of LA.

Phosphines produced polymers with more narrow polydispersity index (1.11 – 1.40) and predicted molecular weights (target DPs between 30 – 100). The substitution on the phosphine is a dominant feature in controlling reactivity. Phosphine catalyst activity toward LA polymerization decreased according to the following order: $P(n\text{-Bu})_3 > P(\text{tert-Bu})_3 > P\text{PhMe}_2 > P\text{Ph}_2\text{Me} > P\text{Ph}_3$. The more basic and nucleophilic alkyl-substituted phosphines the more effective LA polymerization catalysts were than phosphines with one or more aryl groups. Supposed polymerization pathway was through a monomer-activated mechanism (Figure 16) [40, 42].

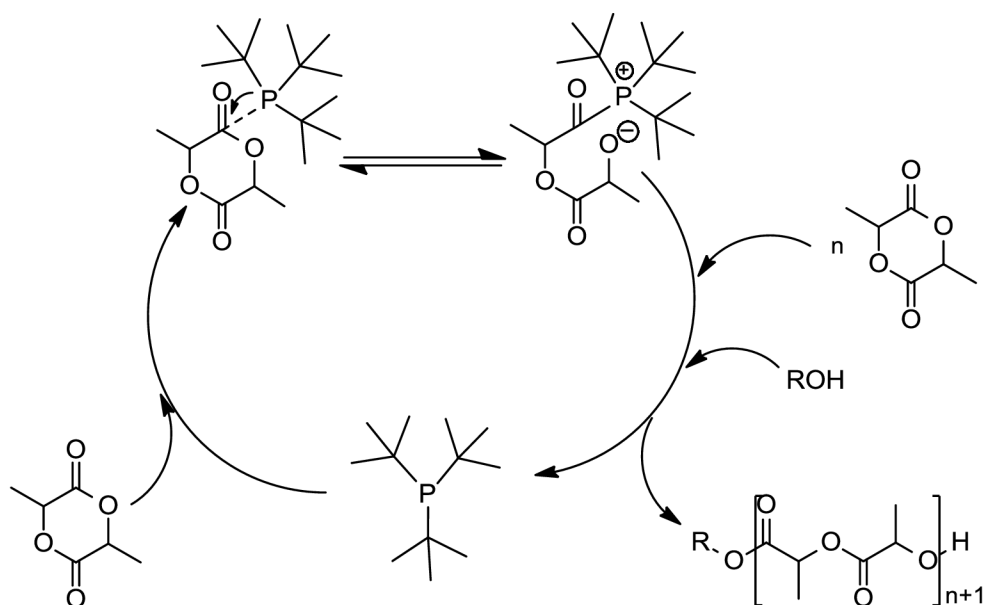


Figure 16 Proposed mechanism for the ROP of LA using $P(\text{tert-Bu})_3$ catalyst.

2.4.2.3 (Thio)urea/amine Based Catalysts

The first Dove and co-workers reported use of a variety thiourea-containing bifunctional organocatalyst for ROP of LA. Mechanistic and theoretical studies support a bifunctional mechanism involving activation of both the LA monomer and the alcohol nucleophile. The carbonyl group of the lactide monomer is activated toward electrophilic attack by the thiourea via hydrogen bonding, and the initiating/propagating alcohols are activated as nucleophiles by the tertiary amine (Figure 17) [43, 44].

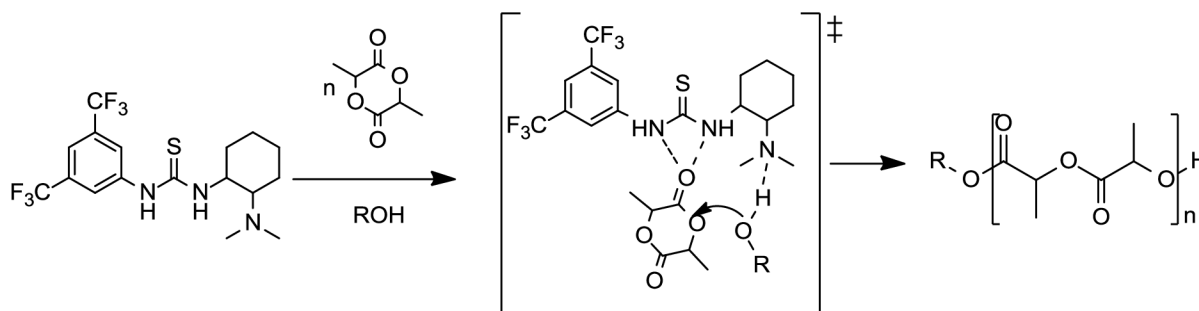


Figure 17 Proposed activation pathway for LA ROP using a bifunctional thiourea catalyst.

Thiourea-amine catalyst (Figure 17) in the presence of 4-pyrenebutanol as the initiator generated PLAs at room temperature in CH_2Cl_2 with monomer conversion reached 97 % after 48 hrs with very narrow polydispersity (1.05). The polymerization exhibited characteristics of a living polymerization as evidenced by the linear correlation between and monomer conversion [43].

2.4.2.4 Amidines and Guanides Organocatalysts

Following the successful development of 4-aminopyridines and phosphines as well as the bifunctional amino-thioureas, Pratt et al. have recently investigated the commercially available guanidine 1,5,7-triazabicyclo[4.4.0]dec-5-ene (TBD, Figure 18) for ROP of cyclic esters [45]. TBD proved to be more active for the ROP of LA than any other organocatalysts even competing with the most efficient metal systems [46].

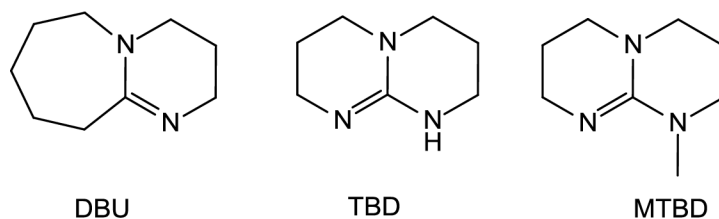


Figure 18 Chemical structures DBU, TBD and MTB.

Using 4-pyrenebutanol as the initiator, polymerization was achieved in only 1 minute at room temperature in CH_2Cl_2 for a monomer/initiator/catalyst (M/I/C) ratio of 500/1/0.5 and $[\text{M}]_0 = 1 \text{ mol}\cdot\text{dm}^{-3}$. Both the N-methylated analogue of TBD (MTBD) and 1,8-diaza[5.4.0]bicycloundec-7-ene (DBU, Figure 18) were found to be much less active under the same conditions, despite only slightly lower basicities ($\text{pK}_{\text{aH}} = 25.5$ and 24.3) [46]. Monomer-activated mechanism for the ROP by TBD involved acylation of TBD by the lactone, followed by displacement of the acylated TBD to the chain-end alcohol (Figure 19).

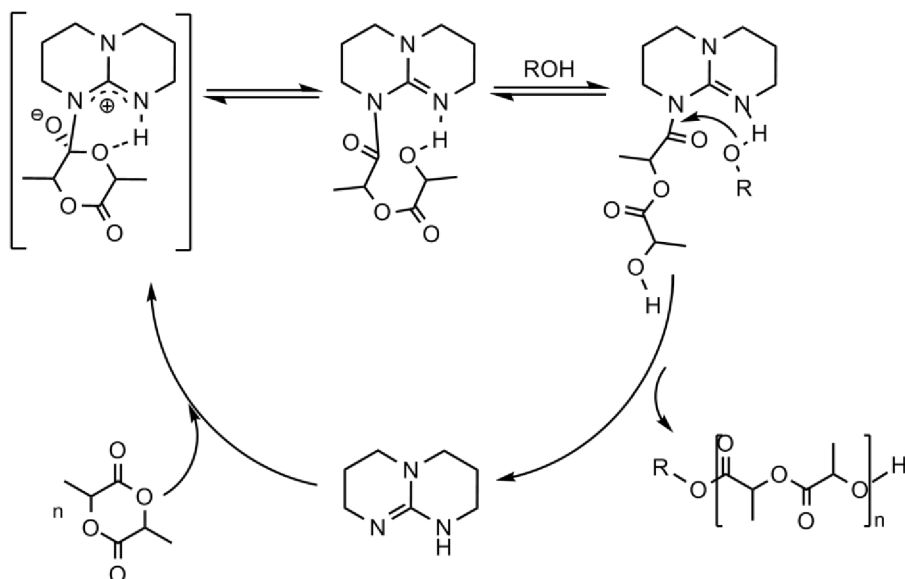


Figure 19 Proposed dual activation of monomer and initiator for ROP of lactones.

Block copolyesters of LA, δ -VL, and/or ϵ -CL have been synthesized using TBU by sequential addition of two different cyclic esters monomers. Copolymerization was controlled by first ring-opening the slower-propagating monomer (CL or VL). Consequently faster-propagating monomer (VL or LA) were added and finally the reaction of the second monomer was quenched. Copolyesters of high molecular weights ($M_n = 23000 - 27000 \text{ g}\cdot\text{mol}^{-1}$) and low polydispersity index (1.17 – 1.21) were obtained [47].

Hoye et al. [48] reported a strategy for the successful controlled “random” copolymerization of glycolide and a racemic mixture of D- and L-LA using poly(ethylene glycol) monomethyl ether (PEG-OH) as a macroinitiator. The resulting amphiphilic PEG-*b*-PLGA block copolymers had well-controlled molecular weights and narrow polydispersity index (1.05 – 1.17).

2.4.2.5 Enzymes

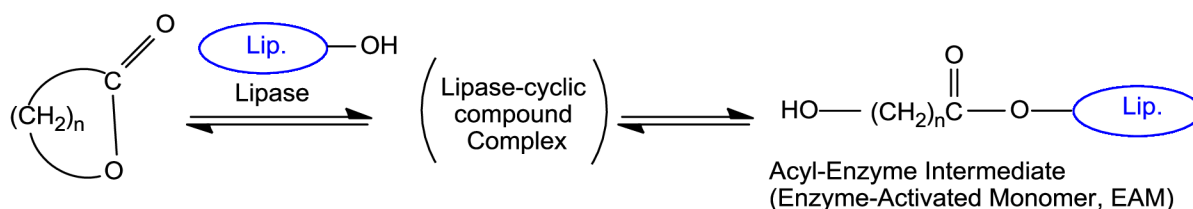
The enzymatic polymerizations also appear as an alternative technique for producing metal-free polyesters [26]. Kobayashi [50], and Knani [51] first reported in 1993 the enzymatic bulk and solution ROP of ϵ -CL and δ -VL with the enzyme *Candida Antarctica Lipase B*. Generally, enzymes catalysts have a several advantages: reactions with high enantio- and regio-selectivity, mild reaction conditions (*i.e.* temperature, pressure, pH, etc.), and nontoxic natural catalyst. There are also some disadvantages: long reaction time or low molecular weight.

Lipase, a member of the hydrolase family, is an enzyme which catalyzes the hydrolysis of fatty acid esters normally in an aqueous environment in living systems. On the other hand, some lipases are stable in organic solvents and can be used as catalyst. The lipases that have been reported for the polyester synthesis are of mammalian (porcine pancreatic lipase, [52]) or fungal (*Candida antarctica* lipase B [53], *Candida rugosa* [54], *Candida cylindracea* [55], *Aspergillus niger* [53], *Penicillium rorueforti* [54], *Rhizopus delemar* [55]) or bacterial origin (*Pseudomonas cepacia* [56, 57], *Pseudomonas fluorescens* [55], *Pseudomonas species lipase* [58], etc.) [59].

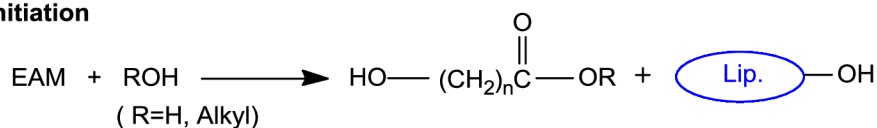
On the basis of reported results [60], it is believed that lipase-catalyzed ROP of lactones proceeded by an enzyme-activated monomer mechanism (Figure 20). The key step is the reaction of the catalytic active serine residue of the enzyme with the cyclic ester leading to the formation of the

acyl-enzyme intermediate. This intermediate reacts with water or alcohol to regenerate the enzyme and a ω -hydroxycarboxylic acid or ester. In the next propagation step, nucleophile attack of the terminal hydroxyl group of the propagating polymer on the acyl-enzyme intermediate leads to the addition of one more unit to the chain and regeneration of the enzyme.

Monomer Activation



Initiation



Propagation

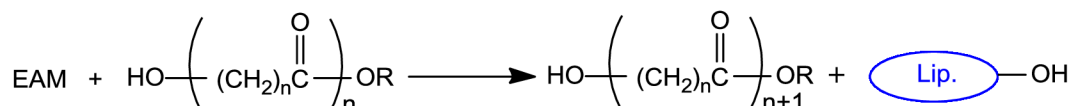


Figure 20 Proposed enzymatic ROP of cyclic esters.

2.4.2.6 Carbenes

Since the 1950s carbenes have shown great potential in the field of organic and organometallic chemistry [61]. These neutral compounds with general formula XYC : see Figure 21, where X and Y may be alkyl, aryl, H, or heteroatoms (O, N, S, halogens) contain divalent carbon atom, which possess two non-bonding electrons and six valence electrons [62]. Because the central carbon atom does not possess an octet of electrons, free carbenes are electron deficient and extremely reactive [63].

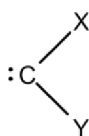


Figure 21 General formula of free carbenes.

The free carbenes exist in two different electronic states: singlet and triplet, which are represented in Figure 22. The singlet state has one lone electron pair, while the triplet state has two unpaired electrons [61].

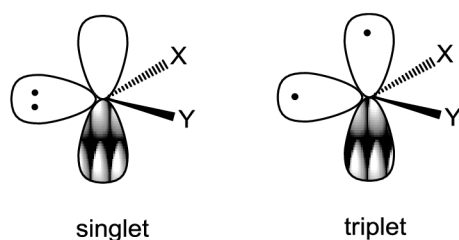


Figure 22 Orbital presentation of carbenes.

The most studied members of the family of nucleophilic carbenes are N-heterocyclic carbenes (NHCs). They are generally known as excellent ligands for metal-based catalysis, but there is also increasing interest in the role of nucleophilic carbenes as organocatalysts. Metal-free catalyzed processes are interesting alternatives to classical organic transformations since they are often more economical and environmentally friendly. This type of organocatalyst will be discussed into more detail in the next section.

N-heterocyclic carbenes

N-heterocyclic carbenes (NHCs) are a specific class of carbene compound in which a singlet carbenic carbon is flanked by two nitrogen atoms within a heterocyclic ring [64]. NHCs were first prepared independently by Wanzlick and Schönher [65] and Öfele [66] in 1968. They attracted much attention after the discovery of first stable NHC 1, 3-bis(adamantyl)imidazole-2-ylidene (IAd) by Arduengo [67] in 1991. The potential of this class of compounds to serve as spectator ligands was recognized by Herrmann et al. in 1995 [68]. Soon thereafter, the exploitation of the potential of NHC ligands in catalysis began [69].

NHCs can be synthesized with considerable diversity by varying the heteroatom in the ring (N or S), the steric and electronics of the groups attached to the imidazole ring (R_{1-2}) and the nitrogen(s) ($R_{3,4}$), and the ethylene backbone (*i.e.* saturated versus unsaturated) (Figure 23) [70]. NHCs form stable complexes with the transition metals, with lithium or beryllium, as well as lanthanides and actinides. They also form stable neutral adducts with a variety of organic species, including alcohols, amines and chloroform [71].

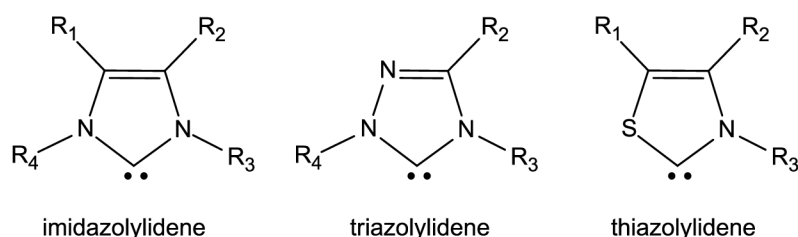


Figure 23 Structural diversity of N-heterocyclic carbenes.

Due to the high reactivity of carbenes as well as their extreme sensitivity to the air and moisture, several strategies for generating these reactive compounds “in situ” under controlled conditions have been developed. The choice of methods depends on the nature of the carbene as well as on the compatibility of the generation method to the reaction interest [40]. Hedrick et al. reported that both

unsaturated imidazolylidene and saturated imidazolylidene carbenes could be generated by treatment of the corresponding imidazolium salts with *tert*-butoxide (t-BuOK) and used directly for the ROP of cyclic esters (Figure 24) [72]. This strategy requires the addition of a strong base, which, if not completely consumed, could also initiate ROP resulting in limited molecular weights and broader polydispersity index [73].

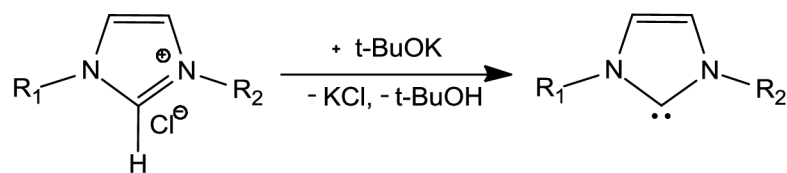


Figure 24 “In situ” generation of free NHC using t-BuOK salt.

An extension of this methodology involves the use of imidazolium-derived ionic liquids both as environment-friendly solvents and catalyst reservoirs. Polymerizations using ionic liquids have been performed using two different ways. In the first method, the polymerization was performed in neat ionic liquid, which serves as both the solvent and catalyst source. But much better results were obtained with THF/ionic liquid biphasic system [40]. Indeed, “in situ” deprotonation of an imidazolium-based liquid with potassium *tert*-butoxide generated the corresponding imidazol-2-ylidene, which migrates to the THF phase and initiates the ROP of cyclic esters (Figure 25) [46].

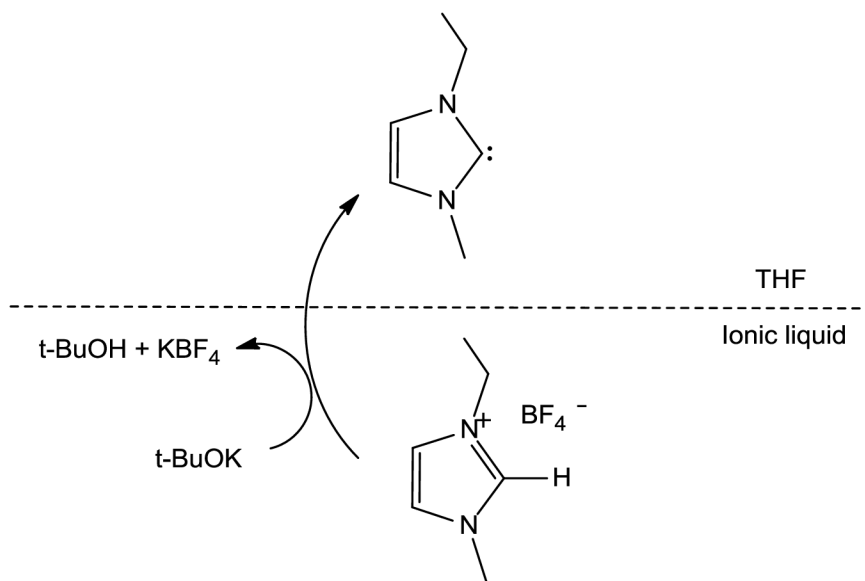


Figure 25 Generation of the NHC catalyst from the ionic liquid reservoir.

The use of silver(I) carbene complexes as transmetalling agents to generate other transition of transition metal complexes prompted the investigation of these silver complexes as potential delivery agents for free carbenes (Figure 26) [72]. Silver carbene complexes are also active catalysts for the ROP of L-LA at 160 °C in the bulk.

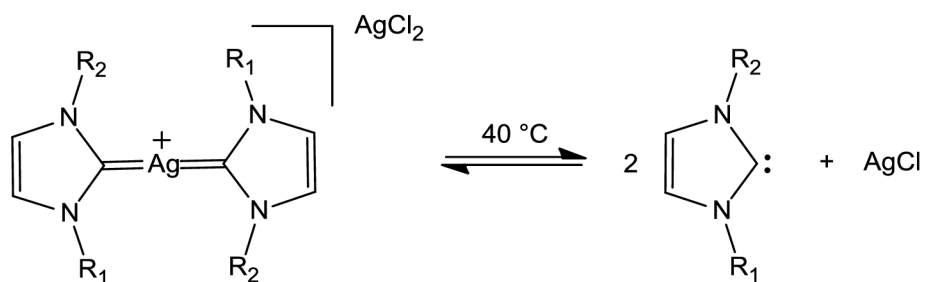


Figure 26 Generation of free carbene from silver(I) carbene complex.

Hedrick et al. also described an alternate strategy for generating saturated imidazolinylidene carbenes by thermolysis of stable chloroform and pentafluorobenzene adducts (Figure 27). At elevated temperature, the carbene-adduct bond is cleaved and the free carbene is released into solution [74].

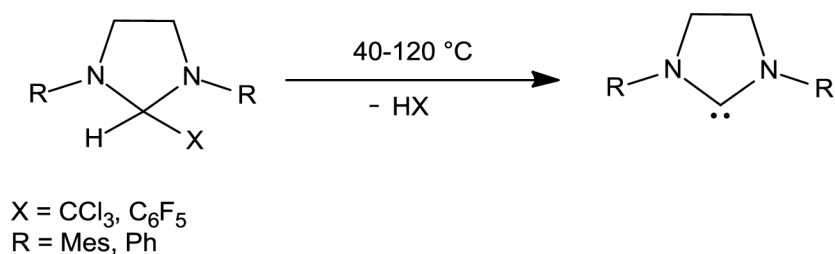


Figure 27 Generation of free carbene from stable chloroform and pentafluorobenzene adducts.

Grubbs demonstrated that alcohol adducts of imidazolin-2-ylidenes can be used to generate the free carbene “in situ” to form NHC-coordinated transition metal complexes in a greatly simplified process (Figure 28). Hedrick et al. have recently showed that these alcohol adducts can be isolated and used directly as both catalysts and initiators for the ROP of lactones [73, 75].

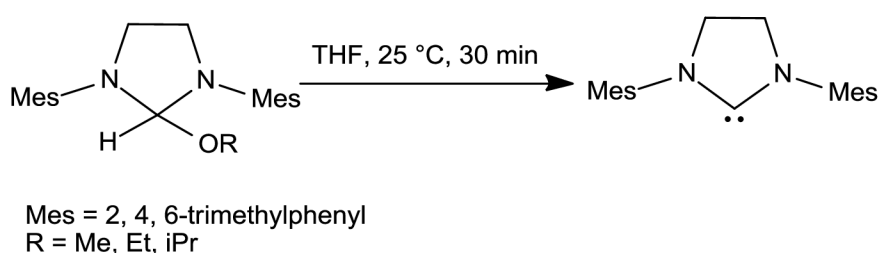


Figure 28 Elimination of alcohol from methoxyimidozolin-2-ylidene.

It is known that NHCs are versatile ligands for transition metals as well as potent nucleophilic organic catalysts for a wide variety of organic transformations. It was found that structural and electronic variations significantly affected the carbene activity, which could be correlated with the carbene basicity. Sterically demanding and electron-withdrawing substituents of NHCs dramatically decrease their activity as well as the thiazole-based carbenes in comparison with their imidazole-based analogues. The saturated/unsaturated nature of the NHC backbone has no appreciable

influence [46]. The rates and selectivity for ROP depend on both the nature of the NHC and the monomer. For example, while the 1,3-bis(2,4,6-(trimethylphenyl)imidazol-2-ylidene) (**1**, IMes) is very active for the ROP of lactide, it is much less active for the ROP of ϵ -caprolactone [76]. In Table 2 a summary of NHCs catalyzed ROP with respect to the used type of NHCs, monomers, initiators and polymerization conditions is presented. Based on the literature, twelve NHCs structures were studied for ROP of LA, CL, VL and BL. The most studied NHC catalysts include IMes (**1**), 1,3,4-triphenyl-4,5-dihydro-1H-1,2-triazol-5-ylidene (**5**) and 1,3-dimethylimidazol-2-ylidene (**7**).

The polymerization behavior of NHCs is sensitive to the ratio of catalyst to initiator (C/I) and monomer concentration. C/I ratios ranging from 0.25 to 1.5 and 1 mol·dm⁻³ lactide solutions were found to be optimal for $DP > 100$, leading to M_w/M_n lower than 1.15, whereas much lower C/I ratios of about 0.01 – 0.02 and 2 mol·dm⁻³ lactide solutions were preferred to obtain oligomers ($DP \sim 10$) with low M_w/M_n (< 1.16). Higher concentrations or catalyst to initiator ratios led to broadened M_w/M_n . Polymerization can be carried out in dichloromethane, tetrahydrofuran and toluene, without significant modification of the polymerization rate [46, 70].

The NHC-catalyzed polymerization can be proposed by two types of mechanisms including a monomer-activated mechanism in which the nucleophilic carbene activates the cyclic ester to form an acyl-imidazolium intermediate for transesterification to the growing polymer chain and chain-end activated mechanism, whereby the NHC activates the alcohol toward nucleophilic attack [40].

A key feature of the monomer-activated mechanism (Figure 29) is the formation of a zwitterionic acylimidazole intermediate generated from nucleophilic attack of the NHC on the cyclic monomer. The protonation of the intermediate by the alcohol initiator is followed by attack of the resulting alkoxide on the activated acyl intermediate and displacement of the NHC catalyst. The resultant hydroxyl-terminated monomer unit serves as the nucleophilic alcohol in subsequent propagation. The generated polyester bears the ester from the initiating alcohol as the R-chain end and a hydroxyl group as the ω -chain end [76]. Polymerization can be terminated by deactivation of the carbene with addition of acetic acid, CO₂ or CS₂, the latter of which forms a zwitterionic species that is readily removed from polymer upon precipitation [70].

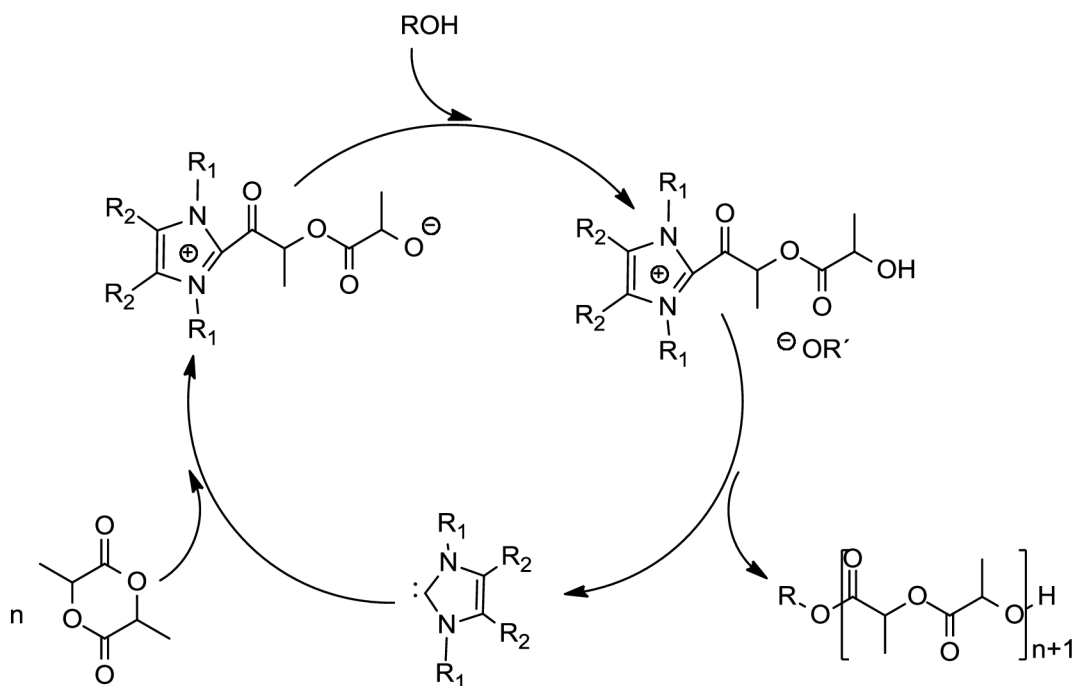


Figure 29 Proposed mechanism for the ROP of lactide in the presence of carbene and alcohol.

It was found that the polymerization of lactide by NHCs without the alcohol yields cyclic PLAs of defined molecular weight [78]. The proposed mechanism for these reactions (Figure 30) involves nucleophilic attack of the carbene initiator to generate a zwitterionic intermediate. Addition of monomers to the zwitterion leads to chain growth by generation of higher zwitterions; macrocyclization of the zwitterions generates cyclic PLAs with liberation of the carbene [78]. The polymerization of rac-lactide with IMes occurs rapidly (5 – 900 s) at room temperature to yield PLAs with molecular weights from 7 to 26 000 g·mol⁻¹ [78].

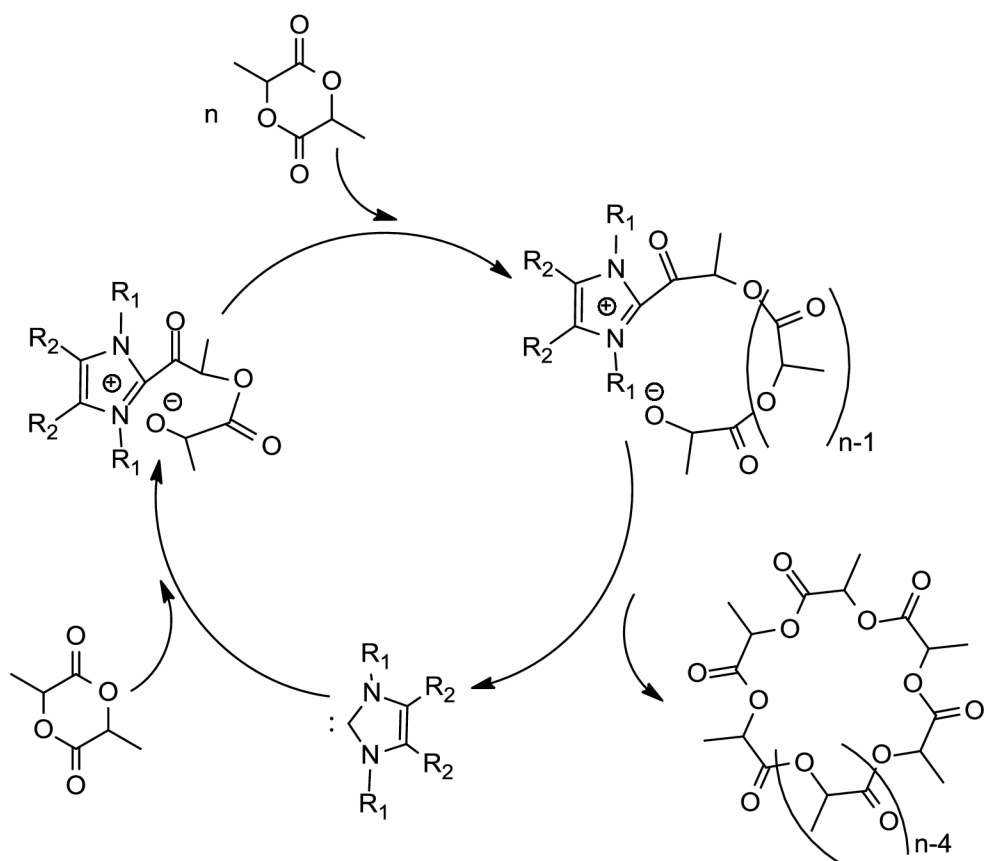
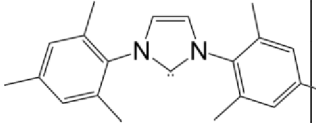
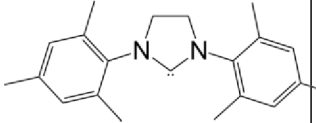
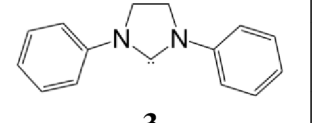
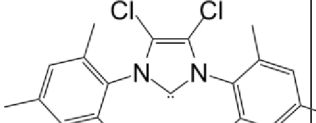
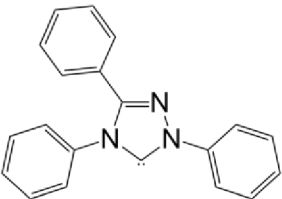
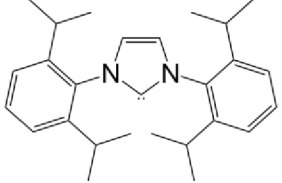
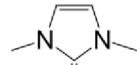
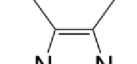
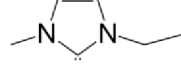
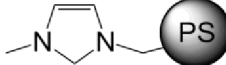


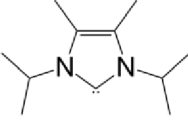
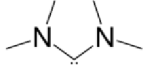
Figure 30 Proposed zwitterionic polymerization of lactide to generate cyclic polylactide.

Table 2 N-heterocyclic carbene catalyzed ring-opening polymerization.

Catalyst	Momomer	Initiator	T [°C]	[M] [mol·dm ⁻³]	I/C	M/I	t [h]	DP	Yield [%]	M _w /M _n	Ref.
 1	LA	BnOH	20 ^a	0.16	1.50	200	0.25	173	85	1.18	70
	L-LA	BnOH	25 ^a	1.00	1.50	50	2.00	47	90	1.12	80
	L-LA	BnOH	25 ^a	1.00	1.50	100	2.00	92	92	1.15	80
	L-LA	BnOH	25 ^a	1.00	1.50	200	2.00	110	60	1.08	80
	L-LA	PBuOH	25 ^a	1.00	1.50	30	2.00	30	99	1.11	80
	L-LA	BnOH	25 ^a	2.00	0.02	10	2.00	12	98	1.16	80
	L-LA	BnOH	25 ^a	2.00	0.01	10	2.00	11	98	1.10	80
	ε-CL	BnOH	25 ^a	2.00	2.00	50	24.00	-	10	-	76
	ε-CL	BnOH	25 ^a	-	0.50	60	24.00	56	99	1.30	80
	ε-CL	6-arm PPG	25 ^a	-	0.50	40 per arm	24.00	35	95	1.15	80
	ε-CL	BnOH	25 ^a	-	0.50	100	24.00	97	99	1.33	80
	β-BL	PBuOH	25 ^a	-	1.50	50	24.00	44	90	1.15	80
	 2	LA	BnOH	20 ^a	0.16	1.50	200	0.25	190	99	1.23
 3	LA	BnOH	20 ^a	0.16	1.50	200	0.25	197	99	1.46	70
	ε-CL	BnOH	-	-	-	100	0.50	98	99	1.55	72
	δ-VL	BnOH	-	-	-	108	0.50	105	99	1.52	72
 4	L-LA	BnOH	20 ^a	0.16	1.50	200	0.25	-	15	-	70

Catalyst	Momomer	Initiator	T [°C]	[M] [mol·dm ⁻³]	I/C	M/I	t [h]	DP	Yield [%]	M _w /M _n	Ref.	
 <p style="text-align: center;">5</p>	L-LA	PBuOH	50 ^a	1.00	-	100	89.00 167.00 306.00	20 16 17	44 59 88	MMD	75	
	L-LA	PBuOH	90 ^b	1.00	-	100	2.60 17.70 44.20 94.80	19 58 69 71	16 67 80 85	1.08 1.17 1.08 1.09	75	
	L-LA	MeOH	90 ^b	1.00	-	42	4.30 5.80 17.50	41 38 37	97 96 98	1.13 1.27 1.29	75	
	L-LA	PEG	90 ^b	1.00	-	100	63.00	-	88	1.17		
	L-LA	PS40-OH	90 ^b	1.00	-	25	15.00	-	93	1.14	75	
	L-LA	PS70-OH	90 ^b	1.00	-	25	15.00	-	92	1.05	75	
	L-LA	PMMA140-OH	90 ^b	1.00	-	100	14.00	-	25	1.15	75	
	L-LA	PDMAEMA100-OH	90 ^b	1.00	-	100	14.00	-	27	1.30	75	
	β-BL	PBuOH	80 ^b	1.00	-	100	25	3.00	-	95	1.19	
							50	4.50	-	92	1.09	
							100	5.40	-	81	1.11	75
							200	14.00	-	89	1.15	
	β-BL	PBuOH	80 ^b	1.00	-	100	300	24.00	-	92	1.10	
							200	14.00	-	89	1.15	
							300	24.00	-	92	1.10	
	β-BL	PEG(2000) monomethyl ether	90	1.00	-	100	-	-	-	1.02	75	

Catalyst	Momomer	Initiator	T [°C]	[M] [mol·dm ⁻³]	I/C	M/I	t [h]	DP	Yield [%]	M _w /M _n	Ref.
 6	L-LA	BnOH	25 ^a	0.16	1.50	200	0.25	185	92	1.18	72
	ε-CL	BnOH	25 ^a	0.50	2.00	100	24.00	-	0	-	76
 7	β-BL	BnOH	25 ^a	-	-	200	3.00	192	100	1.04	72
	δ-VL	BnOH	25 ^a	-	-	200	3.00	185	98	1.32	72
	ε-CL	BnOH	25 ^a	-	-	200	6.00	188	98	1.16	
	ε-CL	BnOH	25 ^a	-	-	20	2.00	20	100	1.32	72
	ε-CL	PEG(1900) monomethyl ether	25 ^a	-	-	100	-	-	-	1.22	
	ε-CL	PEG(1900) monomethyl ether	25 ^a	-	-	150	-	-	-	1.30	72
	ε-CL	PEG(1900) monomethyl ether	25 ^a	-	-	200	-	-	-	1.24	
CL/LLA	BnOH	25 ^a	-	-	-	2.00 (CL) + 12.00 (LLA)	-	-	1.38	72	
LA	BnOH	25 ^a	-	-	200	1.00	123	60	1.16	72	
 8	ε-CL	BnOH	25 ^a	1.00	-	200	6.00	194	99	1.40	72
	ε-CL	BnOH	25 ^a	1.00	2.00	200	0.03	21	18	1.11	76
	ε-CL	BnOH	25 ^a	1.00	2.00	200	3.33	76	63	1.14	76
 9	LA	BnOH	25 ^a	-	1.50	200	0.25	194	97	1.31	72
 10	LA	BnOH	25 ^a	-	1.50	200	1.00	190	95	1.52	72

Catalyst	Momomer	Initiator	T [°C]	[M] [mol·dm ⁻³]	I/C	M/I	t [h]	DP	Yield [%]	M _w /M _n	Ref.
 11	ε-CL	ethylene glycol	25 ^a	1.00	2.00	100	1.00	254	95	1.37	76
	ε-CL	1,1,1-tris(hydroxymethyl)propane	25 ^a	0.50	2.00	100	1.70	255	90	1.15	76
	ε-CL	2,2-bis(hydroxymethyl)1,3-propanediol	25 ^a	0.50	2.00 8.00	100	0.75	190 130	90 60	1.24 1.09	76
	ε-CL	BnOH	25 ^a	0.90	1.00	200	0.17	53	21	1.19	76
	ε-CL	BnOH	25 ^a	0.90	2.00	200	0.17 1.55 5.00	30 150 285	12 47 77	1.20 1.16 1.30	76
 12	LA	BnOH	70 ^a	-	1.50	100	3.00	70	76	1.09	81

Polymerizations were carried out in ^a THF or ^b toluene.

MMD – multimodal distribution, BnOH – benzyl alcohol, MeOH – methanol, PDMAEMA - poly(*N,N*-dimethylaminoethyl methacrylate), PMMA - poly(methyl methacrylate), PBuOH - 4-pyrene-1-butanol, PS – polystyrene, PEG - poly(ethylene glycol).

2.4 Smart Hydrogels

Hydrogels are three-dimensional cross-linked networks which have the ability to hold water within the spaces available among the polymeric chains. They can be classified into two groups depending on the nature of the crosslinking reaction. If the crosslinking reaction involves formation of covalent bonds, then the hydrogels are termed as permanent hydrogel. If the hydrogels are formed due to the physical interactions, g.e. molecular entanglement, ionic interaction and hydrogen bonding among the polymeric chains, then the hydrogels are termed as physical hydrogels. Hydrogels can also be categorized as conventional and stimuli responsive hydrogels [82]. This part of review will focus just on stimuli responsive hydrogels, so called “smart hydrogels”.

Stimuli responsive hydrogels are polymers that undergo reversible large, physical or chemical changes in response to small external changes in the environmental conditions, such as temperature, pH, light, magnetic or electric field, ionic factors, biological molecules, etc. [83]. These hydrogels have very promising applications in the biomedical field as delivery systems of therapeutic agents, tissue engineering scaffolds, cell culture supports, bioseparation devices, sensors or actuators systems [84]. This chapter is focused on temperature sensitive polymers.

Temperature-responding polymers present a fine hydrophobic-hydrophilic balance in their structure, and small temperature changes around the critical temperature, make the chains to collapse or to expand responding to the new adjustments of the hydrophobic and hydrophilic interactions between the polymeric chains and the aqueous media. One of the polymers that exhibits temperature-sensitive properties hydrogels is a triblock copolymer (ABA-type) composed of poly(D,L-lactic acid-co-glycolic acid) (A-block) as the hydrophobic segment and poly(ethylene glycol) (B- block) as the hydrophilic segment. These copolymers were first prepared by Zentner et al. [85]. They are very attractive because of its biodegradability, biocompatibility, and ease of formulation and application. PLGA–PEG–PLGA hydrogels has been developed as a biologically degradable system for drugs delivery carries. They were used to produce many different commercial products, such Regel® and OncoGel®. The copolymer aqueous solutions exhibit sol-to-gel-to-sol phase transition with increasing temperature. Their phase diagram and gelation mechanism will be discussed in more details.

2.4.1 Phase Diagrams

Biodegradable block copolymers prove thermogelling abilities and exhibit a phase transition behavior. Amphiphilic PLGA–PEG–PLGA triblock copolymers showed two phase transitions from sol to gel and gel to sol with increasing temperature [86]. The phase diagrams of these triblock copolymers in water demonstrate a critical gel concentration (CGC), a critical gelation temperature (CGT), a lower transition temperature curve from sol to gel and an upper transition temperature curve from gel to sol [87]. The hydrogels presented three basic physical states: solution, gel, and precipitate. The gel window can be composed of two regions, translucent gels and opaque gels [88]. Figure 31 shows typical phase diagram of PLGA–PEG–PLGA triblock copolymer in water. The diagram will be described in more detail in the following part.

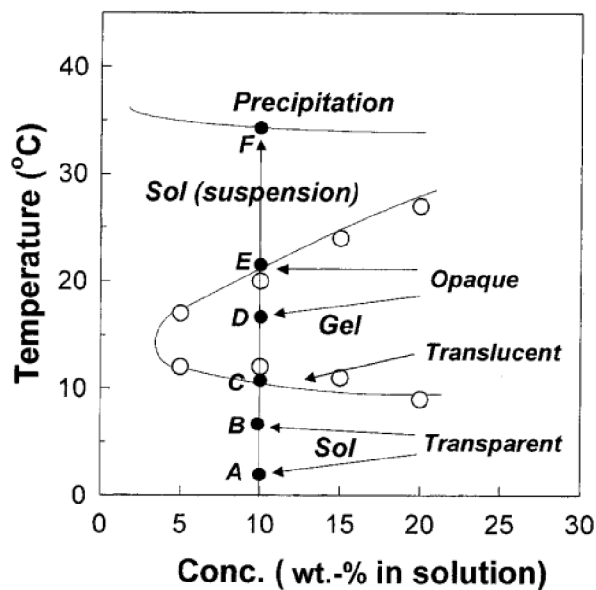


Figure 31 Phase diagram of PLGA-PEG-PLGA copolymers in water [89].

2.4.2 Mechanism of Gelation

Micelle formation and micellar behavior of the copolymer are dependent on the molecular structure and its hydrophobic/hydrophilic balance, which plays an important role in the gelation of ABA-type copolymer in water. In aqueous solution polymeric micelles have core-shell structure for PLGA-*b*-PEG-*b*-PLGA copolymers: hydrophobic PLGA blocks forms core and hydrophilic PEG blocks forms shell [89]. For this type of copolymer two theories to explain the sol-gel and gel-sol transition were published.

Shim et al. suggested PLGA-*b*-PEG-*b*-PLGA triblock copolymers micellar topology and micellar bridging gelation mechanism. They characterized micellar topology in aqueous solution of the copolymer by the micellar size and distribution as a function of temperature measured by dynamic laser scattering. The smallest micelles (unimers) had a size below 5 nm. At temperature lower than the CGT individual micelle of about 10 nm and grouped micelle >20 nm (bridged structures of micelles) were observed. If the temperature was increased, the size of the individual micelles does not change much because the associated number in a micelle is independent on temperature but determined by molecular structure. On the other hand, the size of the grouped micelles increases gradually to 41 nm. This indicates that the grouped micelle expands through bridging individual micelles. When temperature is raised the peak grows up dramatically to 95 nm, and becomes wider and larger [89].

The temperature-dependent micellar bridging gelation mechanism is schematically illustrated in Figure 32. At a lower temperature than CGT unimers, individual micelles, and grouped micelles coexist in the sol state (see Figure 31A) and Figure 32A). The fraction of unimer decreases with temperature (see Figure 31B) and Figure 32B). The size of grouped micelle grows rapidly resulting in sol-gel transition (see Figure 32C). The aggregation and packing interaction between micelles increases to form more dense gel by raising temperature (see Figure 32 D), while the gel changed from translucent to opaque (C and D in Figure 31). If the temperature was raised further, the hydrophobic chains in the micelle core shrink tightly and the hydrophilic PEG block underwent dehydration. The shrunk micelle groups are

restored from the tight aggregation and strong packing interaction, and tend to flow in water and gel-sol transition begins see Figure 31 E) and Figure 32 E). Above the second gel-sol transition the solution became two separated parts of water and polymer see Figure 31 F) and Figure 32 F) [89].

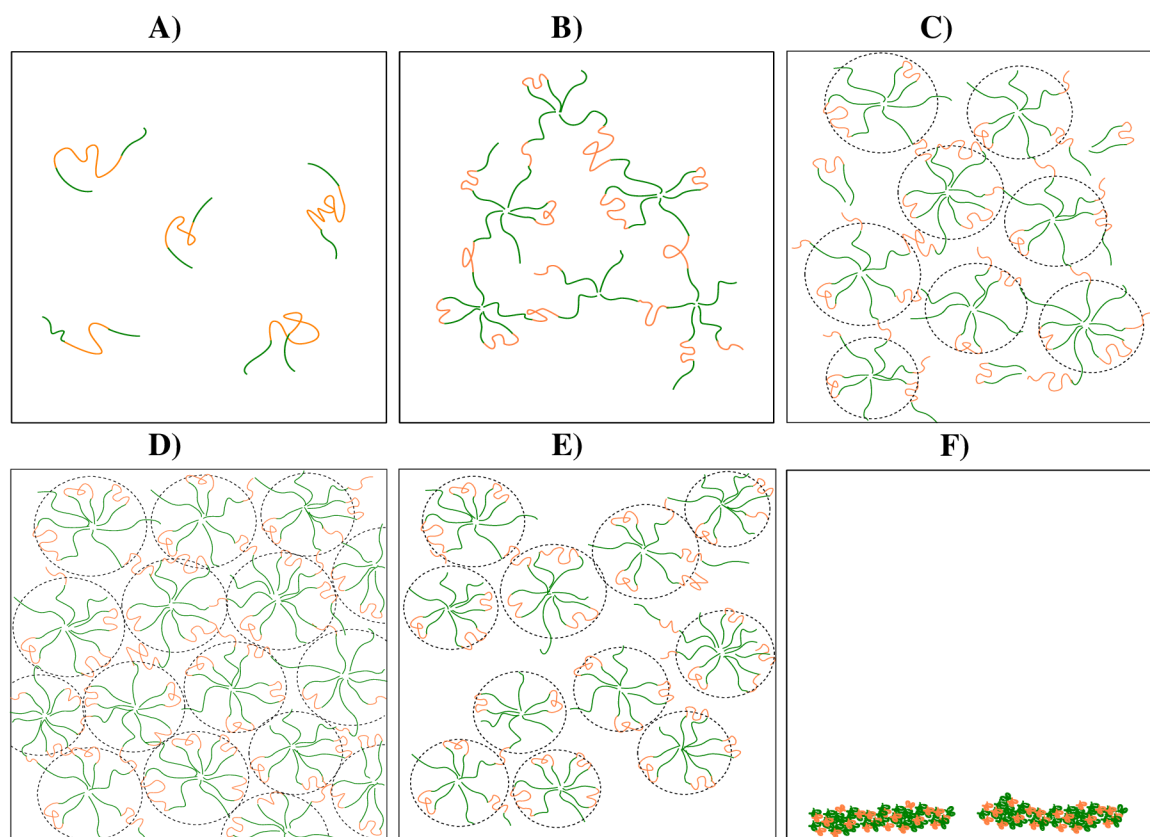


Figure 32 Schematic diagram of the micellar gelation mechanism for PLGA-PEG-PLGA copolymer in aqueous solution [89].

Another principle of gelation described Yu et al. [88]. They supposed that linked micelles are already in solution phase. Therefore, gel formation cannot be adequately explained only bridging between micelles. In solution the amphiphilic block copolymers are aggregated into micelles via self-assembly see Figure 33 A). At gradual increase in a temperature the micelles are further percolated to form a macroscopic gel with an inhomogeneous micelle network. The phase transition of sol-gel is achieved intact micellar structure see Figure 33 B). When the hydrophobic force is so strong that it can induce macroscopic self-assembly of the micelles, the sol-gel transition thus happens. The micelle network might be coarsened with a further increase in the temperature see Figure 33 C). When the size of the micelle clusters or the interval between the micelle clusters falls in the range of the wavelength of visible light, the gel might be opaque to the eye. It is also possible that the micelles are not spherical in gel formation and evolution, or alternatively, a micelle cluster could be a large deformed micelle. Precipitates must occur when the micellar structure is broken due to the over hydrophobicity of the block copolymers at higher temperatures see Figure 33 D) [88].

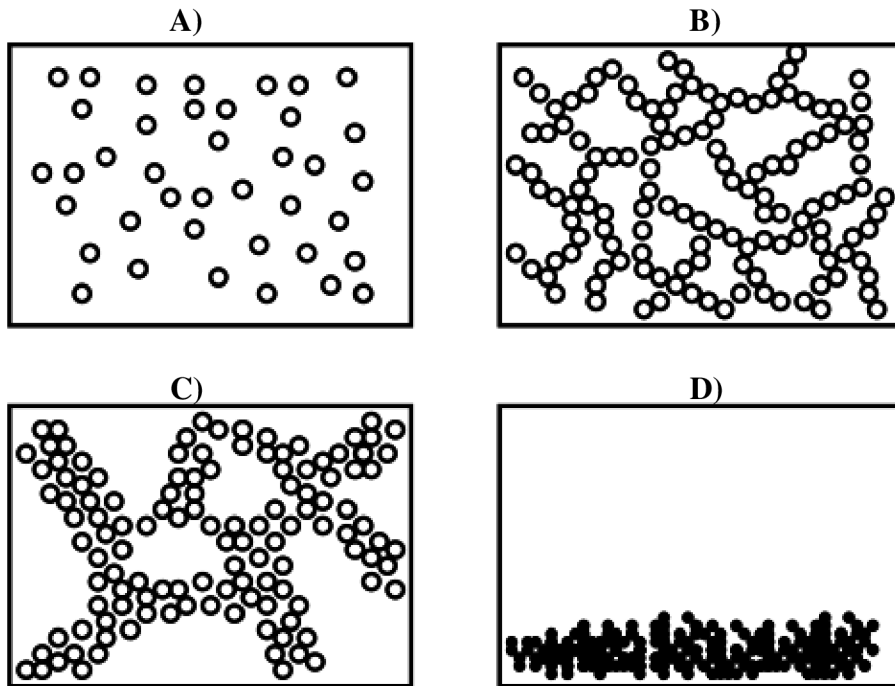


Figure 33 Schematic diagram of a spontaneous thermogelling mechanism of PLGA-PEG-PLGA copolymers in water via a micelle network [88].

3. Main Goal of the Thesis

The main aim of proposed dissertation work is the synthesis of selected free N-heterocyclic carbenes and the study of their potential as the nucleophilic organocatalysts for ring opening polymerization of lactide and lactone in order to prepare well-defined polymer materials with controlled molecular weight, polydispersity index and end-groups. The next goal of proposed work is evaluation of prepared free NHCs for the synthesis and characterization of thermosensitive triblock poly(D,L-lactic acid-co-glycolic acid)-b-poly(ethylene glycol)-b-poly(D,L-lactic acid-co-glycolic acid) (PLGA-PEG-PLGA) copolymers. Synthesized polymers will be studied with respect to their chemical and physical properties. The optimization of reaction conditions in order to achieve living type of ring opening polymerization of cyclic esters will be characterized on molecular level. The sol-gel transition behaviors (both critical gel temperature and critical gel concentration) of amphiphilic polymer hydrogels will be evaluated both by the test tube inverting method and by the dynamic rheological analysis. Finally, behaviors of copolymers prepared with free carbene catalysts will be confirmed with copolymers synthesized using common tin catalyst.

4. Experimental Part

4.1 Chemicals

- 1,3-di-*tert*-butyl-1H-imidazol-3-ium chloride (NHC) purchased from Rhodia Company (Lyon, France) and used as received.
- Butyllithium (BuLi, 1.6 mol·L⁻¹ solution in hexane) purchased from Sigma-Aldrich and used as received.
- Calcium hydride (CaH₂, coarse granules, < 20 mm, reagent grade, 95 %) was purchased from SigmaAldrich, Germany and used as received.
- D, L – lactide (≥ 99.9 %) was purchased from Polysciences inc., Pennsylvania
- Dimethyl sulfoxide (DMSO, p.a.), ordered from Penta, Czech Republic, was dried by CaH₂ and then freshly distilled prior to use.
- Gaseous nitrogen (99.999 %, SIAD Czech spol. s r.o.) was refined over the drying column filled with molecular sieves and Cu catalyst.
- Glycolide (≥ 99.9 %) was purchased from Polysciences inc., Pennsylvania and was purified by sublimation under vacuum at 60 °C.
- Chloroform-d (99.8 Atom % D) for NMR spectroscopy was purchased from ISOSAR GmbH, Germany.
- L-lactide (≥99.9 %) purchased from Polysciences, Inc., Pennsylvania and was purified by sublimation under vacuum at 60 °C.
- Liquid nitrogen was purchased from Linde Gas, a.s., Czech Republic.
- Poly(ethylene glycol) (PEG1500, average $M_n = 1500 \text{ g}\cdot\text{mol}^{-1}$) purchased from SigmaAldrich was purified by degassing under vacuum for 3 hours at 130 °C.
- Potassium *tert*-butoxide (*t*-BuOK, 1 mol·L⁻¹ solution at THF) purchased from SigmaAldrich and used as received.
- Tetrahydrofuran (THF, p.a. ≥99.5 %) purchased from Lach-Ner s. r. o. (CZ) was dried by metal sodium wire and benzophenone and freshly distilled prior to use from the violet solution.
- Toluene (p.a. ≥99 %), purchased from Lach-Ner s. r. o. (CZ) was dried over CaH₂ and then freshly distilled prior to use.
- Ultrapure water (UPW of type II according to ISO 3696, Milli-Q quality) was prepared by Elix5 UV Water Purification System (Millipore,) at FCH BUT, CZ.
- Xylene (p.a. ≥99 %) purchased from Lach-Ner s. r. o. (CZ) was dried over CaH₂ and then freshly distilled prior to use.

4.2 Equipment

- All-glass high vacuum line (hand-made at BUT, Faculty of chemistry)
- Vacuum drying oven (Vacucell 22, BMT a.s., Czech Republic)
- Thermoblock TK 23 (DITABIS AG, Germany)
- Scale PB1502-S (Mettler-Toledo, s.r.o., Czech republic)
- Elix® Essential 5 (Merck Millipore Co., Germany)
- Analytical scale AB204-S (Mettler-Toledo, s.r.o., Czech republic)
- TGA Q500 (TA Instruments, USA)
- Differential scanning calorimeter 204 F1 (NETZSCH GmbH & Co, Germany)
- FTIR-ATR, Tensor 27 (Bruker Co., Germany)
- Christ Alpha 2-4 LSC freeze dryer (Martin Christ Gefriertrocknungsanlagen GmbH, Germany)
- Drying oven (Venticell 111, BMT a.s., Czech Republic)
- GPC Agilent Technologies 1100 Series instrument equipped with autosampler, RI and UV-VIS detector (Agilent Technologies, Inc., USA)
- Rheometer TA Instruments AR-2 (TA Instruments, USA)
- 700 MHz NMR spectrometer Bruker AVANCE III (Bruker Co., Germany)
- 500 MHz NMR spectrometer Bruker AVANCE III (Bruker Co., Germany)

4.3 Methods

All manipulations were carried out under a dry nitrogen atmosphere (99.999 %, Siad, CZ) using vacuum/inert manifold and standard Schlenk's techniques (Figure 34). Nitrogen was purified passing through the drying columns filled with molecular sieves and Cu catalysts to remove the traces of moisture and oxygen.



Figure 34 Vacuum line-manifold for experiments under inert atmosphere in Polymer Synthesis Laboratory at Faculty of chemistry BUT.

4.3.1 Characterization of Polymers

4.3.1.1 Proton Nuclear Magnetic Resonance (^1H NMR)

Molecular weight, composition ratios and polymer structure characterizations were recorded at 500 and 700 MHz Bruker AVANCE III instrument using 128 scans using CDCl_3 as solvent.

4.3.1.2 Gel Permeation Chromatography (GPC)

Number average molecular weights (M_n) and polydispersity index (M_w/M_n) of the polymers were determined by GPC method using Agilent Technologies 1100 Series instrument equipped with isocratic pump, autosampler, RI and UV-VIS detector, fraction collector, column thermostat up to 80 °C and 300×7.5 mm PLgel 5 μm MIXED B;C column. THF was used as mobile phase ($1.0 \text{ mL}\cdot\text{min}^{-1}$). The apparatus was calibrated with linear polystyrene standards, and THF was use as flow rate marker.

4.3.1.3 Thermogravimetric Analysis (TGA)

The thermal degradation of polymers was performed by thermogravimetric analysis on TA Instruments TGA Q500 using nitrogen as purge gas. Samples were heated from ambient temperature to 700 °C at a heating rate of 10 °C·min⁻¹ and nitrogen flow of 60 mL·min⁻¹.

4.3.1.4 Differential Scanning Calorimeter (DSC)

Glass transition temperatures (T_g) were measured by using NETZSCH differential scanning calorimeter 204 F1 (DSC). Copolymers were crimped in an open aluminum pan, cooled to – 40 °C and heated up to 160 °C for two times. Cooling and heating rates were 10 °C·min⁻¹ and steady stream of nitrogen gas was supplied at 50 mL·min⁻¹. Temperatures were obtained from second heating cycle by Proteus Analysis software.

4.3.1.5 Fourier Transformed Infrared Spectroscopy (FTIR)

FTIR spectra of NHC-*t*Bu free carbene catalyst were recorded in the region between 400 - 4000 cm⁻¹ (128 scans at 4 cm⁻¹ resolution) on a Bruker TENSOR 27 in the form of KBr pellets prepared in dry a box under nitrogen atmosphere (measured at Masaryk University in Brno).

4.3.1.6 Attenuated Total Reflectance Fourier Transformed Infrared Spectroscopy (ATR-FTIR)

IR spectra of triblock copolymers were confirmed by attenuated total reflectance Fourier transformed infrared spectrometer (ATR-FTIR) Bruker Tensor 27 with diamond ATR crystal in a range between 4000 – 600 cm⁻¹. All spectra (128 scans at 4 cm⁻¹ resolution) were recorded at laboratory temperature and evaluated by OPUS software.

4.3.1.7 Sol-gel Phase Transitions

The test tube inverting method (TTIM) was used to determinate the sol-gel phase transition temperature. The vials containing copolymer water solutions were immersed in a thermoblock HLC TK 23 BioTech at designated temperature for 7 min. Condition of flow (sol phase) or no flow (gel phase) were observed by inverting a vial vertically. The sample was regarded as a “gel” in the case of no visual flow within 30 s by inverting the vial with a temperature increment of 1 °C per step.

4.3.1.8 Dynamic Rheological Analysis

The sol-gel-suspension phase transitions and other visco-elastic properties of the copolymer aqueous solution were investigated by a dynamic stress-controlled rheometer (AR-2 TA Instruments) with Cone Plate geometry (angle 2°, 40 mm diameter and gap of 60 μm). Cold polymer solution (600 μl) was transferred to the Peltier (temperature control system) by micropipette. Before each measurement the solvent trap was filled with distilled water and the liquids were used to prevent evaporation of the sample.

4.3.2 Preparation of Free Carbene

4.3.2.1 General Procedure for "In situ" 1,3-di-*tert*-butylimidazol-2-ylidene Formation Using *Tert*-butoxide

In situ generation of NHC was performed in a specially designed glass reactor. To a dry activation part of the reactor equipped with a magnetic stirring bar, 44 mg of 1,3-di-*tert*-butylimidazolium chloride and 3.6 mL of tetrahydrofuran were introduced followed by potassium *tert*-butoxide (1 mol·L⁻¹ solution at THF, ratio NHC/*t*-BuOK = 1/0.9). Solution was stirred for 50 minutes to ensure the reaction between the carbene precursor and potassium *tert*-butoxide. A suspension was observed during this carbene formation period. The reaction mixture was then filtered through a sintered glass frit (S3) to the polymerization part of the reactor as light yellow solution.

4.3.2.2 General Procedure for Preparation of 1,3-di-*tert*-butylimidazol-2-ylidene Using *tert*-butoxide

In a dry 100 mL Schlenk's flask, 3.1 g of 1, 3-di-*tert*-butylimidazolium chloride was suspended in 14.9 mL dry THF. The mixture was stirred at 23 °C and 15.7 mL of potassium *tert*-butoxide (1 mol·L⁻¹ solution at THF) was added. The reaction was stirred for 2 h. The reaction mixture was transferred via canula to filtration apparatus and filtered through celpure. The filter cake was washed with 20 mL of THF. The filtrate was concentrated under vacuum. To the crude product 20 mL of hexane was added, the obtained solution was kept at -18°C overnight. After that the solution was concentrated to one half. The brownish white crystals in the yield of 35 % (0.9 g) were recovered by decantation of mother liquor (removed by a syringe).

4.3.2.3 General Procedure for Preparation of 1,3-di-*tert*-butylimidazol-2-ylidene Using *Butyllithium*

Synthesis of free 1,3-di-*tert*-butylimidazol-2-ylidene carbene was performed in a sublimation apparatus. To the dry sublimation apparatus equipped with a magnetic stirring bar, 2.7 g (12.5 mmol) of catalytic precursor and 35.5 mL of dry tetrahydrofuran were introduced. The medium was heterogeneous. After cooling to -78 °C, 12.5 mL (20.0 mmol) of *n*-butyllithium solution (1.6 mol·dm⁻³ in *n*-hexane) was added dropwise over a period of 30 min. The brown reaction mixture was kept stirring and warming up to laboratory temperature. Then the solvent and light derivatives were stripping off under nitrogen. The free carben was isolated by sublimation at 40 °C (temperature of oil bath) under vacuum in the form of white powder in the yield of 38 % (0.9 g).

4.3.3 Polymerization of L-lactide

The polymers were prepared via ring opening polymerization (ROP) method in THF as a solvent.

4.3.3.1 *Catalyzed by NHC-*t*Bu Carbene Prepared “In Situ” Reaction*

In a typical reaction, PEG macroinitiator ($M_n = 1500 \text{ g}\cdot\text{mol}^{-1}$, 0.49 mmol) was placed in the two-neck round-bottom reaction vessel (25 mL) equipped with magnetic stirring bar. Prior the polymerization the PEG was degassed and dewatered at 130 °C for 3 h under the vacuum. After cooling down the PEG initiator, sublimated 6.82 mmol of L-lactide was added against the nitrogen flow and the reaction flask was kept for 30 min under the vacuum. Then 4.2 mL of THF ($\text{THF/LA} = 5 \text{ cm}^3\cdot\text{g}^{-1}$) was added to dissolve the initiator and monomer. Prepared THF solution of initiator and monomer was added to the polymerization part of the reactor containing solution of in situ formed free NHC-*t*Bu carbene. Reaction proceeded for 1 h.

4.3.3.2 *Catalyzed by Free NHC-*t*Bu Carbene*

PEG macroinitiator ($M_n = 1500 \text{ g}\cdot\text{mol}^{-1}$, 0.34 mmol) was placed in the two-neck round-bottom reaction vessel (25 mL) equipped with magnetic stirring bar. Prior the polymerization the PEG was degassed and dewatered at 130 °C for 3 h under the vacuum. After cooling down sublimated 8.61 mmol of L-lactide was added against the nitrogen flow and the reaction flask was kept for 30 min under the vacuum. Then 6.2 mL of THF ($\text{THF/LA} = 5 \text{ cm}^3\cdot\text{g}^{-1}$) was added. After dissolving the initiator and monomer, the solution of free NHC-*t*Bu carbene in THF was added to start up the polymerization. Reaction proceeded for 1 h.

4.3.4 **Synthesis of PLGA–PEG–PLGA Copolymers**

The PLGA–PEG–PLGA triblock copolymers (ABA type) were prepared via ring-opening polymerization of D,L-lactide with glycolide using poly(ethylene glycol) as macroinitiator and 1,3-di-*tert*-butylimidazol-2-ylidene as organocatalyst. Polymers were prepared under nitrogen atmosphere in glass reactor, which was purged by nitrogen and vacuum for three times prior the reaction.

In a typical reaction, PEG macroinitiator ($M_n = 1500 \text{ g}\cdot\text{mol}^{-1}$, 2.18 mmol) was placed in the two-neck round-bottom reaction vessel (25 mL) equipped with magnetic stirring bar. Prior the polymerization, the PEG was either degassed and dewatered at 130 °C for 3 h under the vacuum. After cooling down D,L-lactide (44.75 mmol) and glycolide (14.91 mmol) monomers were added against the nitrogen outflow and the reaction flask was kept for 30 min under the vacuum. Then 41 mL of THF ($\text{THF/LA} = 5 \text{ cm}^3\cdot\text{g}^{-1}$) was added. After dissolving initiator and monomer the solution of free NHC-*t*Bu carbene in THF was added to start up the polymerization. Reaction proceeded for 1 h.

5. Results and Discussion

5.1 Synthesis and Polymerization Behavior of 1,3-di-*tert*-butylimidazol-2-ylidene

A variety of techniques have been reported for the generation of free carbenes from more readily available precursors. These techniques were discussed into more detail in the literature review. The choice among various methods depends on the nature of the carbene as well as the compatibility of the generation method to the reaction of interest.

This thesis builds on my diploma thesis [92] and Fantišek Surman's diploma thesis [93], where we studied polymerization behavior of 1,3-di-*tert*-butyl imidazole-2-ylidene for polymerization of lactide and lactone. 1,3-di-*tert*-butylimidazol-2-ylidene (NHC-*t*Bu) was "In situ" generated by treatment of the corresponding imidazolium salts with potassium *tert*-butoxide (Figure 35).

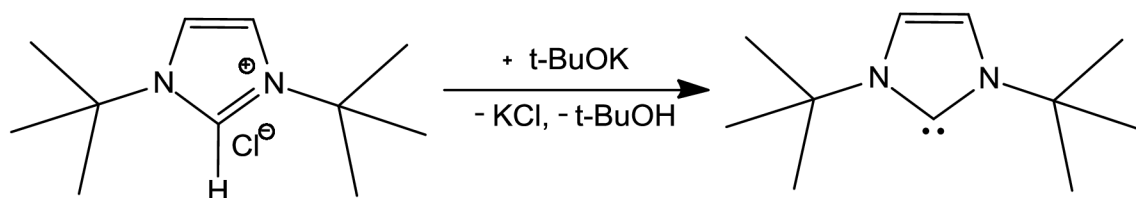


Figure 35 "In situ" generation of 1,3-di-*tert*-butylimidazol-2-ylidene free carbene using *t*-BuOK salt.

Based on previous studies it was found that the precursor salt, due to the presence of impurities, did not provide a defined system. From this reason it was not possible to ensure a quantitative response with *t*-BuOK and formation of equivalent amount of active centers. Therefore, at the beginning of my work I was focused on finding other ways for preparing NHC-*t*Bu.

Based on the literature review I have chosen both the procedure published by Denk [90] and also procedure published by Arduengo [91]. In the first case the reaction of imidazolium salt with butyllithium at a very low temperature (-78 °C) has been used for preparing NHC-*t*Bu (Figure 36).

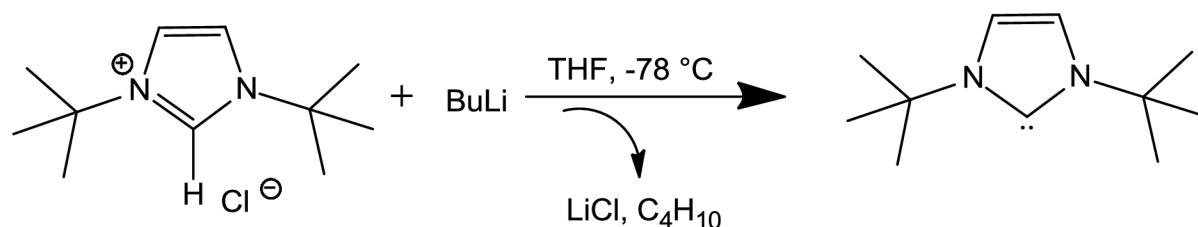


Figure 36 Schematic illustration of imidazolium salt reaction with butyllithium at low temperature to gain 1,3-di-*tert*-butylimidazol-2-ylidene free carbene.

In the second case the reaction of imidazolium salt with *t*-BuOK at laboratory temperature followed up by isolation of free carbene has been applied.

Starting (original) imidazolium salt and prepared NHC-*t*Bu via above mentioned three methods are shown in Figure 37.

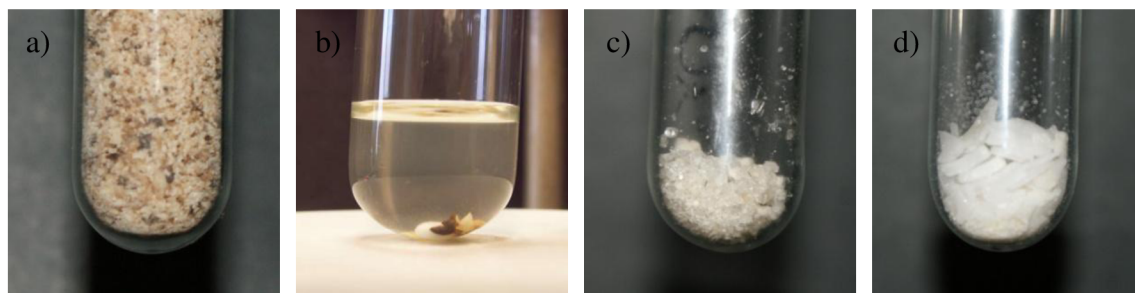


Figure 37 Photos of a) Starting imidazolium salt, b) NHC-*t*Bu generated “In situ” in THF, c) NHC-*t*Bu generated according to Arduengo, d) NHC-*t*Bu generated according to Denk.

Polymerizations of L-lactide were carried out to compare polymerization ability of free NHC-*t*Bu generated by three different ways:

- “In situ” reaction (sample 1)
- Using butyllithium (sample 2)
- Using *tert*-butoxide (sample 3)

All reactions proceeded in the presence of poly(ethylene glycol) ($M_n = 1500 \text{ g}\cdot\text{mol}^{-1}$) as macroinitiator and in THF at laboratory temperature. Since PEG has two hydroxyl functional groups at both α - and ω - ends thus P(L-LA)-*b*-PEG-*b*-P(L-LA) triblock copolymers were prepared. Figure 38 shows schema of triblock copolymer synthesis.

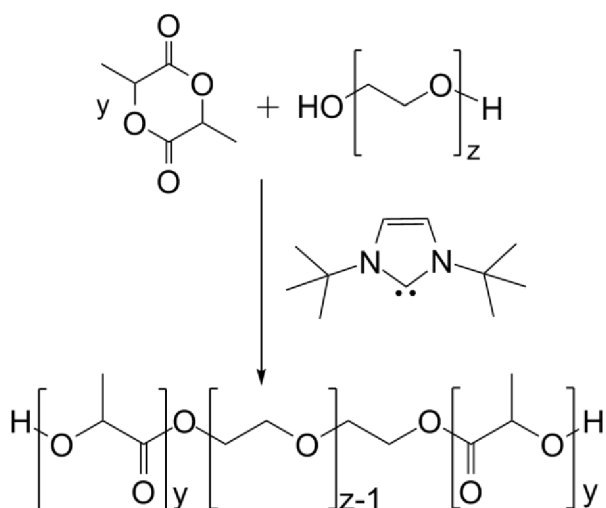


Figure 38 Synthesis of P(L-LA)-*b*-PEG-*b*-P(L-LA) triblock copolymers using NHC-*t*Bu free carbene.

The molecular weight and molecular weight distribution of the polymers were determined by GPC and ^1H NMR. Results are listed in Table 3.

Table 3 Properties of prepared polylactides.

Sample	[L-LA] ₀ [mol·dm ⁻³]	Yield ^a [%]	M _n ^b [g·mol ⁻¹]	M _n ^c [g·mol ⁻¹]	M _w /M _n ^b	M _n (theor)/ M _n (GPC)/M _n (NMR)
1	1.47	71	3496	4208	1.73	1.0/1.1/0.9
2	1.38	85	5562	4133	1.20	1.0/0.8/1.1
3	1.39	70	3278	3420	2.11	1.0/1.0/1.1

Conditions of polymerization: THF, $T_p = 23$ °C, $t_p = 1$ h, $[C]_0 = 0.1$ mol·dm⁻³, $[I]_0/[C]_0 = 1/2$, $[L-LA]_0/[I]_0 = 25$

^a Determined gravimetrically.

^b Determined by GPC against PS standards in THF.

^c Determined by ¹H NMR.

It is obvious that using NHC-*t*Bu generated by butyllithium (sample 2) the obtained P(L-LA)-*b*-PEG-*b*-P(L-LA) copolymer exhibited narrow polydispersity index ($M_w/M_n = 1.20$) controllable molecular weight and simultaneously high yield (85 %). Other L-LA polymerizations (sample 1 and 3) provided triblock copolymer with a relatively high yield (70 %), but also with higher polydispersity index ($M_w/M_n = 1.73$ and 2.11, respectively) corresponding to the change of the activity of polymer centers due to the presence of impurities and side reactions. Based on the results above, preparation of NHC-*t*Bu using butyllithium (see Figure 36) was selected for further work. 1,3-di-*tert*-butylimidazol-2-ylidene free carbene was prepared in the form of a white crystals with a conversion of 40 %. The structure was confirmed by ¹H NMR and FTIR analyses.

¹H NMR was measured in deuterated benzene (C₆D₆) under nitrogen atmosphere. In Figure 39 the spectrum confirms that peak with shifting $\delta = 1.59$ ppm corresponds to protons of CH₃ groups and a peak with shift $\delta = 6.86$ ppm belongs to groups of NCH protons. Furthermore, no other peaks of impurities were observed.

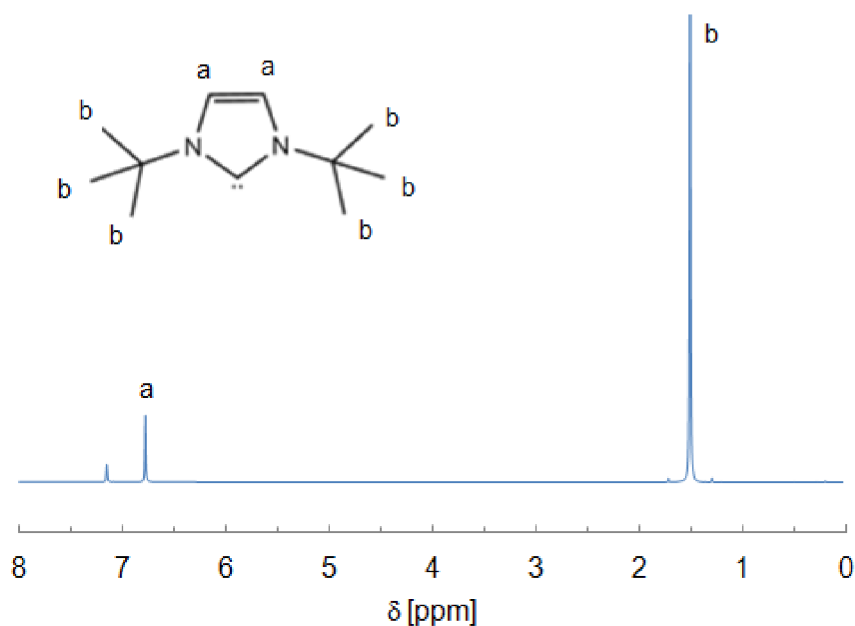


Figure 39 The measured ¹H NMR spectrum of 1,3-di-*tert*-butylimidazol-2-ylidene free carbene in C₆D₆ under nitrogen atmosphere.

The spectrum obtained by FTIR for 1,3-di-*tert*-butylimidazol-2-ylidene is presented in Figure 40. Table 4 gives the absorption bands of NHC-*t*Bu with their respective attributions. Thoroughly Eva Kulovaná was focused on the study of FTIR spectra of free carbene in her diploma thesis [94].

Table 4 Assignment of the absorption bands observed in the FTIR spectra of 1,3-di-*tert*-butylimidazol-2-ylidene (Nujol, KBr).

Experimental frequencies [cm ⁻¹]	Assignment	Experimental frequencies [cm ⁻¹]	Assignment
3110	=CH (wagging vibration)	1319	=C-N, CH ₃ - (stretching)
3073	=CH (wagging vibration)	1234	CH ₃ - CH, C-C (stretching)
2976	CH in CH ₃ - (stretching)	827	CH ₃ - (wagging vibration)
1462	CH ₃ - (stretching)	721	=CH (stretching)
1366	=CH, =C-N (stretching)	632	=CH (wagging vibration)

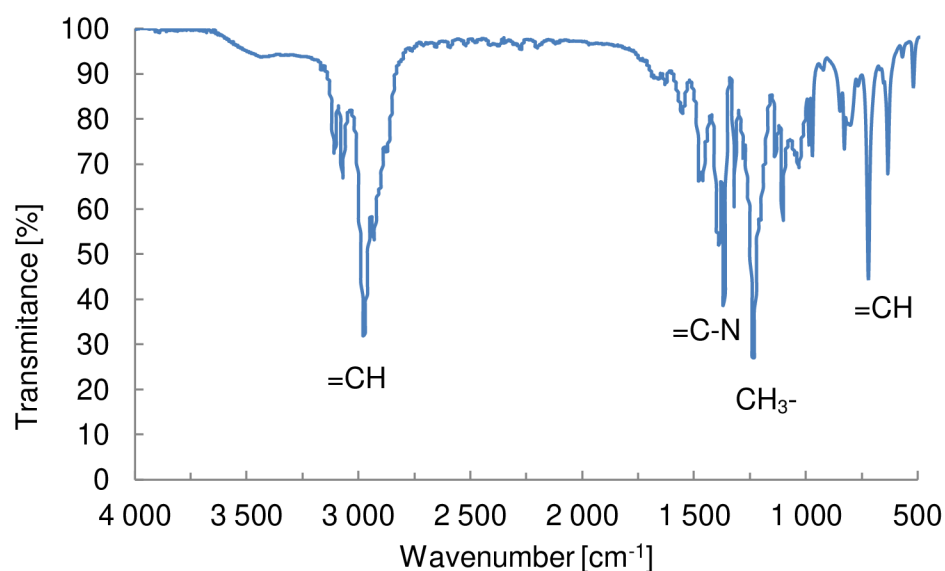


Figure 40 FTIR spectrum of 1,3-di-*tert*-butylimidazol-2-ylidene.

5.2 Polymerization of Cyclic Esters Using NHC/PEG Catalytic System

In earlier experiments it was shown that the studied NHC-*t*Bu created with PEG effective catalyst for ring opening polymerization of L-LA. Based on previous studies NHC-*t*Bu and PEG were tested for the polymerization of other cyclic esters, namely D,L-lactide (D,L-LA), glycolide (GA) and ϵ -caprolactone (CL). In all cases ABA triblock copolymer were obtained,

where A acts for certain cyclic ester and B for PEG. The results of each polymerization are shown in Table 5.

Table 5 Properties of prepared triblock copolymers.

Monomer	Yield ^a [%]	M_n^b [g·mol ⁻¹]	M_n^c [g·mol ⁻¹]	M_n^d [g·mol ⁻¹]	M_w/M_n	$M_{n(\text{theor})}/M_{n(\text{GPC})}/M_{n(\text{NMR})}$
L-lactide	85	5562	4133	4338	1.20	1.0/0.8/1.0
D,L-lactide	70	3176	4660	3675	1.28	1.0/1.2/0.8
ϵ -caprolactone	71	3929	2329	3728	1.88	1.0/0.9/1.6
glycolide	83	3019	N.D.	4358	1.07	1.0/1.4/-

Conditions of polymerization: THF, $T_p = 23$ °C., $t_p = 5$ min, $[C]_0 = 0.1$ mol·dm⁻³, $[I]_0/[C]_0 = 1/2$,

^a Determined gravimetrically.

^b Determined by GPC against PS standards in THF.

^c Determined by ¹H NMR.

^d Calculated from initial molar ratio $[M]_0/[I]_0 \times M_w(\text{monomer}) \times \text{conversion yield}$.

N.D. = not detected, due to poor solubility of the copolymer.

The catalytic efficiency of NHC-*t*Bu toward ROP of D,L-LA, GA and CL was demonstrated. Polymers were synthesized within 5 minutes at room temperature with high yield.

P(L-LA)-*b*-PEG-*b*-P(L-LA) triblock copolymer was prepared with the highest conversion of monomer (85 %) and narrow polydispersity index ($M_w/M_n = 1.20$). Similar polydispersity index ($M_w/M_n = 1.28$) and a little bit lower conversion (70 %) showed synthesized P(D,L-LA)-*b*-PEG-*b*-P(D,L-LA) triblock copolymer. For both L- and D,L- forms of polylactide M_n calculated from ¹H NMR spectra was in a very good agreement with M_n found by GPC as well as with theoretically calculated M_n of polymer showing the catalyst efficiency ($M_{n(\text{theor})}/M_{n(\text{GPC})}$) higher than 80 %. However, polymerization of L-lactide exhibited better polymerization results than D,L- form, which could be due to the regular structure of L-lactide. ¹H NMR spectroscopy was used to characterize both forms of prepared polylactides (Figure 41). Characteristic peaks of lactic acid protons were found in range between $\delta = 1.38 - 1.66$ ppm [multiplet, 3H, (O-(CH₃)CHO)] (d) and $\delta = 5.10 - 5.29$ ppm [multiplet, 1H, (O-(CH₃)CHO)] (a). Peak of PEG protons were found in a range between $\delta = 3.55 - 3.75$ ppm [multiplet, 3H, (OCH₂CH₂O)] (c). The peak in the area of $\delta = 1.67$ ppm (unmarked) belongs to protons of residual organic catalyst. The peak assigning to residual protons of the deuterated chloroform solvent was found at $\delta = 7.25$ ppm.

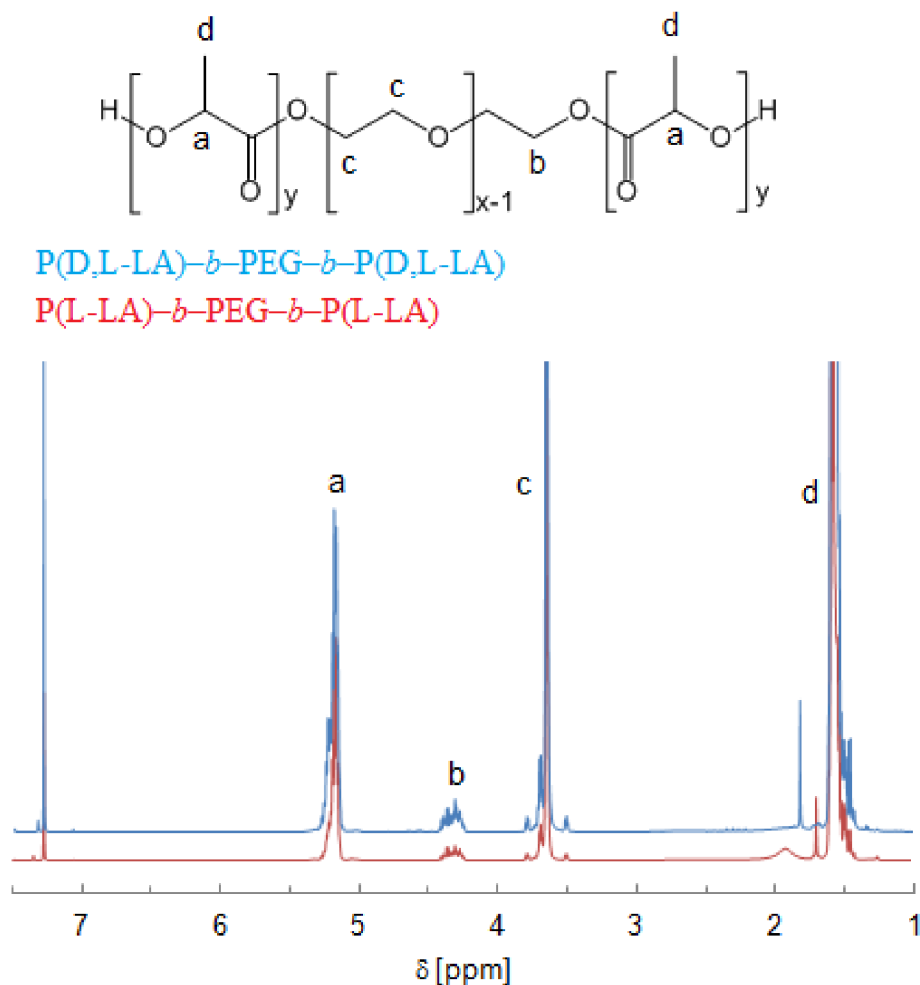


Figure 41 Obtained ^1H NMR spectra of $\text{P(L-LA)-}b\text{-PEG-}b\text{-P(L-LA)}$ and $\text{P(D,L-LA)-}b\text{-PEG-}b\text{-P(D,L-LA)}$ triblock copolymers prepared via ROP using NHC-tBu at room temperature in 5 minutes in THF.

Prepared $\text{PGA-}b\text{-PEG-}b\text{-PGA}$ triblock copolymer showed very narrow polydispersity index ($M_w/M_n = 1.07$) with high conversion (83 %) of glycolide monomer. Polyglycolide-based triblock copolymer was characterized by ^1H NMR spectroscopy with a spectrum shown in Figure 42. A characteristic peak of glycolic acid protons was found in a range between $\delta = 4.78 - 4.88$ ppm [multiplet, 2H, (OCH_2O)] (a) and peak of PEG protons in a range between $\delta = 3.45 - 3.85$ ppm [multiplet, 3H, $(\text{OCH}_2\text{CH}_2\text{O})$] (c). The peaks in the area of $\delta = 1.70$ and $\delta = 1.80$ ppm (unmarked) belong to protons of residual organic catalyst. The peak assigning to residual protons of the deuterated chloroform solvent was found at $\delta = 7.27$ ppm.

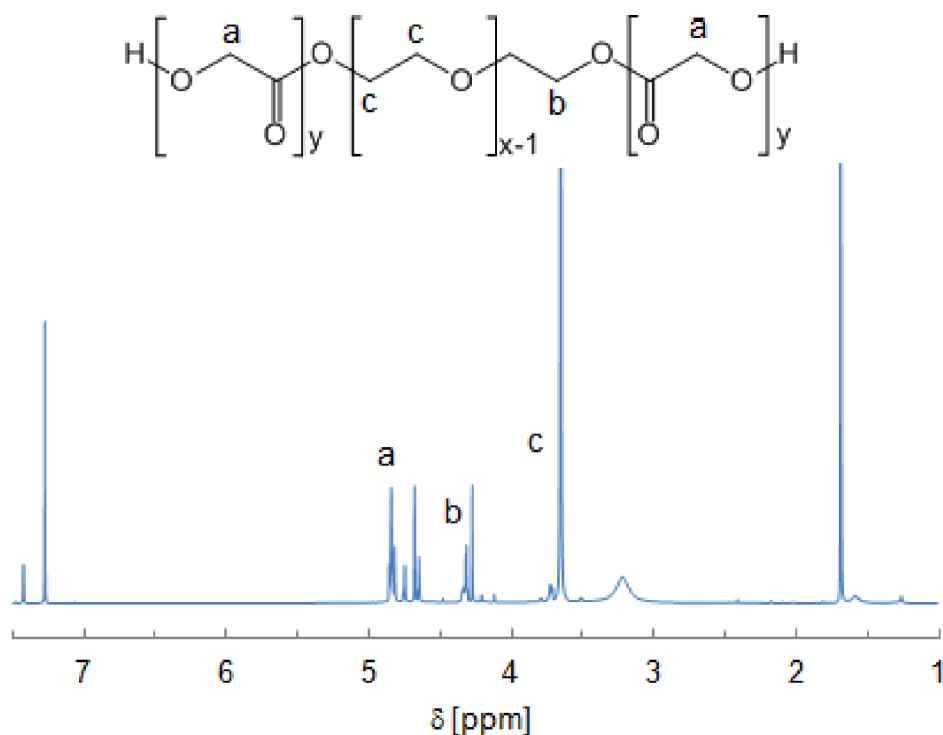


Figure 42 Obtained ^1H NMR spectrum of $\text{PGA-}b\text{-PEG-}b\text{-PGA}$ prepared via ROP using $\text{NHC-}t\text{Bu}$ at room temperature in 5 minutes in THF.

Prepared $\text{PCL-}b\text{-PEG-}b\text{-PCL}$ triblock copolymer had quite high conversion (71 %) but the highest polydispersity index ($M_w/M_n = 1.88$), probably due to side reactions such as inter- or intra-molecular transesterification and formation of cyclic oligomers. It is known that the efficiency of the ROP of $\epsilon\text{-CL}$ is very sensitive to the steric and electronic nature of the carbene [76, 95]. In the future work it will be better to use another type of carbene catalyst for the preparation of PCL-base copolymers with narrow polydispersity index. ^1H NMR spectrum of $\text{PCL-}b\text{-PEG-}b\text{-PCL}$ copolymer is shown in Figure 43. Characteristic peaks of $\epsilon\text{-caprolactone}$ were found in range between $\delta = 1.33 - 1.44$ ppm [m, 2H, (-CH₂-)] (f), $\delta = 1.60 - 1.70$ ppm [m, 4H, (-CH₂-)] (e), $\delta = 2.27 - 2.34$ ppm [t, 2H, (-CH₂CO-)] (d) and $\delta = 4.01 - 4.08$ ppm [t, 2H, (-CH₂O-)] (b). Peak of PEG protons were assigned in a range between $\delta = 3.58 - 3.72$ ppm [multiplet, 3H, (OCH₂CH₂O)] (c). The peak in the area of $\delta = 1.67$ ppm (unmarked) belongs to protons of residual organic catalyst. The peak belonging to the residual protons of the deuterated chloroform solvent was found at $\delta = 7.27$ ppm.

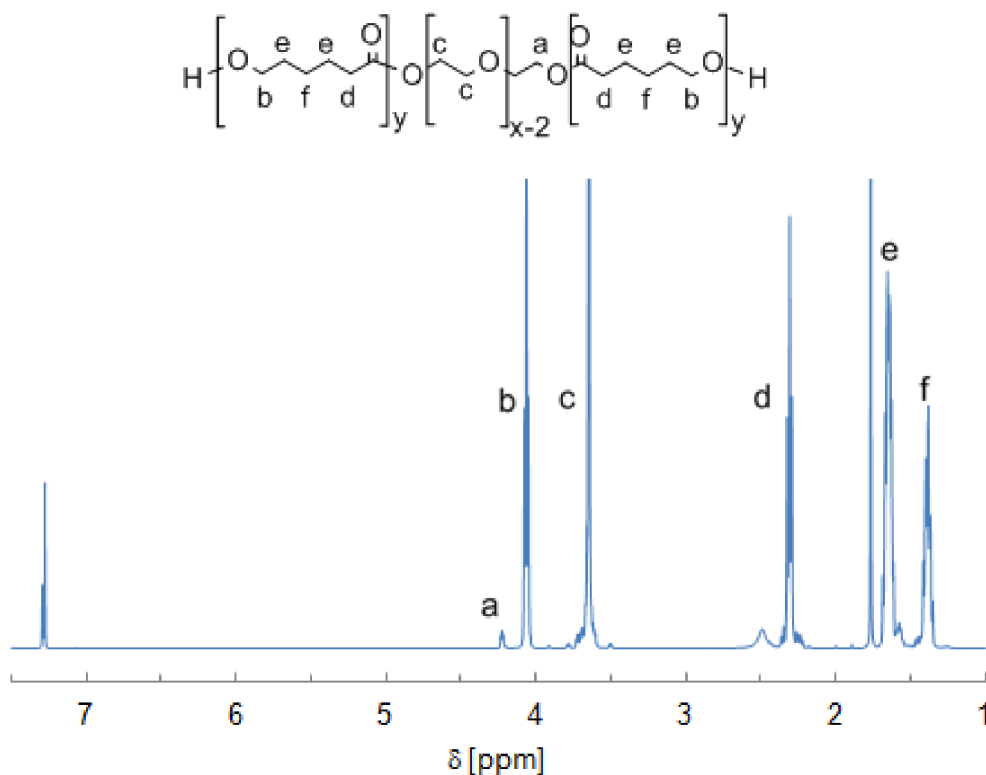


Figure 43 Obtained ¹H NMR spectrum of PCL-*b*-PEG-*b*-PCL prepared via ROP using NHC-*t*Bu at room temperature in 5 minutes in THF.

Based on the obtained results it can be expected that the preparation of biodegradable thermosensitive PLGA-PEG-PLGA copolymers using 1,3-di-*tert*-butylimidazol-2-ylidene is possible. The next part of work will be focused on the preparation and characterization of these thermosensitive triblock copolymers.

5.3 Synthesis of PLGA-PEG-PLGA Copolymers

PLGA-PEG-PLGA copolymers were synthesized via ring-opening polymerization of D,L-lactide with glycolide using poly(ethylene glycol) as macroinitiator and NHC-*t*Bu as organocatalyst (Figure 44). The molar ratio between lactide and glycolide units affects the rate of degradation, which was theoretically set to the value of LA/GA = 3. The weight ratio between the poly(D,L-lactide-*co*-glycolide) and poly(ethylene glycol) controls the solubility of the resulting copolymer and gelation behaviours in water. The ratio was theoretically set to PLGA/PEG = 2.5. Reaction proceeded in a THF solution at laboratory temperature and prepared copolymers after purification by ultrapure water were characterized by GPC, ¹H NMR, DSC, TGA and ATR-FTIR.

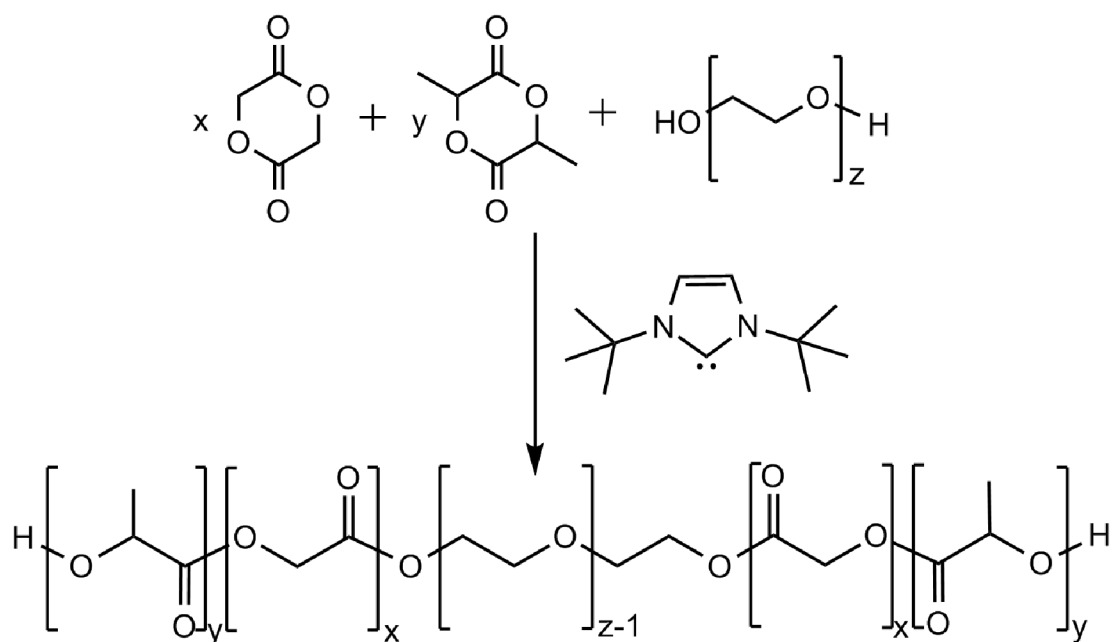


Figure 44 ROP polymerization of PLGA-PEG-PLGA triblock copolymers using NHC-tBu free carbene.

GPC results were used as a qualitative tool to check the peak shape, molecular weight's properties and size distribution of copolymer. Figure 45 shows GPC chromatograms of prepared PLGA-PEG-PLGA copolymer. Obtained elution curves was symmetrical and unimodal. Properties of prepared copolymer are shown in Table 6.

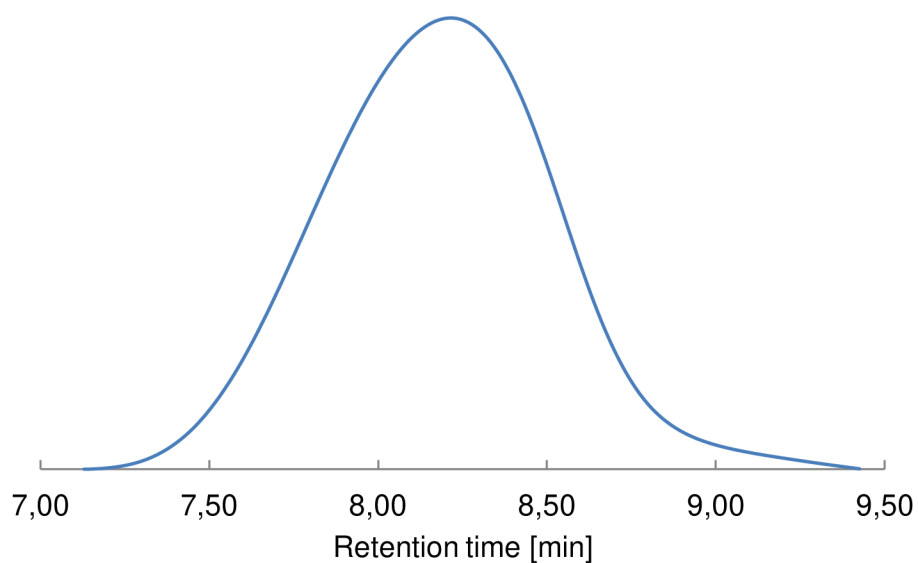


Figure 45 GPC diagram of PLGA-PEG-PLGA copolymer.

Table 6 Properties of prepared PLGA–PEG–PLGA triblock copolymer.

Yield ^a [%]	M_n^b [g·mol ⁻¹]	M_n^c [g·mol ⁻¹]	M_n^d [g·mol ⁻¹]	M_w/M_n	PLGA/PEG ^c [wt/wt]	LA/GA ^c [mol/mol]
79	5648	5007	4148	1.17	2.34	3.10

Conditions of polymerization: THF solvent, $T_p = 23$ °C, $t_p = 2h$, $I/C = 0.5$, $S/M = 5$.

^a Determined gravimetrically.

^b Determined by GPC against PS standards in THF.

^c Determined by ¹H NMR.

^d Calculated from initial molar ratio $[M]_0/[I]_0 \times M_w(\text{monomer}) \times \text{conversion yield}$.

Real M_n and composition of copolymer were determined by ¹H NMR spectroscopy. Molecular weight was calculated from integral of peak (a) belongs to PLA and from integral of peak (b) belongs to PGA. In the PLGA–PEG–PLGA spectrum shown in Figure 46 characteristic peaks of lactic acid were found in a range between $\delta = 5.10 - 5.35$ ppm [multiplet, 1H, (O(CH₃)CHO)] (a) and protons at $\delta = 1.50 - 1.75$ ppm [multiplet, 3H, (OC(CH₃)CHO)] (e), of glycolic acid at $\delta = 4.60 - 4.90$ ppm [multiplet, 2H, (OCH₂O)] (b) and PEG at $\delta = 3.55 - 3.75$ ppm [multiplet, 3H, (OCH₂CH₂O)] (d). The peak in the area of $\delta = 1.67$ ppm (unmarked) belongs to protons of residual organic catalyst. The peak belonging to the residual protons of the deuteriochloroform solvent was found at $\delta = 7.25$ ppm.

The M_n calculated from ¹H NMR spectra was in a very good agreement with M_n found by GPC as well as with theoretical M_n of copolymer ($M_{n(\text{theor})}/M_{n(\text{GPC})}/M_{n(\text{NMR})} = 1/0.95/1.06$).

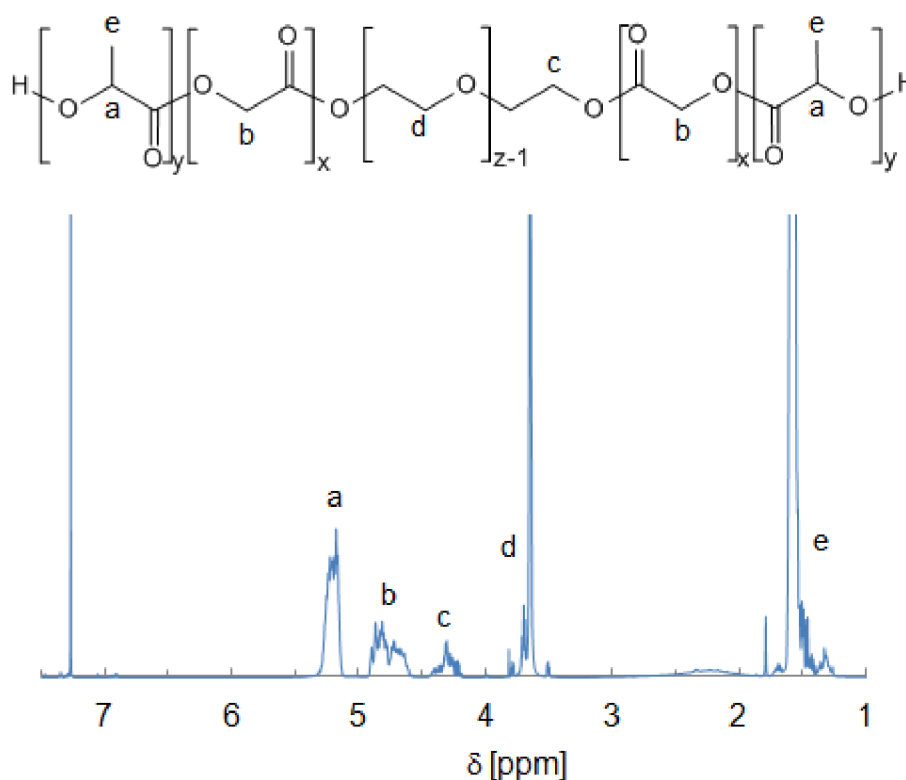


Figure 46 Obtained ¹H NMR spectrum of PLGA–PEG–PLGA copolymer prepared via ROP using NHC-*t*Bu at room temperature in THF.

Structure of PLGA–PEG–PLGA copolymer was characterized also using Fourier transform infrared spectroscopy. FTIR spectrum for the PLGA–PEG–PLGA copolymer is shown in Figure 47. The absorption bands at 1720 - 1760 cm^{-1} are attributed to the C=O stretching vibrations of the ester carbonyl group of LA and GA units. The absorption bands at 1350 - 1520 cm^{-1} are assigned to the $-\text{CH}_2-$ and CH_3- . The absorption bands from 1005 to 1350 cm^{-1} are attributed to the characteristic C–O–C stretching vibration of the repeated $-\text{OCH}_2\text{CH}_2$ units of PEG and the $-\text{COO}$ bonds stretching vibrations of LA and GA. The CH, CH_2 , CH_3 stretching bonds are centered at 2950 and 2800 cm^{-1} . The absorption bands of hydroxyl functional end-groups of PLGA–PEG–PLGA were found at 3530 cm^{-1} . Table 7 gives the absorption bands with their respective attributions. All these signals indicate the PLGA–PEG–PLGA copolymer was formed.

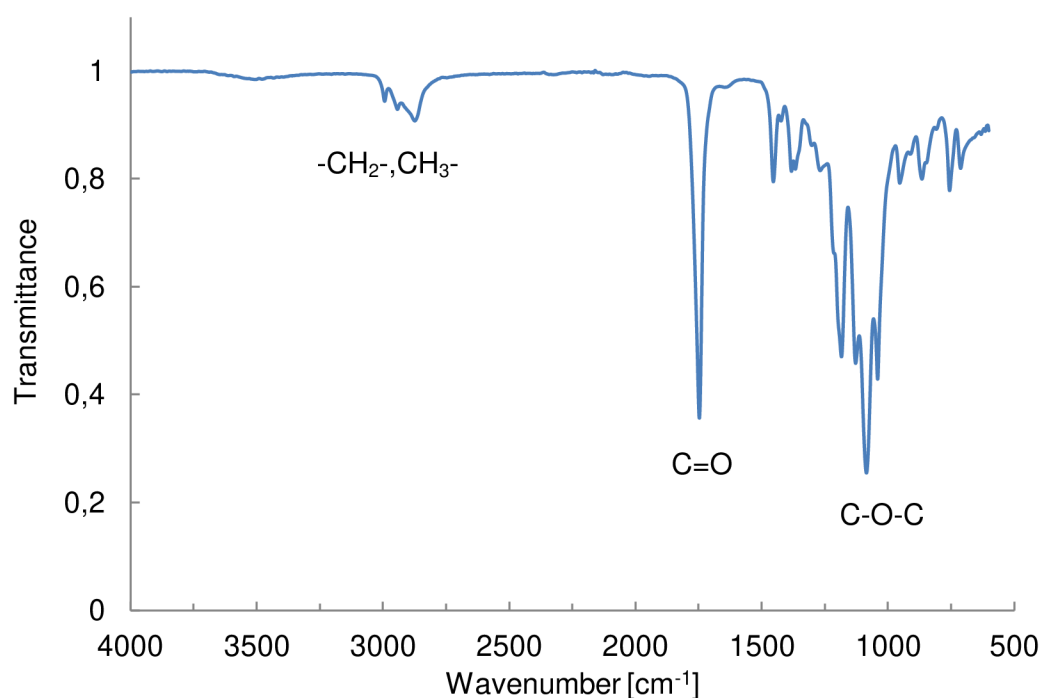


Figure 47 FTIR of PLGA–PEG–PLGA copolymer.

Table 7 Assignment of the absorption bands observed in the FTIR spectra of PLGA–PEG–PLGA copolymer.

Experimental frequencies [cm^{-1}]	Assignment
2950 - 2800	CH, CH_3 , CH_2 (stretching)
1760 - 1720	C=O (stretching)
1520 - 1350	CH_3 , CH_2 (deformation)
1350 - 1005	CH_2 , CH (wagging vibration)
1350 - 1005	C-O (stretching)

Kinetics of polymerization of PLGA–PEG–PLGA copolymer was investigated by gravimetric method. Aliquots were withdrawn during the polymerization after particular time intervals. Figure 48 shows dependence of the conversion on the time during copolymerization of D,L-lactide and glycolide. The illustrated dependence shows that the polymerization takes place very quickly after the first 5 minutes is achieved maximum monomer conversion of 89 %. From literature it is known that the ROP of cyclic esters by NHCs exhibit several notable features. Reaction rates can be extremely high. For example the IMes carbene catalyzes the ROP of LA in the presence of an alcohol initiator within seconds at room temperature (turnover frequency TOF = 18 s⁻¹) with catalyst loadings as low as 0.5 mol %. In addition to the rapid rate of polymerization, the ROP of LA mediated by NHCs is remarkably well-controlled and exhibits many of the features of a living polymerization [40].

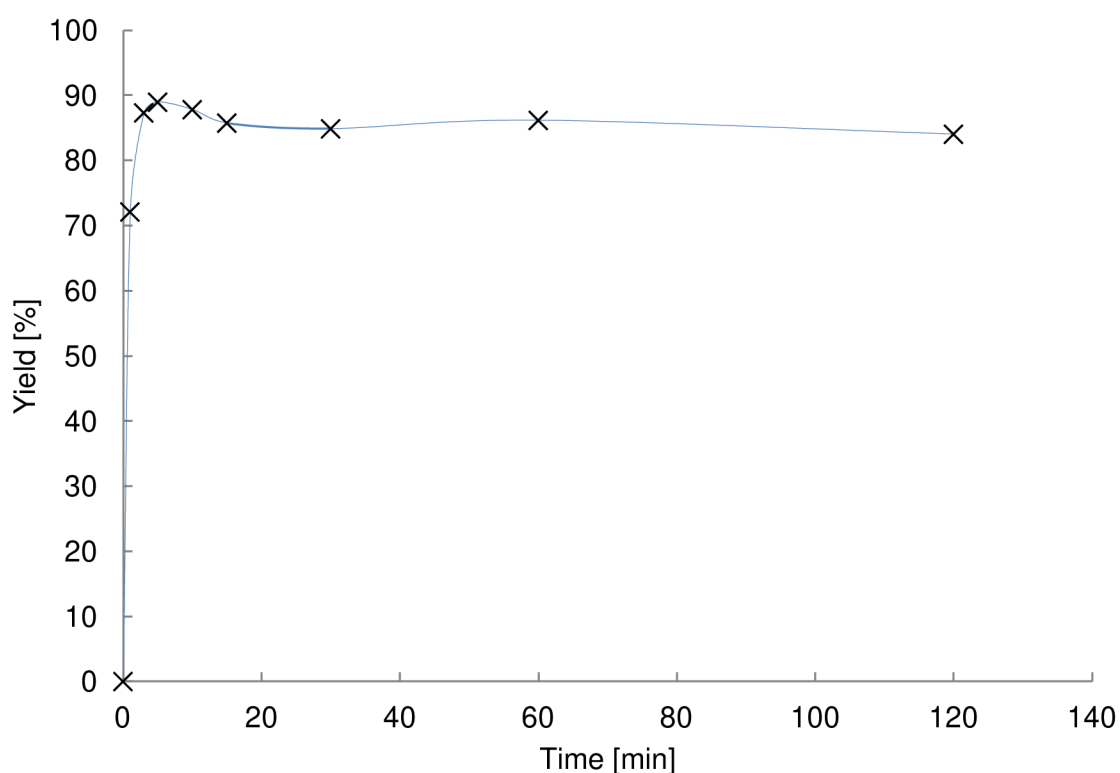


Figure 48 Dependence of monomers conversion on the time of D,L-lactide and glycolide copolymerization using NHC/PEG catalytic system.

Dependence of molecular weight and polydispersity index on polymerization time during copolymerization of D,L-lactide and glycolide is shown on Figure 49. The dependence of molecular weight on the polymerization time only slightly increases. Dependence on polydispersity index on the polymerization time is linear at all times. From this it is evident that the properties of copolymers are during polymerization almost unchanged. In future work the kinetic studies should be focus on the first minute or better on the first seconds of polymerization.

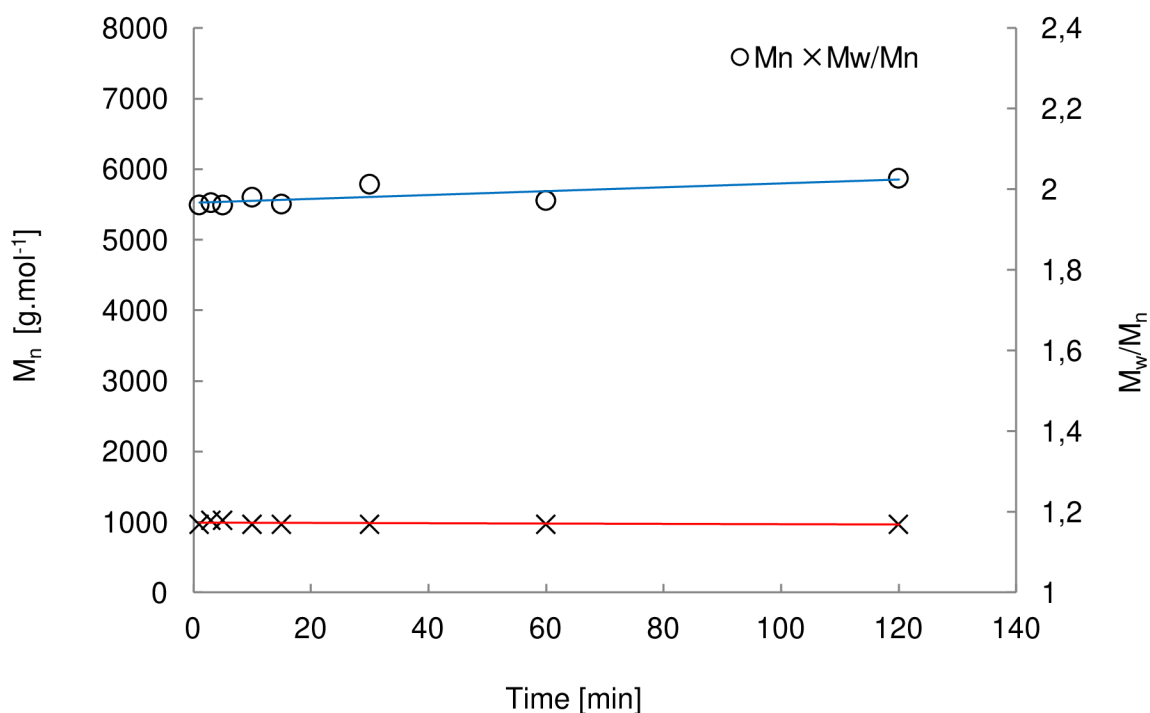


Figure 49 Dependence of molecular weight and polydispersity index on polymerization time during copolymerization of D, L-lactide and glycolide.

The thermal stability of copolymers was studied by thermogravimetric analysis. TGA was carried out to measure change in mass with increased temperature, thermal stability, and maximum degradation temperature for the sample. Thermograms (Figure 50) of PLGA–PEG–PLGA copolymer exhibited two-stage changes in the weight loss corresponding to decomposition of ester bonds in PLGA (total weight loss at the end of first stage $\Delta W^1 = 71.55$ wt.%) and ether bonds in PEG (total weight loss at the end of second stage $\Delta W^2 = 26.34$ wt.%). As can be seen, copolymer starts degradation at temperature $T_d = 204$ °C, first degradation step with the temperature at max. rate of $T_{dm}^1 = 275$ °C and second stage with the temperature at maximum rates of $T_{dm}^2 = 387$ °C.

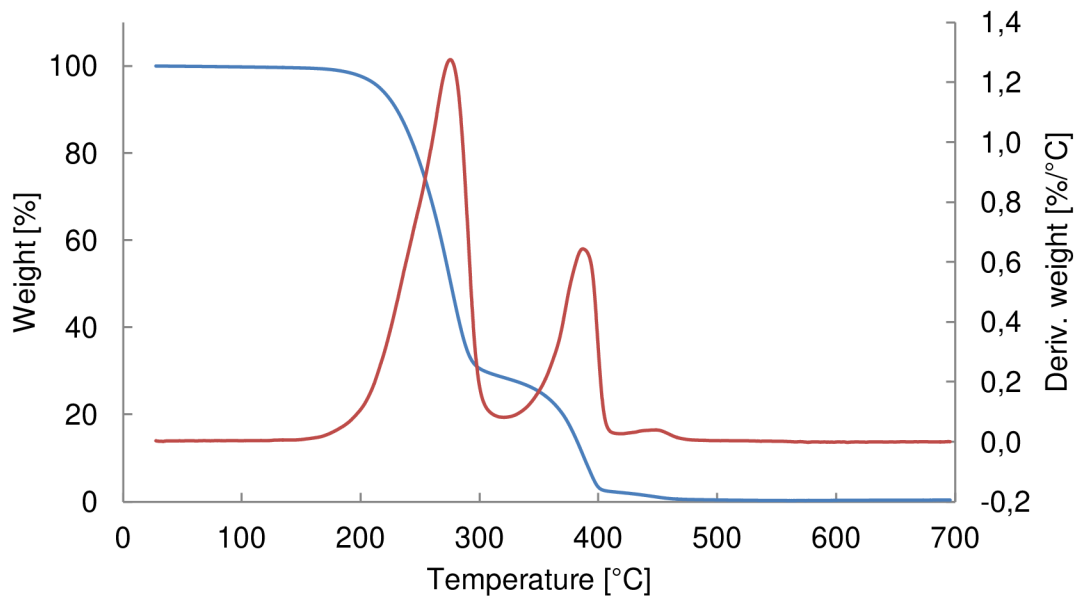


Figure 50 TGA of PLGA-PEG-PLGA copolymer.

Figure 51 shows the DSC curve for the PLGA-PEG-PLGA copolymer. The DSC data were recorded for the second heating run from -40 to 160 °C. From these DSC curve it is possible to see the thermal transitions related to the glass transition (change in the angle of the DSC curves to the baseline). Glass transition temperature (T_g) calculated from DSC analysis was found to be -10 °C. The absence of a melting transition phase suggests that the analyzed copolymer is amorphous. It can be seen that there is no indication of residual monomers in the prepared copolymers, since no endothermic event characteristic of glycolide melting is observed on the respective DSC curves.

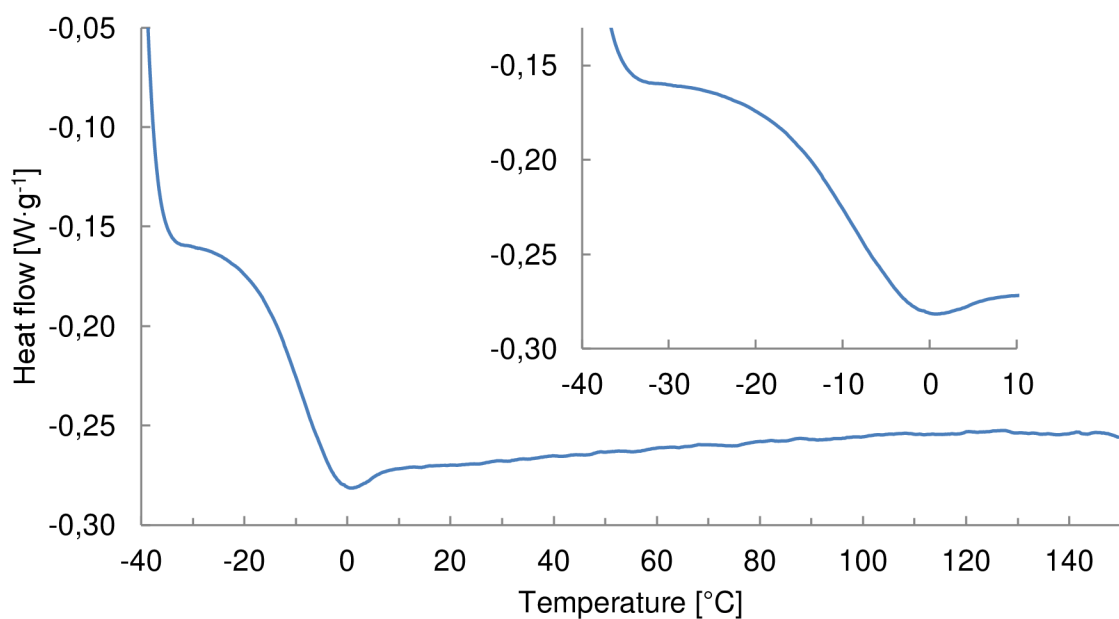


Figure 51 DSC of PLGA-PEG-PLGA copolymer.

The sol-gel phase transition of aqueous solutions of PLGA–PEG–PLGA copolymer was evaluated by inverting test tube method (Figure 52). The phase diagram of copolymer is shown in Figure 53. These phase diagram demonstrates three basic areas sol, gel and suspension. They are separated by sol-gel curve. Copolymer dissolved in water forms free-flowing solution (sol) and with increases temperature spontaneously gels (first sol-gel transition), further increasing the temperature causes the second gel sol transition, the copolymer is separated from the water (suspension).



Figure 52 Inverting test tube method: a) the solution in phase sol b) the phase gel at 37 °C, c) the phase suspension.

The solutions of PLGA–PEG–PLGA in ultrapure water were prepared in a concentration range of 6 – 42 w/v %. At concentrations above 20 w/v % the copolymer solution becoming viscous with gradually increasing temperature and changed to transparent gel at the temperature of about 36 °C. With further increasing temperature the transparent gel is transferred to a white gel. At the temperature around 43 °C the copolymer precipitated and dividing the sample into two phases (copolymer and water). When the copolymer suspension is cooled down, sample dissolved and again exhibits a sol-gel transition. At concentrations of the copolymer solution lower than 20 % only increasing the viscosity was observed with increasing temperature. Thus 20 % was set as CGC and 36 °C as CGT.

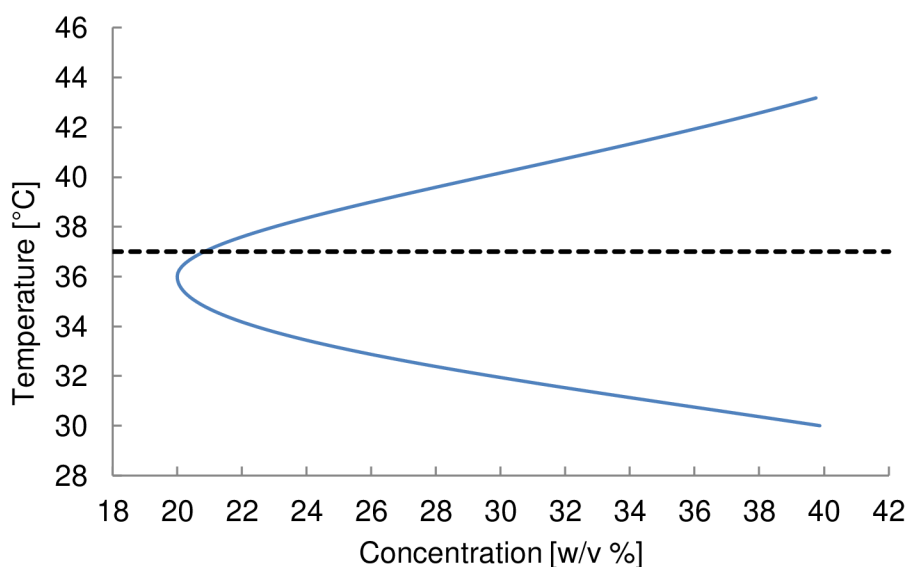


Figure 53 Phase diagram of PLGA–PEG–PLGA copolymer.

The rheological behavior of the temperature-sensitive block copolymer was described by the storage modulus (G'). Figure 54 shows the temperature-dependent storage modulus of the hydrogel in the temperature range of interest, between 25 °C and 50 °C for the concentrations between 18 – 42 %. G' was zero until the onset of the sol–gel transition, after which G' increased to a maximum. With further increase in the temperature G' decreased. The sample was in the gel state up to the 49 °C. The highest stiffness 176 Pa had copolymer solution with the concentration of 42 w/v %.

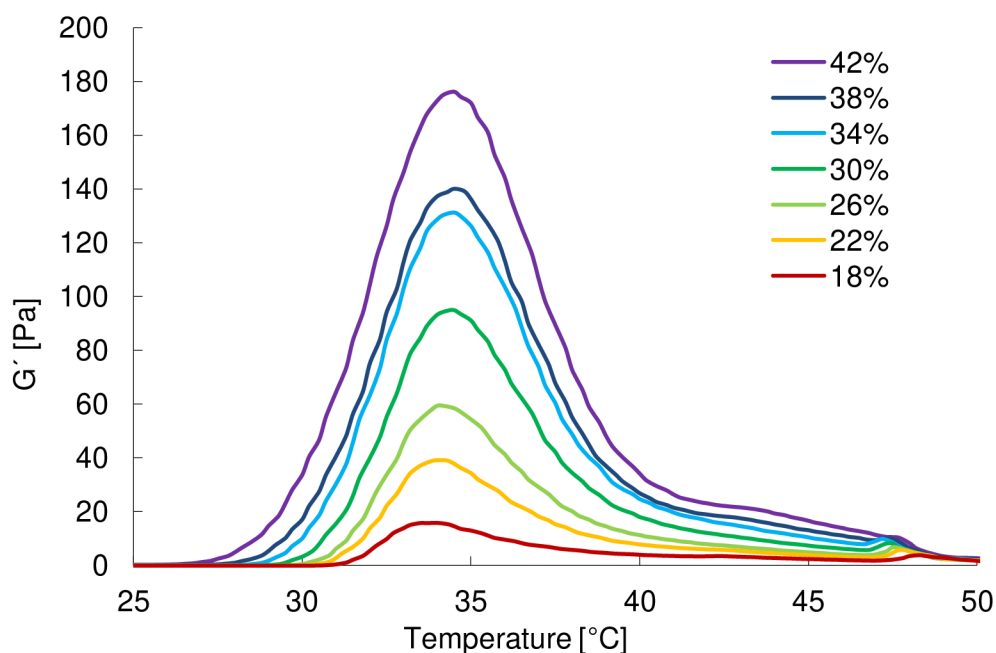


Figure 54 Effect of polymer solution concentration (18 – 42 w/v %) on the storage modulus.

5.3.1 Optimization of Copolymerization Conditions

In this study, the goal was to achieve optimal conditions to slow-down the ring opening polymerization to keep “living” well-controlled conditions of polymerization. Therefore, the synthesis of PLGA–PEG–PLGA copolymer was carried out in a range of different temperatures of polymerization, in different solvents or in a bulk and different ratio solvent to monomer or initiator to catalyst in order to optimize the physical conditions with a view of predicted M_n , narrow polydispersity index and gelation behavior of copolymers. The effect of D,L-lactide and glycolide purification prior the use on the copolymer characteristics was studied as well. The PLGA–PEG–PLGA triblock copolymers theoretical composition was same as above, so PLGA/PEG weight ratio was set to 2.5 and LA/GA molar ratio was equal to 3.0.

5.3.1.1 Influence of Monomer Purification

At the beginning the effect of monomer purification prior the use on the copolymer characteristics was monitored. PLGA–PEG–PLGA copolymers with sublimated and original

unsublimated monomers were successfully synthesized. All samples were purified by ultrapure water. Polymers characteristics are listed in Table 8.

Table 8 Properties of the prepared PLGA–PEG–PLGA copolymers.

Sample	Yield ^a [%]	M_n^b [g·mol ⁻¹]	M_n^c [g·mol ⁻¹]	M_n^d [g·mol ⁻¹]	M_w/M_n	PLGA/PEG ^c [wt/wt]	LA/GA ^c [mol/mol]
sublimated	89	6046	4561	4673	1.21	2.04	2.65
unsublimated	74	6498	4526	3885	1.17	2.02	2.70

Conditions of polymerization: THF solvent, $T_p = 23$ °C, $t_p = 5$ min, $I/C = 0.5$, $S/M = 5$.

^a Determined gravimetrically.

^b Determined by GPC against PS standards in THF.

^c Determined by ¹H NMR.

^d Calculated from initial molar ratio $[M]_0/[I]_0 \times M_w(\text{monomer}) \times \text{conversion yield}$.

Copolymer from sublimated monomers reached higher monomer conversion (89 %) than copolymer from original unsublimated monomers (74 %). Molecular weight calculated from ¹H NMR for copolymers sublimated was 4561 g·mol⁻¹ which was comparable with theoretical molecular weight (4673 g·mol⁻¹) and for unsublimated copolymer the M_n was considerably higher (4526 g·mol⁻¹) than theoretical molecular weight (3885 g·mol⁻¹). The efficiency of NHC/PEG system for sublimated monomers was higher ($M_{n(\text{theor})}/M_{n(\text{GPC})} = 0.77$) in comparison to unsublimated monomers ($M_{n(\text{theor})}/M_{n(\text{GPC})} = 0.60$). Polydispersity index were for both copolymers narrow $M_w/M_n = 1.2$. These results indicate that the polymerization proceeds better with sublimed monomers, due to the higher purity of the entering monomers. There is no significant difference between ¹H NMR spectra of individual PLGA sequences from PLGA–PEG–PLGA copolymers either from sublimated or unsublimated monomers (see Figure 55).

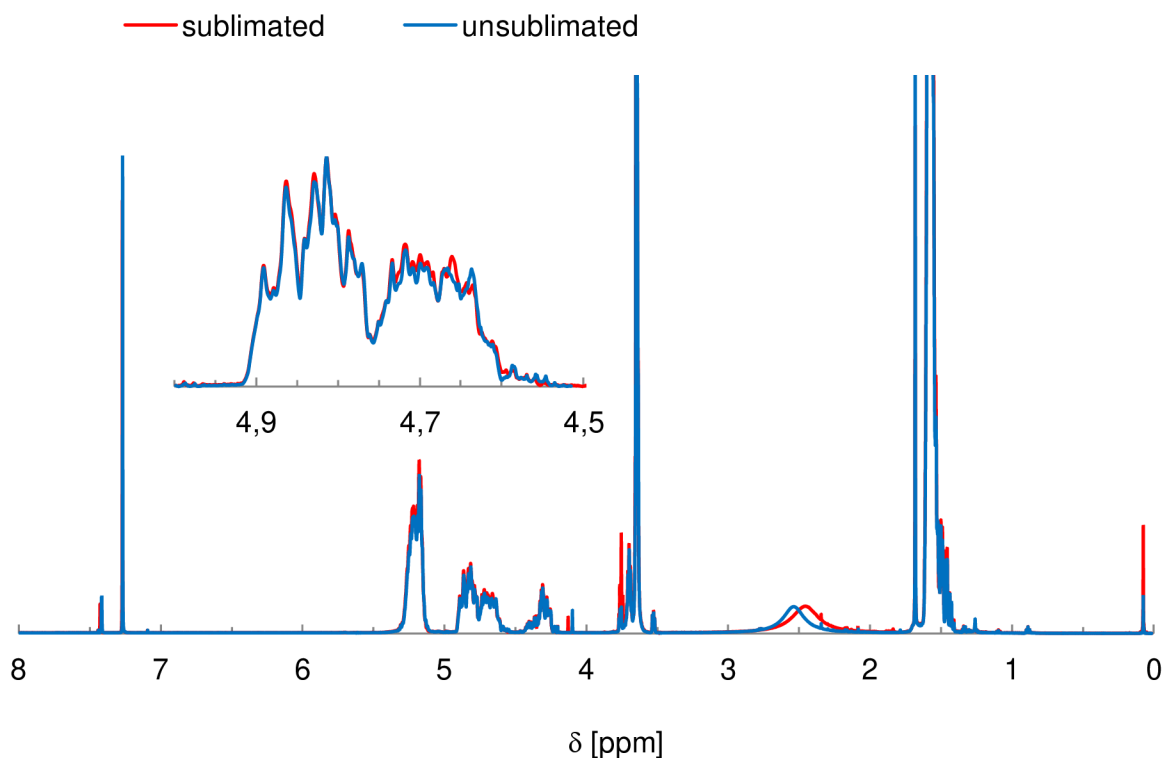


Figure 55 ^1H NMR spectra of PLGA-PEG-PLGA copolymers from both sublimated and unsublimated monomers and detail in a range from 5.0 – 4.5 ppm.

Rheological properties of the copolymers prepared from sublimated and original unsublimated monomers were evaluated. Figure 56 shows elastic modulus of copolymer solutions (24 w/v %). The copolymer solution from sublimated monomers exhibited elastic modulus only 8.5 Pa at 35.7 °C, while copolymer from original unsublimated monomers exhibited G' equal to 46.0 Pa at 35.0 °C.

The lower elastic modulus found at the sublimated copolymer can be caused by the presence of higher amount of carbene catalyst bound to copolymer chain ends. Presented molecules of catalyst might disrupt hydrophobic interactions between chains and thus did not allow the formation of strong micelles interactions. Higher presence of the carbene catalyst in the copolymer from sublimated monomers was confirmed by ^1H NMR.

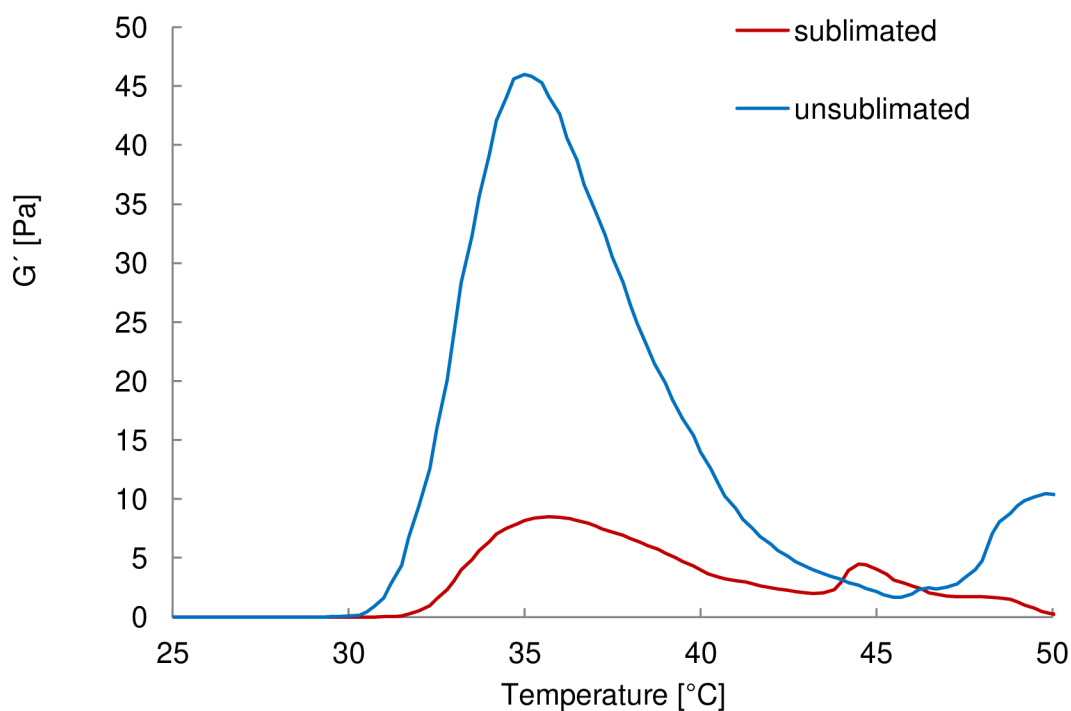


Figure 56 Rheological properties of PLGA–PEG–PLGA copolymers from either sublimated or unsublimated monomers (24 w/v % in ultrapure water).

Monomers purification have not significantly influenced the chemical properties of resulted copolymers, but essentially influenced the physical properties such as gelation behavior (gel stiffness). Moreover, sublimation of monomers is very economically and time-consuming. Based on these results next samples were prepared only from original unsublimated monomers.

5.3.1.2 Influence of Copolymerization Temperature

It is generally known that increasing the polymerization temperature leads to faster both polymerization reactions and the transmission frequency responses. Influence of temperature on polymerization behavior catalytic system NHC/PEG in copolymerization of D,L-lactide and glycolide was investigated. Series of experiments were carried out in the temperature equal to 0, 10, 23 and 40 °C in THF for 120 minutes. Properties of prepared copolymers are shown in Table 9.

Table 9 Summary of the properties of copolymers PLGA–PEG–PLGA prepared at different temperatures.

T_p [°C]	Yield ^a [%]	M_n^b [g·mol ⁻¹]	M_n^c [g·mol ⁻¹]	M_n^d [g·mol ⁻¹]	M_w/M_n	PLGA/PEG ^c [wt/wt]	LA/GA ^c [mol/mol]
0	74	4133	5003	3885	1.39	2.34	3.23
10	71	4609	5042	3728	1.26	2.36	3.09
23	79	5648	5007	4148	1.17	2.34	3.10
40	77	4312	4689	4043	1.14	2.13	3.12

Conditions of polymerization: THF solvent, $t_p = 5$ min, $I/C = 0,5$, $S/M = 5$.

^a Determined gravimetrically.

^b Determined by GPC against PS standards in THF.

^c Determined by ¹H NMR.

^d Calculated from initial molar ratio $[M]_0/[I]_0 \times M_w(\text{monomer}) \times \text{conversion yield}$.

Prepared copolymers reached conversion of monomer in the range of 71 – 79 %. With decreasing the polymerization temperature it can be observed lowering in molecular weight of copolymers and broadening their polydispersity index. The ratios of LA/GA and PLGA/PEG approached theoretically set values (LA/GA = 3.0, PLGA/PEG = 2.5). The lowest polydispersity index ($M_w/M_n = 1.14$) was achieved at $T_p = 40$ °C, the highest temperature tested, which surprisingly is not consistent with the expected change of the polymerization rate.

Differences in the structure of the prepared copolymers were observed by ¹H NMR at individual sequences for PLGA in a range from 4.56 to 4.93 ppm (Figure 57).

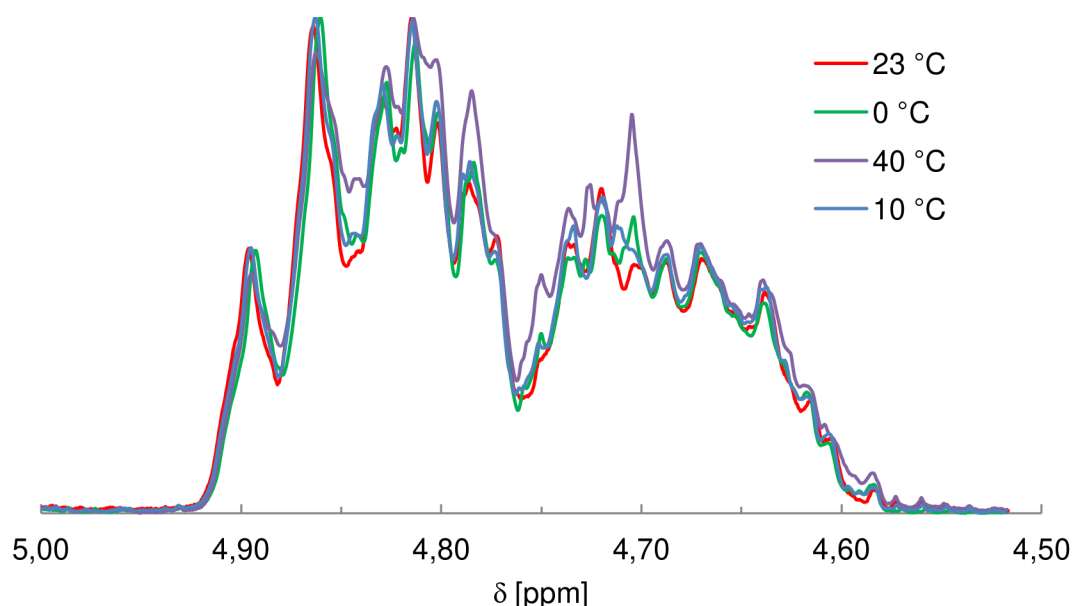


Figure 57 Detail in ¹H NMR spectra of PLGA–PEG–PLGA in a range from 5.00 – 4.50 ppm for ROP at different temperature.

J. Kasperczyk performed detailed characterization of the glycolide/lactide copolymer chain microstructure, including expected structural changes resulting from transesterification processes using proton nuclear magnetic resonance (Figure 58) [96].

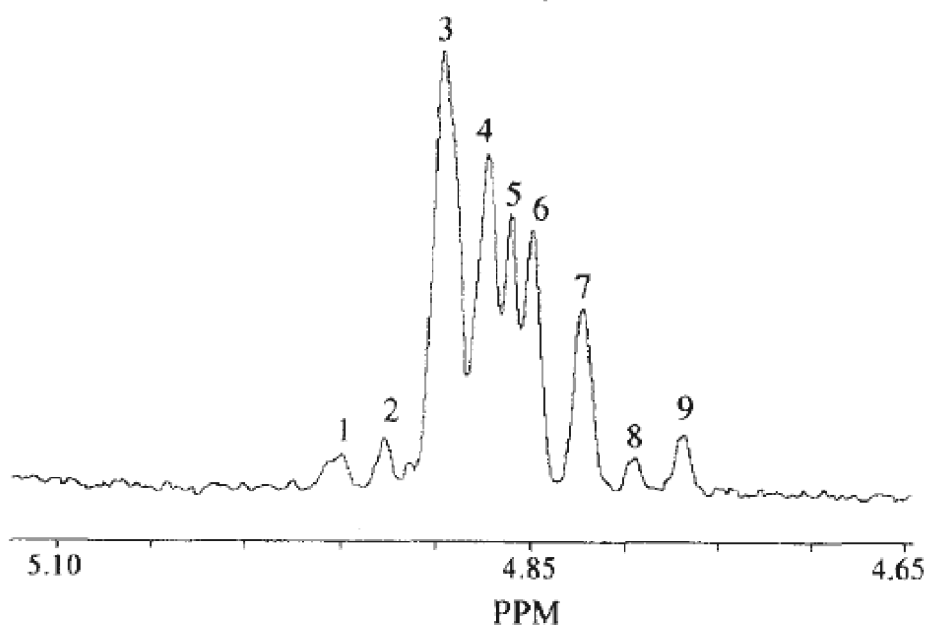


Figure 58 ^1H NMR spectra of poly(lactide-co-glycolide) obtained in the region of glycolide methylene protons [96].

Assignment of resonance lines to appropriate sequences in ^1H NMR spectrum of poly[(lactide)-co-(glycolide)] in the region of the glycolide methylene proton are listed in Table 10.

Table 10 Sequences in the region of the glycolide methylene proton [96].

Line number	Sequences	δ [ppm]
1	GLGGG or GGGLG	4.96
2	LGGLG or GLGGL	4.94
3	GGGGG	4.90
4	LLGGL + LGGLL	4.88
5	GGGGL + LGGGG	4.87
6	LLGGG + GGGLL	4.86
7	LLGLL + GLGLL + LLGLG + GLGLG	4.83
8	GGGLG or GLGGG	4.80
9	LGGGL + GLGGL or LGGLG	4.78

The peaks in the ^1H NMR spectra of samples prepared at 0 °C, 10 °C and 23 °C are similar, but peaks of copolymer prepared at 40 °C are different. Generally, transesterification reaction depends on the reaction temperature. Inter-molecular transesterifications cause the redistribution of sequences in the polyester chain, resulting in the change of sequence structure and even the length distribution of PLGA blocks. Contrary, intra-molecular transesterifications result in copolymer degradation [97]. Results show that lower ROP

temperatures lead to the application of an intra-molecular transesterifications accompanied by expansion of polydispersity index.

Rheological properties of copolymers prepared at different temperature of polymerization were evaluated. Figure 59 shows elastic modulus of copolymer solutions having concentration of 42 w/v %. The solution of copolymer prepared at 40 °C stayed in phase sol in the all temperature scale. Other solutions of copolymers exhibited sol-gel transition. The solution of copolymer prepared at 0 °C exhibited G' equal to 28.3 Pa at 36.0 °C, higher elastic modulus G' equal to 51.7 Pa at 34.2 °C showed the solution of copolymer prepared at 10 °C. The highest stiffness of 176 Pa at 34.5 °C reached copolymer solution prepared at 23 °C.

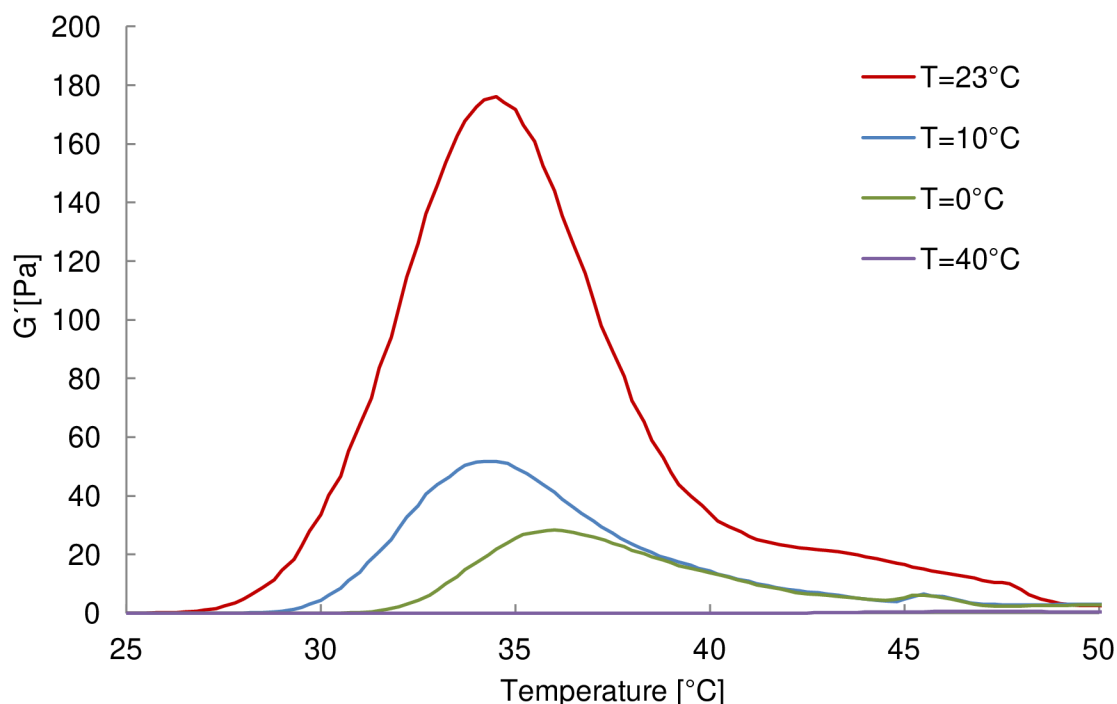


Figure 59 Influence of polymerization temperature on elastic modulus of the polymer solutions (concentration 42 w/v %).

It was demonstrated that different temperatures of polymerization have not overmuch influenced the molecular weight or polydispersity index. Essential affect was observed at visco-elastic behavior. Best visco-elastic behavior was achieved with the copolymer prepared at 23 °C. This temperature is advantageous both from an economical and practical point of view. Based on these results next samples were prepared at laboratory temperature.

5.3.1.3 Influence of Solvents

The effect of the reaction medium on the polymerization was evaluated using tetrahydrofuran (THF), dimethyl sulfoxide (DMSO) and xylene as solvents. These solvents have the dielectric constants, $\epsilon = 7.5$, 47, and 2.4, respectively. For comparison, the polymerization in bulk was also conducted. Experiments in solutions were carried out at laboratory temperature for 60 minutes. The polymerization in bulk was carried out at 130 °C (to melt the monomers) for 60 minutes. The data of polymerizations are summarized in Table 11.

Table 11 Influence of solvent on the properties of prepared PLGA–PEG–PLGA copolymers.

solvent	Yield ^a [%]	M_n^b [g·mol ⁻¹]	M_n^c [g·mol ⁻¹]	M_n^d [g·mol ⁻¹]	M_w/M_n	PLGA/PEG ^c [wt/wt]	LA/GA ^c [mol/mol]
bulk	73	3876	4825	3833	1.32	2.21	2.83
THF	79	5648	5007	4148	1.17	2.34	3.10
DMSO	53	3901	4550	2783	1.30	2.03	2.37
Xylene	45	5151	4416	2415	1.30	1.94	4.74

Conditions of polymerization: $T_p = 23$ °C, $t_p = 60$ min, $I/C = 0.5$, $S/M = 5$.

^a Determined gravimetrically.

^b Determined by GPC against PS standards in THF.

^c Determined by ¹H NMR.

^d Calculated from initial molar ratio $[M]_0/[I]_0 \times M_w(\text{monomer}) \times \text{conversion yield}$.

Prepared copolymers in bulk and in THF solution reached conversion of monomers 73 % and 79 %, respectively. Copolymers prepared in DMSO and xylene solution showed lower conversion of monomers (53 % and 45 %, respectively). Also the ratios of LA/GA and PLGA/PEG did not come close to the theoretically set values (LA/GA = 3.0, PLGA/PEG = 2.5). It is probably due to different polarity of solvents. Xylene is non-polar aprotic solvent and PLA/PGA ratio looks like the glycolide polymerized to lower conversion in comparison to lactide. DMSO belongs to polar aprotic solvent and THF is “Borderline” polar aprotic solvents. THF don’t participate in reactions: it serve only as the medium.

The differences in the structures of the prepared copolymer can be seen from the ¹H NMR spectra shown in Figure 60.

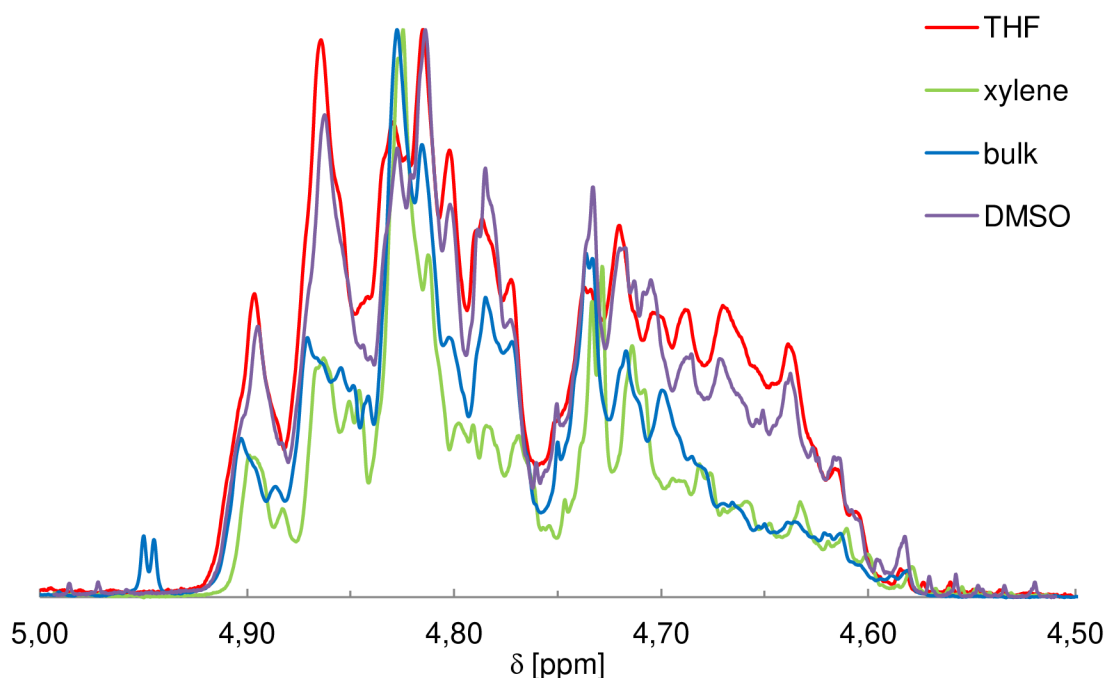


Figure 60 Detail in ¹H NMR spectrum in a range from 5.00–4.50 ppm for copolymers prepared in different medium.

The peaks in the ^1H NMR spectra of samples prepared in THF and DMSO are quite similar. The resonance lines of GA-LA sequences in the region of the glycolide methylene proton are in the similar representation. While in the case of the copolymers prepared in xylene and bulk it is evident that resonance line at $\delta = 4.83$ ppm (peak of LA-GA-LA triad) significantly exceeds the other resonance lines. This peak confirms existence of transesterification reaction. Rheological properties of the copolymers prepared in different polymerization medium were evaluated. Elastic modulus of copolymer solutions (42 w/v %) is shown in Figure 61. The solution of copolymer prepared in solution of DMSO stayed in phase sol in the all temperature scale. The solution of copolymer prepared in bulk exhibited G' only equal to 3.0 Pa at 32.0 °C, higher elastic modulus $G' = 33.06$ Pa at 33.2 °C showed the solution of copolymer prepared in hexane. The highest stiffness 176 Pa at 34.5 °C reached copolymer solution prepared in solution of THF.

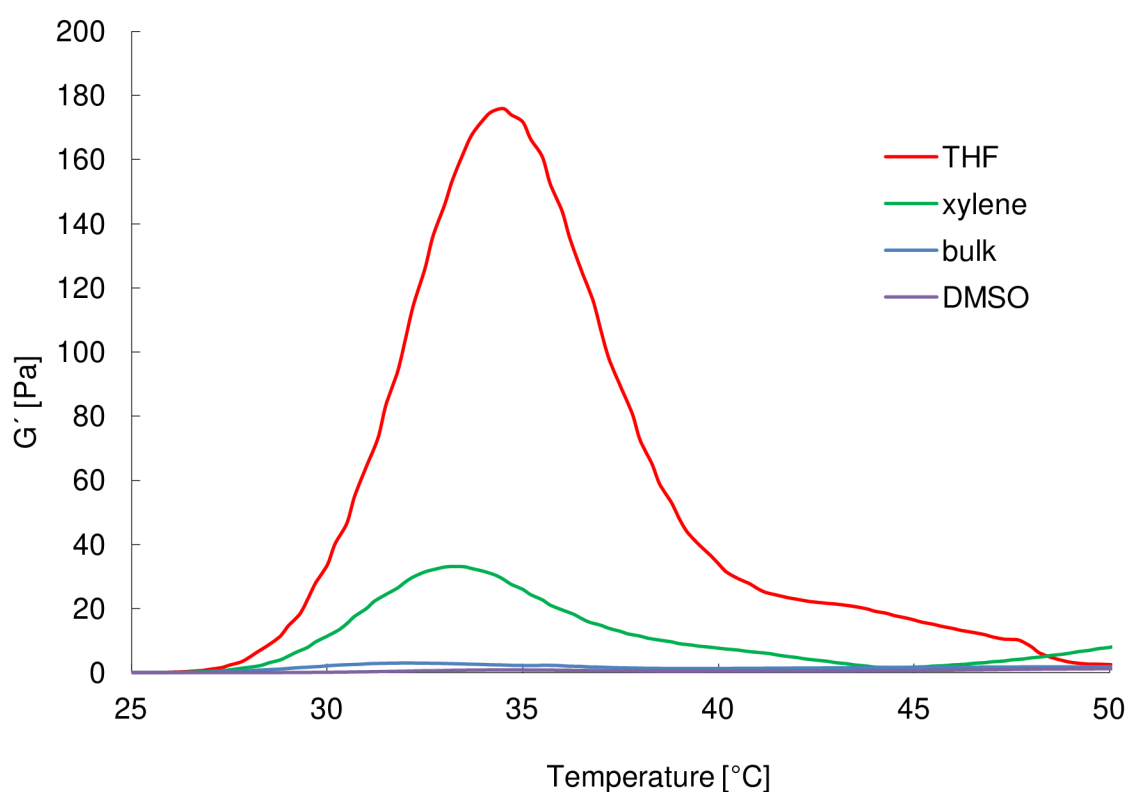


Figure 61 Influence of polymerization solvent on elastic modulus of the polymer solutions (concentration 42 w/v %).

Changes in the reaction medium have essentially influenced the conversion of monomers, molecular weight and also the composition of copolymers. Effect of polymerization solvent also reflected on gelation behavior. Best equals were achieved in THF solvent. Based on these results next samples were prepared in THF.

5.3.1.4 Influence of Different Solvent to Monomer Ratio

The influence of the initial concentration of monomers, which is given by the ratio of solvent to monomer (S/M) was studied. The polymerizations were carried out at concentrations

of monomers $[D,L-LA]_0 = 1.08 - 0.27$ and $[GA]_0 = 0.36 - 0.09$ in the polymerization batch at laboratory temperature in THF for 120 min. Overall results are summarized in Table 12.

Table 12 Properties of prepared copolymers PLGA–PEG–PLGA at different ratio solvent to monomer.

S/M	Yield ^a [%]	M_n^b [g·mol ⁻¹]	M_n^c [g·mol ⁻¹]	M_n^d [g·mol ⁻¹]	M_w/M_n	PLGA/PEG ^c [wt/wt]	LA/GA ^c [mol/mol]
5	79	5648	5007	4148	1.17	2.34	3.10
10	68	4400	5173	3570	1.23	2.45	3.01
20	72	4628	5196	3780	1.12	2.46	2.93

Conditions of polymerization: THF solvent, $T_p = 23$ °C, $t_p = 2$ h, $I/C = 0.5$.

^a Determined gravimetrically.

^b Determined by GPC against PS standards in THF.

^c Determined by ¹H NMR.

^d Calculated from initial molar ratio $[M]_0/[I]_0 \times M_w(\text{monomer}) \times \text{conversion yield}$.

Prepared copolymers reached conversion of monomer in the range of 68 – 79 %. There were no significant differences between molecular weights. The ratios of LA/GA and PLGA/PEG approached theoretically set values (LA/GA = 3.0, PLGA/PEG = 2.5). The lowest polydispersity index ($M_w/M_n = 1.12$) was achieved at ratio solvent to monomer equal to 20. Changes in the structure of prepared copolymers were not observed in ¹H NMR spectrum (Figure 62).

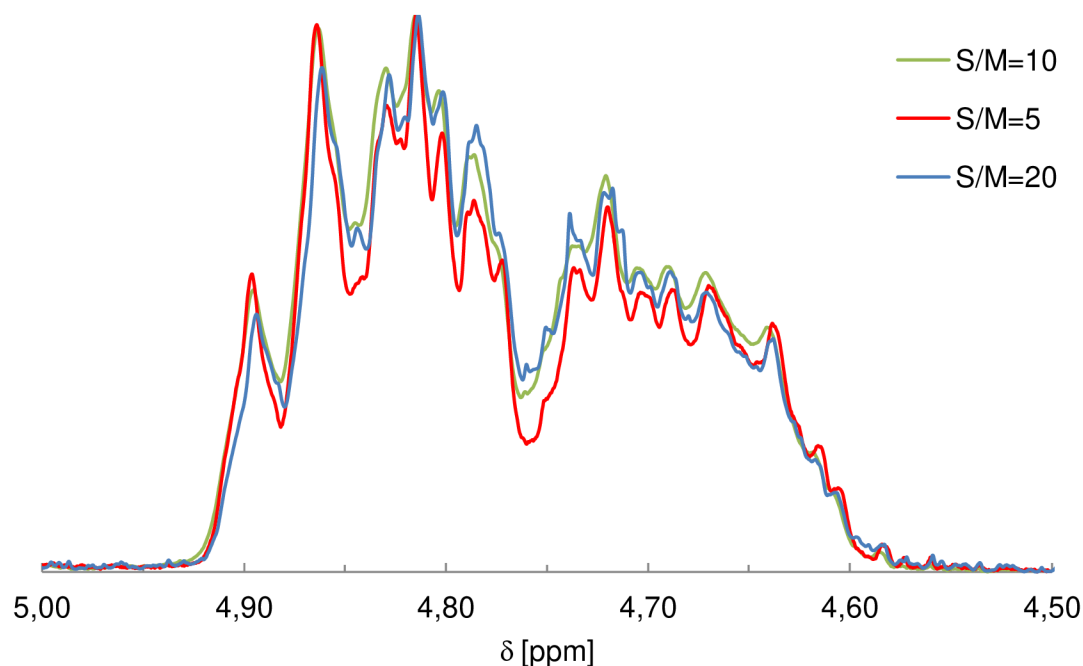


Figure 62 Detail in ¹H NMR spectrum in a range from 5.00 – 4.50 ppm for copolymers prepared with different solvent to monomer ratio.

Rheological properties of the copolymers prepared at different ratio solvent to monomer were evaluated. Figure 63 shows elastic modulus of copolymer solutions (42 w/v %). All solutions

of copolymers exhibited sol-gel transition. The solution of copolymer prepared at ratio solvent to monomer equal to 20 exhibited the lowest elastic modulus $G' = 4.1$ Pa at 37.5 °C, higher elastic modulus G' equal to 20.4 Pa at 35.7 °C showed the solution of copolymer prepared at ratio solvent to monomer equal to 10. The highest stiffness 176.0 Pa at 34.5 °C reached copolymer solution prepared at ratio solvent to monomer equal to 5.

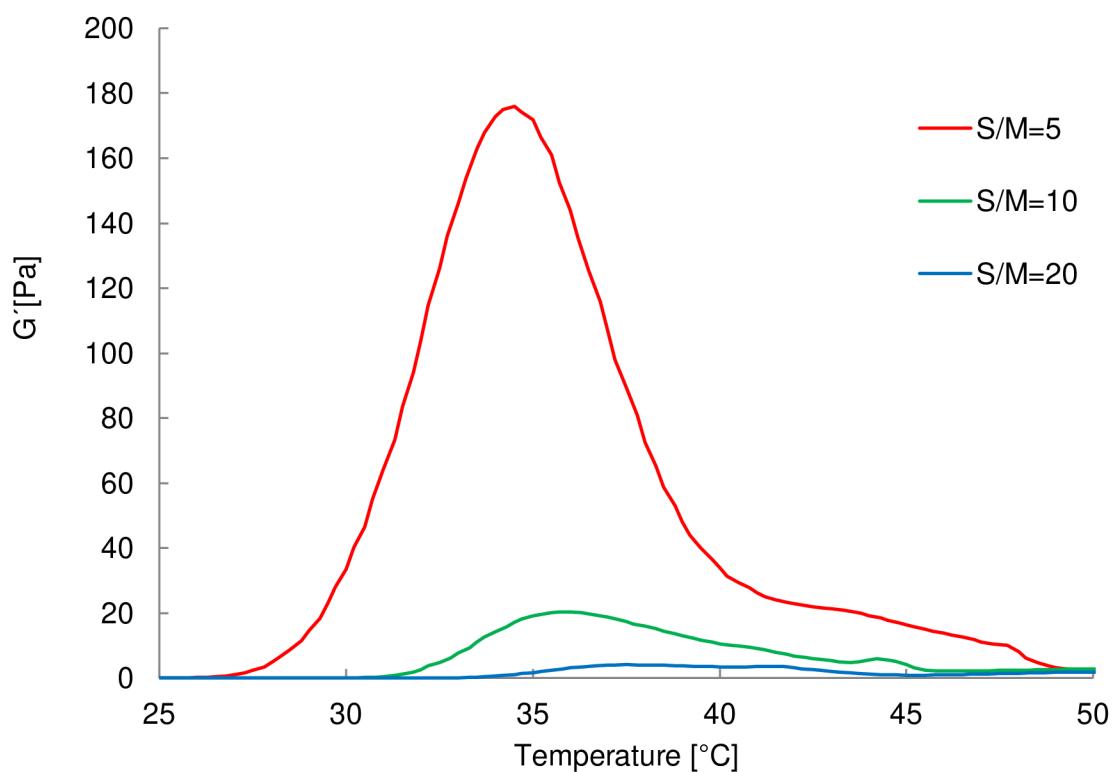


Figure 63 Influence of different solvent to monomer ratio on elastic modulus of the polymer solutions (concentration 42 w/v %).

It was demonstrated that different initial concentrations of monomers in polymerization solution have not overmuch influenced the molecular weight, polydispersity index or the copolymer composition, but again showed essential influence on gelation behavior. Best equals were achieved at ratio solvent to monomer equal to 5. Based on these results next samples were prepared at this ratio.

5.3.1.5 Influence of Different Initiator to Catalyst Ratio

Based on literature review discussing similar catalytic system it is known that polymerization behavior of NHCs is strongly sensitive to the ratio of initiator to catalyst. The experiments with varying molar ratios of initiator to catalyst were performed (Table 13). All the copolymerizations were carried out for 120 min in THF solution.

Table 13 Properties of prepared PLGA–PEG–PLGA copolymers at different initiator to catalyst ratio.

<i>I/C</i>	Yield ^a [%]	M_n^b [g·mol ⁻¹]	M_n^c [g·mol ⁻¹]	M_n^d [g·mol ⁻¹]	M_w/M_n	PLGA/PEG ^c [wt/wt]	LA/GA ^c [mol/mol]
1/2.5	71	4462	5102	3728	1.14	2.16	3.26
1/2	79	5648	5007	4148	1.17	2.34	3.10
1/1.5	80	5376	5357	4200	1.25	2.57	3.01
1/1	85	5152	5065	4463	1.34	2.38	3.05
1/0.5	65	5484	5086	3413	1.36	2.39	3.06

Conditions of polymerization: THF solvent, $T_p = 23\text{ }^\circ\text{C}$, $t_p = 2\text{ h}$, $S/M=5$.

^a Determined gravimetrically.

^b Determined by GPC against PS standards in THF.

^c Determined by ¹H NMR.

^d Calculated from initial molar ratio $[M]_0/[I]_0 \times M_w(\text{monomer}) \times \text{conversion yield}$.

Prepared copolymers reached conversion of monomer in the range of 65 – 85 %. There were no significant differences between molecular weights, only copolymer prepared with ratio catalyst to initiator equal 1/2.5 exhibited lower molecular weight comparable with theoretical molecular weight (3728 g·mol⁻¹). The ratios of LA/GA and PLGA/PEG approached theoretically set values (LA/GA = 3.0, PLGA/PEG = 2.5). It was demonstrated that with decreasing the ratio of initiator to catalyst expands polydispersity index of prepared copolymers. Changes in the structure of prepared copolymers were not observed in ¹H NMR spectrum (see Figure 64).

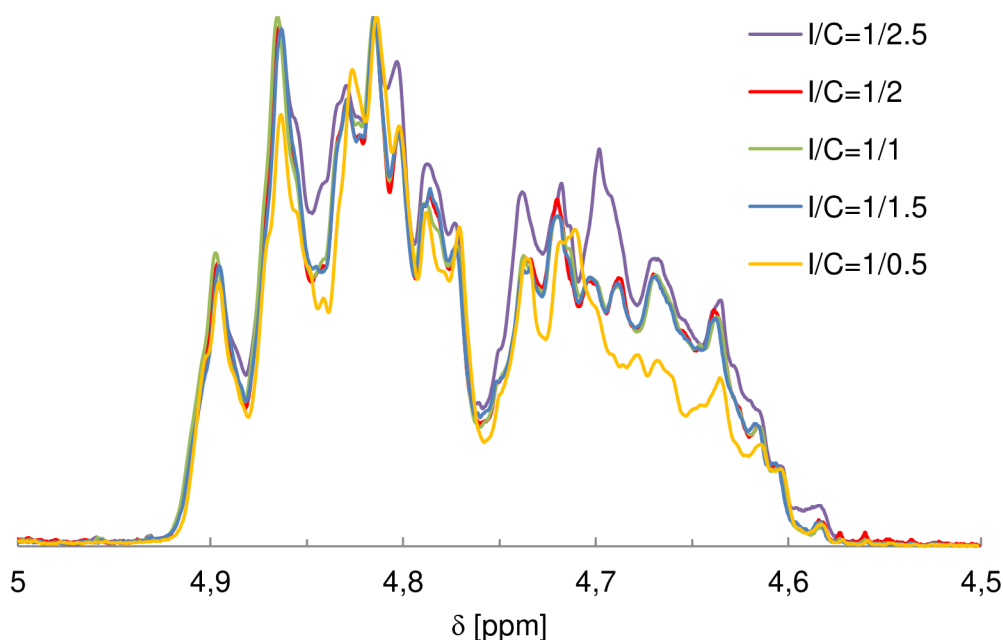


Figure 64 Detail in ¹H NMR spectrum in a range from 5.00 – 4.50 ppm for copolymers prepared with different initiator to catalyst ratio.

Rheological properties of the copolymers prepared with different initiator to catalyst ratio were evaluated. Elastic modulus of copolymer solutions (42 w/v %) is shown in Figure 65. The solution of copolymer prepared with ratio initiator to catalyst equal 1/2.5 stayed in phase sol in the all temperature scale. The highest stiffness 292.1 Pa at 33.7 °C reached copolymer solution prepared with initiator to catalyst ratio equal to 1/1. Furthermore, it was observed that with increasing initiator to catalyst ratio reduces the value of elastic modulus. The solution of copolymer prepared with $I/C = 1/1.5$ exhibited G' equal to 213.2 Pa at 33.0 °C. Elastic modulus $G' = 176.0$ Pa at 34.5 °C showed the solution of copolymer prepared with $I/C = 1/2$.

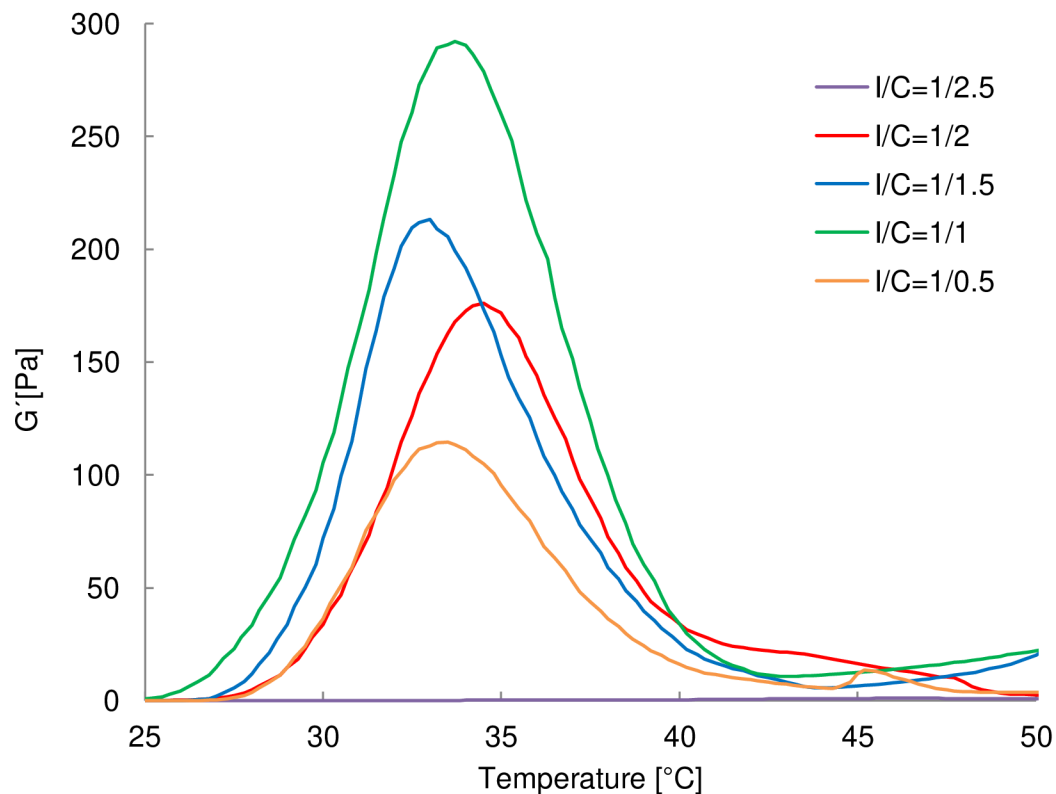


Figure 65 Influence of different initiator to catalyst ratio on elastic modulus of the polymer solutions (concentration 42 w/v %).

Change in the initiator to catalyst ratio had influence on conversion of monomers, molecular weight, polydispersity index and also on gelation behavior. The best gelation behaviors were obtained with initiator to catalyst ratio equal to 1/1.

5.3.2 Comparison of the Copolymers Prepared by the Organic Catalyst and Organometallic Catalyst

Recently, thermoreversible biodegradable “smart hydrogels” based on hydrophilic PEG and hydrophobic PLA and PGA with the swelling or shrinking ability driven by external stimuli have been prepared “in situ” via ROP by our group. Amphiphilic copolymers were additionally modified by itaconic acid to achieve end-functional reactive double bonds and carboxylic acid groups. Resulted copolymers are temperature sensitive and could be cross-linked either chemically by covalent bonds (photopolymerization) or physically by ionic or hydrophobic interaction [98-105].

Since our group has experience with ROP copolymerization of lactide and glycolide using poly(ethylene glycol) as macroinitiator and tin(II)-2-ethylhexanoate (SnOct₂) as the catalyst, utilization of NHCs as catalysts for the ROP of cyclic esters provides an attractive alternative to traditional metal-containing catalysts. Comparison of copolymers prepared using both ways is discussed in this section. The properties of both copolymers are listed in Table 14.

Table 14 Properties of PLGA–PEG–PLGA copolymers prepared using different catalysts.

Sample	Yield ^a [%]	M_n^b [g·mol ⁻¹]	M_n^c [g·mol ⁻¹]	M_n^d [g·mol ⁻¹]	M_w/M_n	PLGA/PEG ^c [wt/wt]	LA/GA ^c [mol/mol]
NHC- <i>t</i> Bu	79	5648	5007	4148	1.17	2.34	3.10
SnOct ₂	90	6785	5275	4746	1.20	2.60	2.95

Conditions of polymerization:

- NHC-*t*Bu - THF solvent, $T_p = 23$ °C, $t_p = 2$ h, $S/M=5$, $I/C = 1/2$.
- SnOct₂– bulk, $T_p = 130$ °C, $t_p = 3$ h, $I/C = 1/0.03$.

^a Determined gravimetrically.

^b Determined by GPC against PS standards in THF.

^c Determined by ¹H NMR.

^d Calculated from initial molar ratio $[M]_0/[I]_0 \times M_w(\text{monomer}) \times \text{conversion yield}$.

Copolymer prepared using SnOct₂ showed higher conversion of monomer (90 %) and higher molecular weight than copolymer prepared using NHC-*t*Bu. At both prepared copolymers higher molecular weight than theoretical was observed. The ratios of LA/GA and PLGA/PEG almost approached theoretically set values (LA/GA = 3.0, PLGA/PEG = 2.5) for both copolymers. Catalyst efficiency for copolymer prepared using SnOct₂ was 69.9 % and for copolymer prepared using NHC-*t*Bu was 73.4 %.

The differences in the structures of the prepared copolymers can be seen in the ¹H NMR spectra shown in Figure 66. Differences were observed especially at individual sequences for both copolymers in the region of the glycolide methylene proton (Figure 67).

Based on the literature review it is known that glycolide has higher reactivity in comparison to lactide, the ring of glycolide is opened and linked to hydroxyl end groups of PEG block in the first step. When large part of GA is already bonded the LA is built in polymer chains. Transesterification in the polymerization process made the redistribution of sequences in the copolymer chain, which results in the more random sequence.

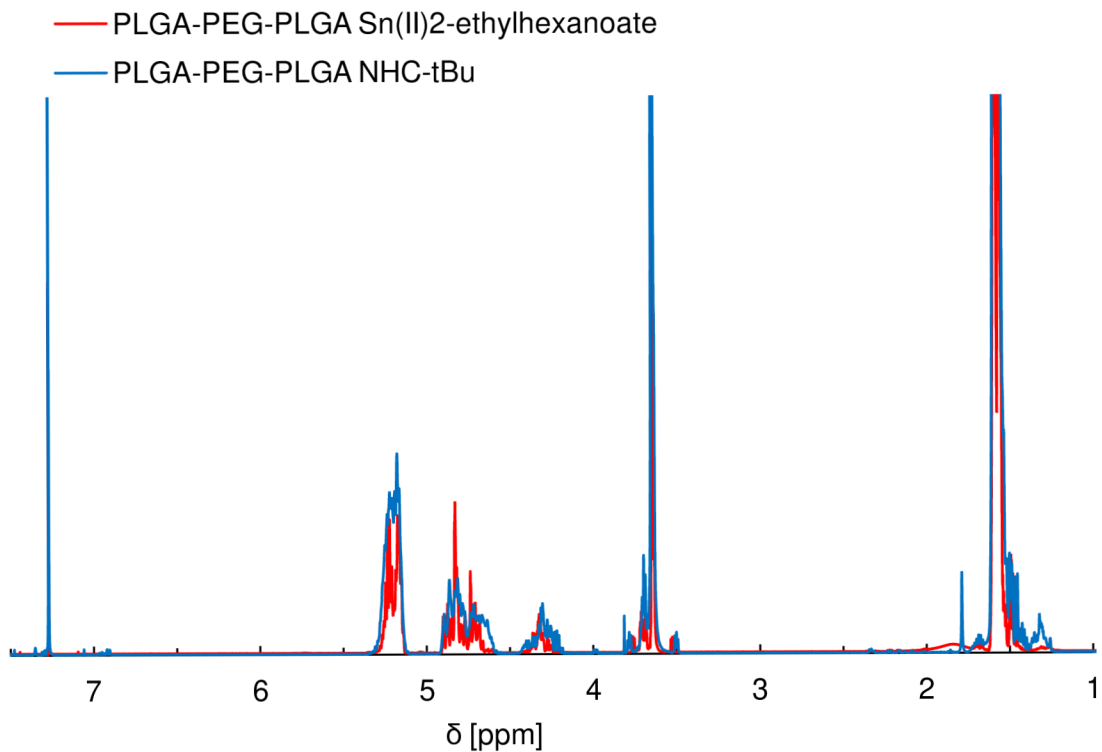


Figure 66 ^1H NMR spectra of copolymers prepared using SnOct_2 and NHC-tBu .

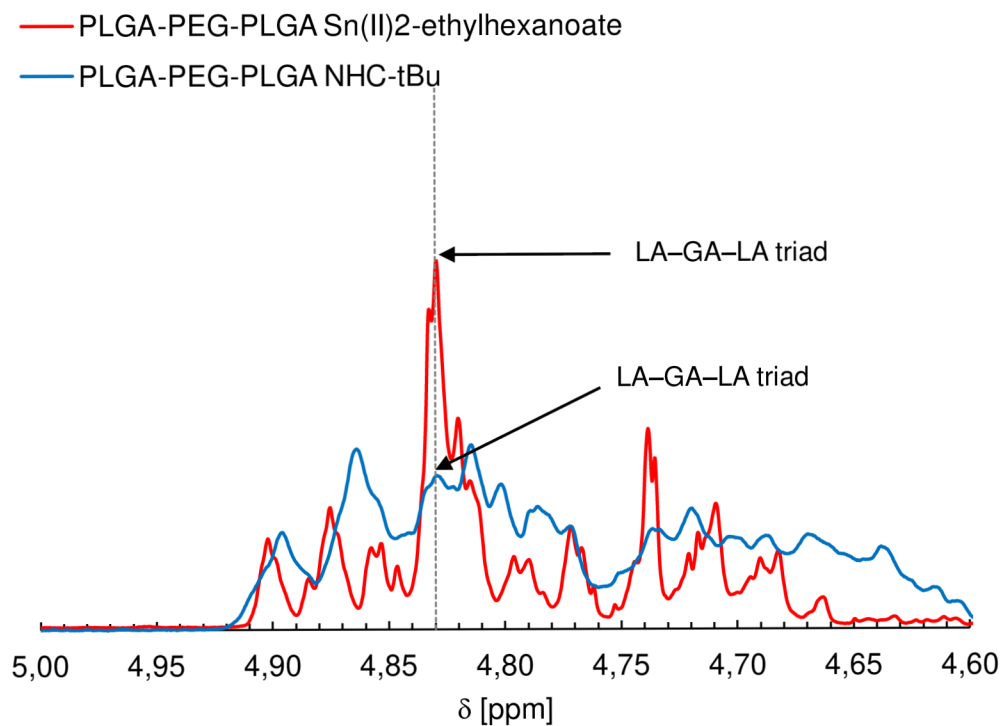


Figure 67 ^1H NMR spectra of copolymers prepared using SnOct_2 and NHC-tBu detail in a range from 5.00 – 4.60 ppm.

For copolymers prepared with SnOct₂ prevails sequence for LA-GA-LA triad at 4.83 ppm, prevails regular alternating LA and GA units corresponds to alternating copolymer. While for copolymer prepared using NHC-*t*Bu resonance lines of GA-LA sequences are in the similar representation, which corresponds to the random structure of copolymer. Resonance lines to appropriate sequences in ¹H NMR spectrum of poly[(lactide)-*co*-(glycolide)] in the region of the glycolide methylene proton are listed in Table 10.

The phase diagrams of aqueous solution investigated PLGA-PEG-PLGA copolymers are shown in Figure 68. Both traces show two phase transitions (first-lower and second-upper) above critical gel concentration (CGC).

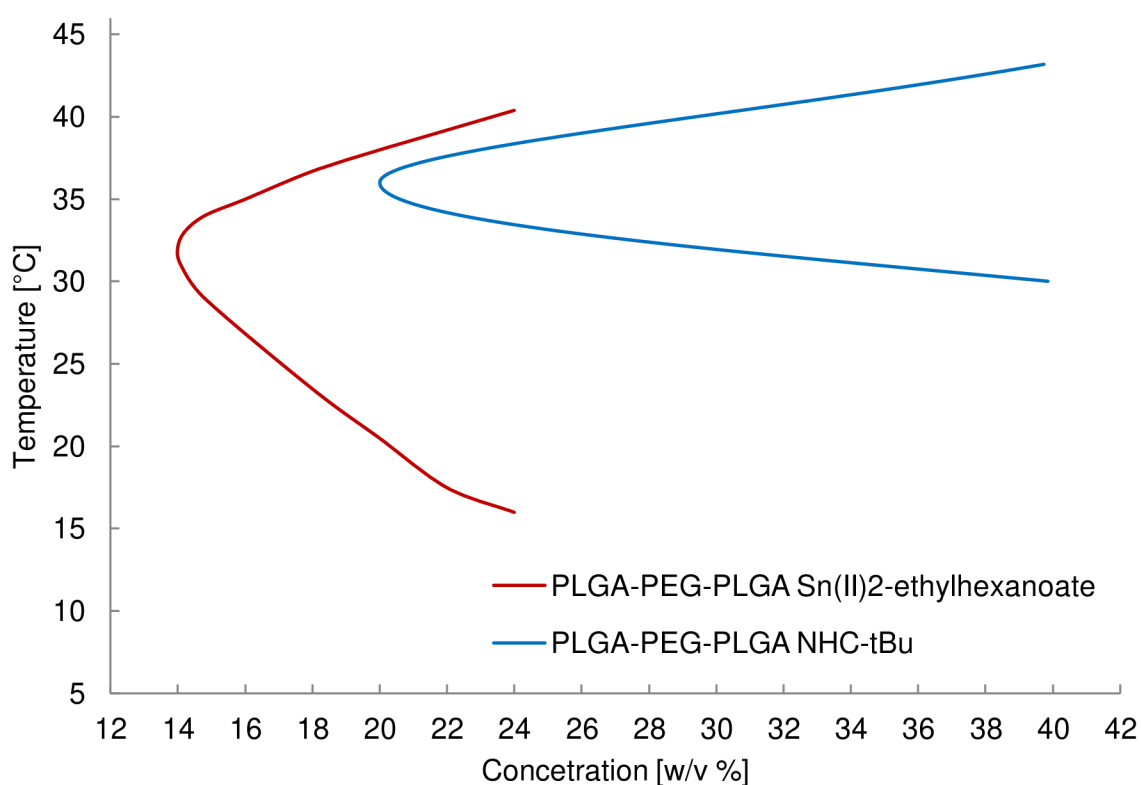


Figure 68 Phase diagrams of prepared copolymers.

Copolymer solution prepared using SnOct₂ exhibits the CGC equal to 14 w/v % at critical gel temperatures (CGT) equal to 32 °C and copolymer solution prepared using NHC-*t*Bu exhibits the CGC equal to 20 w/v % at CTG equal to 36 °C. This finding indicates that the sequence of PLGA blocks in the copolymers have a significant influence on their gelation behaviors and also can modulate the sol-gel transition temperatures. The different sequence structures alter the balance of hydrophobicity and hydrophilicity, which is critical for micellization of the amphiphilic block copolymers in water.

Rheological properties of the prepared copolymers were evaluated. Elastic modulus of copolymer solutions is shown in Figure 69. Micelles formed during gelation were stable. Maximum value of elastic modulus for copolymer solutions (22 w/v %) were equal to 39.1 Pa at 34.0 °C and for copolymer prepared by NHC-*t*Bu and 497.6 Pa at 32.7 °C for copolymer prepared by SnOct₂, due to higher arrangement of PLGA chains.

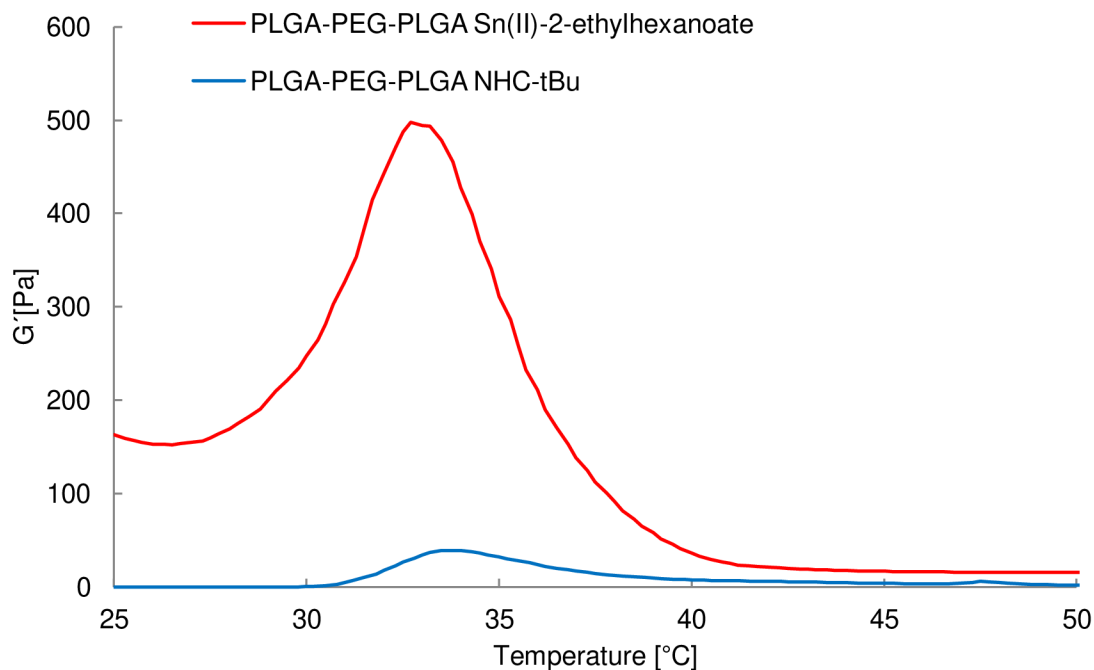


Figure 69 Elastic modulus of the polymer solutions (concentration 22 w/v %) prepared using $SnOct_2$ and NHC-*t*Bu.

Both copolymers have satisfied condition, namely that for injectable biodegradable hydrogels having two sol-gel phase transitions, where they exist in sols at laboratory temperature and change to gels at body temperature. These copolymers can be used as suitable material for injectable resorbable implants in regenerative medicine. Disadvantages of copolymer prepared by NHC-*t*Bu are the need for higher concentration of aqueous solution and lower gel stiffness.

6. CONCLUSION

The main aim of the presented work was synthesis and characterization of biodegradable non-toxic thermosensitive triblock copolymers based on hydrophilic polyethylene glycol (PEG) and hydrophobic aliphatic polyesters poly(lactic acid-*co*-glycolic acid) (PLGA) using “green” organic carbene catalyst in order to replace toxic organometallic catalysts.

The initial part of this work was focused on the preparation of 1,3-di-*tert*-butylimidazol-2-ylidene (NHC-*t*Bu) free carbene from corresponding imidazolium salts. Three ways of NHC-*t*Bu preparation, were tested on polymerization of L-lactide. The best efficiency was obtained with NHC-*t*Bu generated by butyllithium. Resulting P(L-LA)-*b*-PEG-*b*-P(L-LA) triblock copolymer showed narrow polydispersity index ($M_w/M_n = 1.2$), controllable molecular weight ($M_{n\text{theor}}/M_{n\text{GPC}}/M_{n\text{NMR}} = 1.0/1.3/1.1$) and high yield (85 %).

The prepared NHC-*t*Bu was also tested for opening polymerization of other cyclic esters, namely D, L-LA, glycolide and ϵ -caprolactone. As we expected, polymerization of lactone proceeded worse than polymerization of lactides. Prepared polyglycolide showed a very narrow polydispersity index ($M_w/M_n = 1.1$) with high conversion of monomer (83 %). Poly-L-lactide was prepared with the highest conversion of monomer (85 %) and narrow polydispersity index ($M_w/M_n = 1.2$). Poly-D, L-lactide showed a narrow polydispersity index ($M_w/M_n = 1.1$) with 70 % conversion of monomer. Prepared PCL had quite high conversion (71 %) but the worst polydispersity index ($M_w/M_n = 1.9$).

In next part of the work synthesis of thermosensitive amphiphilic triblock copolymers based on hydrophobic biodegradable polylactide and polyglycolide and biocompatible hydrophilic polyethylene glycol (PLGA-PEG-PLGA) using prepared NHC-*t*Bu was investigated. PLGA-PEG-PLGA copolymer as suitable material for injectable resorbable implants in regenerative medicine was successfully prepared and precisely characterized by means of ^1H NMR, ATR-FTIR, GPC, TGA, and DSC methods. Gelling ability of copolymers were studied as well. Results indicate that structure-controlled triblock copolymer was synthesized. Prepared copolymer showed a very narrow polydispersity index ($M_w/M_n = 1.2$) with high conversion of monomer (79 %). The ratios of LA/GA (3.1) and PLGA/PEG (2.3) approached theoretically set values (LA/GA = 3.0, PLGA/PEG = 2.5). Kinetic study showed that polymerization proceeds very fast in the first minutes. Water solution of PLGA-PEG-PLGA copolymer formed free flowing sol at room temperature and gel at body temperature. Copolymer solution exhibited critical gel concentration equal to 20 w/v % at critical gel temperature equal to 36 °C.

The influences of polymerization conditions: monomers purification, reaction temperature, solvent, ratio solvent/monomer (S/M) and ratio initiator/catalyst (I/C) were evaluated. Study showed that the experimental conditions influenced the properties of prepared copolymers. Changes of reaction conditions in most cases had not significantly influence on chemical properties such as molecular weight or polydispersity index, but had essential influence on physical properties like gelation behavior. Optimal conditions under which occurred production of PLGA-PEG-PLGA copolymer with highest stiffness 292.1 Pa at 33.7 °C were

found for unsublimated monomers, at ratio $S/M = 5 \text{ cm}^3 \cdot \text{g}^{-1}$, $I/C = 1/1 \text{ mol} \cdot \text{dm}^{-3}$ in THF solution at laboratory temperature.

Finally, the comparison of copolymers prepared using NHC-*t*Bu and Sn(II)-2-ethylhexanoate catalysts was performed. Both copolymers have two sol-gel phase transitions, where they exist in sols at laboratory temperature and change to gels at body temperature. Differences between the both copolymers were noticeable in structure, in the sol-gel transition as well in the rheological properties. Copolymer prepared by NHC-*t*Bu needed for sol-gel transition higher concentration of aqueous solution (20 %) and had lower elastic modulus ($G' = 39.1 \text{ Pa}$ at $34.0 \text{ }^\circ\text{C}$) than copolymer prepared by tin(II)-2-ethylhexanoate (critical gel concentration 14 %, $G' = 497.6 \text{ Pa}$ at $32.7 \text{ }^\circ\text{C}$).

Part of this work involved in the preparation and properties of the thermosensitive copolymer was published in the form of patent April 8, 2015, which is listed at the end thesis.

References

1. DECHY-CABARET, O., MARTIN-VACA, B., BOURISSOU, D. Controlled Ring-Opening Polymerization of Lactide and Glycolide. *Chemical Reviews*. 2004, 104, p. 6149.
2. GUNATILLAKE, P. A.; ADHIKARI, R. Biodegradable synthetic polymers for tissue engineering, *European Cells and Materials*. 2003, p. 1-16.
3. FIKR, J., *Názvoslovní organické chemie*. [s.l.]: Rubico, 2004. p 244. ISBN 978-80-7346-088-4.
4. ODIAN, G. *Principles of Polymerization*. 4th edition. [s.l.]: Wiley-interscience, 2004, p. 812, ISBN 0-471-27400-3.
5. DUBOIS, P.; COULEMBIER, O.; RAQUEZ, J. - M. *Handbook of Ring-Opening Polymerization*. Weinheim: WILEY-VCH Verlag GmbH & Co. KGaA, 2009. p. 408, ISBN 978-3-527-31953-4.
6. KOLYBBABA, M. et al., Biodegradable Polymers: Past, Present, and Future, *Presentation at the CSAE/ASAE Annual Intersectional Meeting* (2003).
7. MOONEY, B. P. The second green revolution? Production of plant-based biodegradable plastics, *Biochemical Journal* 2009, 418, p. 219–232.
8. BEHRAVESH, E.; YASKO, A.W.; ENGLE, P.S.; MIKOS, A.G. Synthetic biodegradable polymers for orthopedic applications. *Clinical Orthopaedics and Related Research* 1999, 367, p. 118-185.
9. Medical Supplies Producer of Uniform & Quality Surgical Sutures [online]. © 2003 - 2006 [cit. 2012-02-09]. Available from: http://www.scalpel.cn/surgical_suture.htm.
10. HENEBERG, P. Nanotechnologie versus rakovina [online]. Science, © 2008 [cit. 2012-02-09]. Available from: <http://vtm.zive.cz/clanek/nanotechnologie-versus-rakovina>.
11. ROBBINS, M. M.; VACCARO, A. R.; MADIGAN, L. The Use of Bioabsorbable Implants in Spine Surgery [online]. *Neurosurg Focus*. © 2004 [cit. 2012-02-09]. Available from: <http://www.medscape.com/viewarticle/472962>.
12. New Materials June 2011 [online]. © 2012 [cit. 2012-02-09]. Available from: http://www.packagingdigest.com/article/518404-EW_MATERIALS_June_2011.php.
13. JONES, A. C. Analysis of 3D bone ingrowth into polymer scaffolds via micro-computed tomography imaging. *Biomaterials* 2004, 25, p. 4947–4954.
14. WANG, Y.; Miguel A., RODRIGUEZ –PEREZ, M. A.; REIS, R. L.; F. MANO, J. F. Thermal and Thermomechanical Behaviour of Polycaprolactone and Starch/Polycaprolactone Blends for Biomedical Applications, *Macromolecular Materials and Engineering* 2005, 290, p. 792–801.
15. BHAW-LUXIMON, A.; JHURRY, D.; MOTALA-TIMOL, S.; LOCHEE, Y. Polymerization of ϵ -Caprolactone and its Copolymerization with γ -Butyrolactone using Metal Complexes. *Macromol Symposia* 2006, 231, p. 60–68.
16. WUTTICHAROENMONGKOL, P.; SANCHAVANAKIT, N.; PAVASANT, P.; SUPAPHOL, P. Polymerization of ϵ -Caprolactone and its Copolymerization with γ -Butyrolactone using Metal Complexes, *Macromolecular Bioscience* 2006, 6, p. 70–77.
17. ZHANG, W.; OKUBAYASHI, S.; BECHTOLD, T. Fibrillation tendency of cellulosic fibres, Part 1: Effects of swelling, *Cellulose* 2005. 12, p. 275-279.

18. ANG, K.C.; LEONG, K.F.; CHUA, C.K.; CHANDRASEKARAN, M. Compressive properties and degradability of poly(ϵ -caprolactone)/hydroxyapatite composites under accelerated hydrolytic degradation. *Journal of Biomedical Materials Research Part A* 2006, p. 655-660.
19. GÄDDA, T. et al. Poly(ϵ -caprolactone)-Grafted Acetylated Anhydroglucose Oligomer by Ring-opening Polymerization –Synthesis and Characterization, *Journal of Applied Polymer Science* 2006, 100, p. 1633–1641.
20. ALBERTSSON, A-C. *Degradable Aliphatic Polyesters*. [s.l.] : Springer, 2002. p. 179, ISBN 3540422498.
21. HAKKARAINEN, M. Aliphatic Polyesters: Abiotic and Biotic Degradation and Degradation Products. *Advances in Polymer Science*. 2002, 157, p. 113–138.
22. Biodegradable - Bioresorbable Polymers [online]. © 2010 University of Mauritius [cit. 2012-02-09]. Available from: <http://www.uom.ac.mu/polymer/html/Research%20review/reviews/PART1.pdf>.
23. KAITH, B. S. et al. Environment Benevolent Biodegradable Polymers: Synthesis, Biodegradability, and Applications. *Cellulose Fibers: Bio- and Nano-Polymer Composites* 2011, p. 425- 451.
24. NAIR, L. S.; LAURENCIN, C. T. Biodegradable polymers as biomaterials. *Progress in Polymer Science* 2007, 32, p. 762-798.
25. VROMAN, I.; TIGHZERT, L. Biodegradable Polymers. *Materials* 2009, 2, p. 307-344.
26. MAURUS, P. B.; KAEDING, C. C. Bioabsorbable implant material review. *Operative Techniques in Sports Medicine* 2004; 12, p. 158–160.
27. JEROME, Ch., LECOMTE, P. Recent advances in the synthesis of aliphatic polyesters by ROP. *Advanced drug delivery reviews* 2008, vol. 60, p. 1056–1076.
28. CAROTHERS, W. H.; DOROUGH, G. L.; VAN NATTA, F. J. Studies of Polymerization and Ring Formation. X. The Reversible Polymerization of Six-Membered Cyclic Esters. *Journal of the American Chemical Society* 1932, 54, p. 761–772.
29. SRIVASTAVA, R. K. Novel methods to synthesize aliphatic polyesters of vivid architectures. *Royal Institute of Technology Stockholm, Sweden* 2005, ISBN 91-7178-191-9.
30. JOHNS D. B, LENZ R. W. Preparation and polymerization of lactones. *Polym Preprints: American Chemical Society, Division of Polymer Chemistry*. 1984, 25, p. 220–1.
31. ALBERTSSON, A., VARMA, I. Recent developments in ROP of lactones for biomedical applications. *Biomacromolecules*. 2003, 4, p. 1466–1486.
32. COULEMBIER, O., et al. From controlled ring-opening polymerization to biodegradable aliphatic polyester: Especially poly(β -malic acid) derivatives. *Progress in Polymer Science*. 2006, 31, p. 723–747.
33. ALBERTSSON, A., VARMA, I. Aliphatic Polyesters: Synthesis, Properties and Applications. *Advances in Polymer Science*. 2002, 157, p. 2-40.
34. MECERREYES, D., JÉRÔME, R., DUBOIS, P., Novel Macromolecular Architectures Based on Aliphatic Polyesters: Relevance of The ‘‘Coordination-Insertion’’ Ring-Opening Polymerization. *Advances in Polymer Science* 1999, 147, p. 1-59.

35. URUSHIDO, K.; IWASAKI, F. Polymerization of allyl esters of unsaturated acids: Cyclopolymerization of methyl 2-methylallyl fumarate. *Macromolecular Chemistry and Physics*. 1986, 187, p. 711–721.
36. STRIDSBERG, K., RYNER, M., ALBERTSSON, A. Controlled ROP: Polymers with designed macromolecular architecture. *Advances in polymer science: Degradable aliphatic polyesters*. 2000, 157, p. 41–65.
37. KRICHELDORF, H., BERL, M., SCHARNAGL, N. Poly(lactones) 9 polymerization mechanism of metal alkoxide: initiated polymerizations of lactide and various lactones. *Macromolecules* 1988, 21, p. 286–293.
38. DUBOIS, P. et al, Macromolecular Engineering of Polylactones and Polylactides. Kinetics of Ring-Opening Polymerization of ϵ -Caprolactone Initiated with Functional Aluminum Alkoxides. *Macromolecules* 1996, 29, p. 1965-197.
39. SCHWACH, G., et al. Zn lactate as initiator of D,L-lactide ROP and comparison with Sn octoate. *Polymer bulletin*. 1996, vol. 37, p. 771-776.
40. NEDERBERG, F.; CONNOR, E. F.; MOËLLER, M.; GLAUSER, T.; HEDRIK, J. L. New Paradigms for Organic Catalysts: The First Organocatalytic Living Polymerization. *Angewandte Chemie International Edition* 2001, 40, p. 2712.
41. KAMBER, N. E.; JEONG, W.; WAYMOUTH, R. M. Organocatalytic Ring-Opening Polymerization. *Chemical Reviews* 2007, 107, p. 5813-5840.
42. Li, Y.; Li, Q. B.; Li, F. X.; Zhang, H. Y.; Jia, L.; Yu, J. Y.; Fang, Q.; Cao, A. Amphiphilic Poly(L-lactide)-b-dendritic Poly(L-lysine)s Synthesized with A Metal-Free Catalyst and New Dendron Initiators: Chemical Preparation and Characterization. *Biomacromolecules* 2006, 7, p. 224.
43. MYERS, M.; CONNOR, E. F.; GLAUSER, T.; MÖCK, A.; NYCE, G.; HEDRICK, J. L. Phosphines: Nucleophilic Organic Catalysts for the Controlled Ring-Opening Polymerization of Lactides. *Journal of Polymer Science Part A: Polymer Chemistry* 2002, 40, p. 844-851.
44. DOVE, A. P.; PRATT, R. C.; LOHMEIJER, B. G. G.; WAYMOUNT, R. M.; HEDRICK, J. L. Thiourea-Based Bifunctional Organocatalysis: Supramolecular Recognition for Living Polymerization. *Journal of the American Chemical Society* 2005, 127, p. 13798-13799.
45. PRATT, R. et al. Exploration, Optimization, and Application of Supramolecular Thiourea-Amine Catalysts for the Synthesis of Lactide (Co)polymers. *Macromolecules* 2006, 39, p. 7863-7871.
46. PRATT, R.; LOHMEIJER, B. G. G.; LONG, D. A.; WAYMOUNT, R. M.; HEDRICK, J. L. Triazabicyclodecene: A Simple Bifunctional Organocatalyst for Acyl Transfer and Ring-Opening Polymerization of Cyclic Esters. *Journal of the American Chemical Society* 2006, 128, p. 4556-4557.
47. BOURISSOU, D.; MOEBS-SANCHEZ, S.; MARTÍN-VACA, B. Recent advances in the controlled preparation of poly(α -hydroxy acids): Metal-free catalysts and new monomers. *Comptes Rendus Chimie* 2007, 10, p. 775-794.
48. LOHMEIJER, B. G. G. et al. Guanidine and Amidine Organocatalysts for Ring-Opening Polymerization of Cyclic Esters. *Macromolecules* 2006, 39, p. 8574-8583.
49. QIAN, H. et al. A Strategy for Control of “Random” Copolymerization of Lactide and Glycolide: Application to Synthesis of PEG-b-PLGA Block Polymers Having Narrow Dispersity. *Macromolecules* 2011, 44, p. 7132–7140.

50. UYAMA, H.; KOBAYASHI, S. Enzymatic Ring-Opening Polymerization of Lactones Catalyzed by Lipase. *Chemistry Letters* 1993, 22, p. 1149.
51. KNANI, D.; GUTMAN, A. L.; KOHN, D. H.; Enzymatic polyesterification in organic media. Enzyme-catalyzed synthesis of linear polyesters. I. Condensation polymerization of linear hydroxyesters. II. Ring-opening polymerization of ϵ -caprolactone. *Journal of Polymer Science Part A: Polymer Chemistry* 1993, 31, p. 1221-1232.
52. UYAMA, H.; SUDA, S.; KOBAYASHI, S. Enzymic synthesis of terminal-functionalized polyesters by initiator method. *Acta Polymerica* 1998, 49, p. 700–703.
53. KOBAYASHI, S.; UYAMA, H.; NAMEKAWA, S. In vitro biosynthesis of polyesters with isolated enzymes in aqueous systems and organic solvents. *Polymer Degradation and Stability* 1998, 59, p. 195–201.
54. UYAMA, H.; TAKEYA, K.; HOSHI, N.; KOBAYASHI, S. Lipase catalyzed ring-opening polymerization of dodecanolide. *Macromolecules* 1995, 28, p. 7046–50.
55. KOBAYASHI, S.; TAKEYA, K.; SUDA, S.; UYAMA, H. Lipase-catalyzed ring-opening polymerization of medium-size lactones to polyesters. *Macromolecular Chemistry and Physics* 1998, 199, p. 1729–1736.
56. NAMEKAWA, S.; SUDA, S.; UYAMA, H.; KOBAYASHI, S. Lipase-catalyzed ring-opening polymerization of lactones to polyesters and its mechanistic aspects. *International Journal of Biological Macromolecules* 1999, 25, p. 145–151.
57. HUIJSER, S.; STAAL, B.B.P.; HUANG, J.; DUCHATEAU, R.; KONING, C.E. Topology Characterization by MALDI-ToF-MS of Enzymatically Synthesized Poly(lactide-co-glycolide). *Biomacromolecules* 2006, 7, p. 2465-2469.
58. DONG, H.; CAO, S.-G.; LI, Z.-Q.; HAN, S.-P.; YOU, D.-L.; SHEN, J.-C. Study on the enzymic polymerization mechanism of lactone and the strategy for improving the degree of polymerization. *Journal of Polymer Science Part A: Polymer Chemistry* 1999, 37, p. 1265–1275.
59. VARMA, I. K.; ALBERTSSON, A.-CH.; RAJKHOWA, R.; SRIVASTAVA, R. K. Enzyme catalyzed synthesis of polyesters. *Progress in Polymer Science* 2005, 30, p. 949–981.
60. HANS, M.; KEUL, H.; MOELLER, M. Ring-Opening Polymerization of D, D – Lactide Catalyzed by Novozyme 435. *Macromolecular Bioscience* 2009, 9, p. 239–247.
61. MOORE, J. L.; ROVIS, T. Carbene Catalysts. *Topics in Current Chemistry* 2010, 291, p. 77–144.
62. BOURISSOU, D.; GUETRRET, O.; GABBAOË, F. P.; BERTRAND, G. Stable Carbenes. *Chemical Reviews* 2000, 100, p. 39–91.
63. AÇIKEL, M. *Active and Reusable Heterogeneous Catalysts for Mizoroki-Heck Reactions*. Izmir Institute of Technology Izmir, Turkey, 2004. PhD Thesis.
64. SAKER, O. J. *Mono- and tri-nuclear ruthenium complexes incorporating N-heterocyclic carbene ligands*. University of Bath, 2008. PhD Thesis.
65. WANZLICK, H. W.; SCHÖNHERR, H. J. Direct Synthesis of a Mercury Salt Carbene Complex. *Angewandte Chemie International Edition* 1968, 7, p.141-142.
66. ÖFELE, K. 1,3-Dimethyl-4-imidazolinylliden-(2)-pentacarbonylchrom ein neuer übergangsmetall-carben-komplex. *Journal of Organometallic Chemistry* 1968, 12, p. P42-P43.

67. ARDUENGO, A. J.; HARLOW, R. L.; KLINE, M. A Stable Crystalline Carbene. *Journal of the American Chemical Society*. 1991, 113, p. 361–363.
68. HERRMANN, W. A.; ELISON, M.; FISCHER, J.; KÖCHTER, C.; ARTHUS, G. R. J. Metal Complexes of N-Heterocyclic Carbenes—A New Structural Principle for Catalysts in Homogeneous Catalysis. *Angewandte Chemie International Edition* 1995, 34, p. 2371 – 2373.
69. ZINNER, S. C. et al. Synthesis and characterization of asymmetric NHC complexes. *Journal of Organometallic Chemistry* 2008, 693, p. 1543–1546.
70. DOVE, A. P., et al. N-Heterocyclic carbenes: Effective organic catalyst for living polymerization. *Polymer*. 2006, 47, p. 4018–4025.
71. DELAUDE, L. Betaine Adducts of N-Heterocyclic Carbenes: Synthesis, Properties, and Reactivity. *European Journal of Inorganic Chemistry* 2009, p. 1681–1699.
72. NYCE, G., et al. In situ generation of carbenes: A general and versatile platform for organocatalytic living polymerization. *Journal of the American chemical society*. 2003, 125, p. 3046–3056.
73. CSIHONY, S., et al. Single-Component Catalyst/Initiators for the Organocatalytic Ring-Opening Polymerization of Lactide. *Journal of the American Chemical Society*. 2005, 127, s. 9079–9084.
74. NYCE, G.W.; CSIHONY, S.; WAYMOUTH, R. M.; HEDRICK, J.L. A General and Versatile Approach to Thermally Generated N-Heterocyclic Carbenes. *Chemistry - A European Journal* 2004, 10, p. 4073–4079.
75. COULEMBIER, O. et al. Alcohol Adducts of N-Heterocyclic Carbenes: Latent Catalysts for the Thermally-Controlled Living Polymerization of Cyclic Esters. *Macromolecules* 2006, 39, p. 5617-5628.
76. KAMBER, N. E. et al. N-Heterocyclic Carbenes for the Organocatalytic Ring-Opening Polymerization of ϵ -Caprolactone. *Macromolecules* 2009, 42, p. 1634-1639.
77. COULEMBIER, O.; RAQUEZ, J.-M.; DUBOIS, P. N-Heterocyclic carbene catalysis — from simple organic reactions to polymerization of cyclic esters. *Polimery* 2008, 53, p. 259-267.
78. CULKIN, D. A. et al. Zwitterionic Polymerization of Lactide to Cyclic Poly(Lactide) by Using N-Heterocyclic Carbene Organocatalysts. *Angewandte Chemie International Edition* 2007, 46, p. 2627–2630.
79. JEONG, W. Zwitterionic Polymerization: A Kinetic Strategy for the Controlled Synthesis of Cyclic Polylactide. *Journal of the American Chemical Society* 2009, 131, p. 4884–4891.
80. CONNOR, E. F., et al. First Example of N-Heterocyclic Carbenes as Catalysts for Living Polymerization: Organocatalytic Ring-Opening Polymerization of Cyclic Esters. *Journal of the American Chemical Society*. 2002, 124, p. 914–915.
81. CSIHONY, S., et al. Brederecks Reagent Revisited: Latent Anionic Ring-Opening Polymerization and Transesterification Reactions. *Advanced Synthesis & Catalysis* 2004, 346, p. 1081 –1086.
82. PAL, K., BANTHIA, A. K., MAJUMDAR, D.K. Polymeric Hydrogels: Characterization and Biomedical Applications –A mini review. *Designed Monomers and Polymers* 12 (2009), Pages 197–220.

83. JEONG, B., GUTOWSKA, A. Lessons from Nature: Stimuli-Responsive Polymers and their Biomedical Applications. *Trends in Biotechnology*, 2002, vol. 20, no. 7. s. 305-311, ISSN 0167-7799.
84. KHODAVERDI, E. Preparation and analysis of a sustained drug delivery system by PLGA–PEG–PLGA triblock copolymers. *Polymer Bulletin*, 2012, Published online. DOI 10.1007/s00289-012-0747-5
85. ZENTNER, G.M., et al. Biodegradable block copolymers for delivery of proteins and water-insoluble drugs. *Journal of Controlled Release*, 2001, vol. 72, no. 1-3, p. 203-215. ISSN 0168-3659.
86. JEONG, B., BAE, Y.H., KIM, S.W. Thermoreversible Gelation of PEG-PLGA-PEG Triblock Copolymer Aqueous Solutions. *Macromolecules*, 1999, vol. 32, no. 21, p. 7064-7069.
87. LEE, D.S., SHIM, M.S., KIM, S.W., LEE, H., PARK, I., and CHANG, T.Y. Novel thermoreversible gelation of biodegradable PLGA-block-PEO-block-PLGA triblock copolymers in aqueous solution. *Macromolecular Rapid Communications*, 2001, vol. 22, no. 8, p. 587-592. ISSN 1022-1336.
88. YU, L., CHANG, G.T., ZHANG, H., and DING, J.D. Temperature-induced spontaneous sol-gel transitions of poly(D,L-lactic acid-co-glycolic acid)-b-poly(ethylene glycol)-b-poly(D,L-lactic acid-co-glycolic acid) triblock copolymers and their end-capped derivatives in water. *Journal of Polymer Science Part a-Polymer Chemistry*, 2007, vol. 45, no. 6, p. 1122-1133. ISSN 0887-624X.
89. SHIM, M.S., et al. Poly(D,L-lactic acid-co-glycolic acid)-b-poly(ethylene glycol)-b-poly(D,L-lactic acid-co-glycolic acid) triblock copolymer and thermoreversible phase transition in water. *Journal of Biomedical Materials Research*, 2002, vol. 61, no. 2, p. 188-196. ISSN 0021-9304.
90. DENK, M.K.; RODEZNO, J.M.; GUPTA, S.; LOUGH, A. Synthesis and reactivity of subvalent compounds. Part 11. Oxidation, hydrogenation and hydrolysis of stable diamino carbenes. *Journal of Organometallic Chemistry*. 2001, 616-618, p. 242-253.
91. ARDUENGO, A. J., et al. Photoelectron Spectroscopy of a Carbene/Silylene/Germyle Series. *Journal of the American Chemical Society*. 1994, 116, p. 6641–6649.
92. NEUMAYEROVÁ, Z. *Polykaprolakton, jeho syntéza, charakterizace a degradabilita*. Brno: Vysoké učení technické v Brně, Fakulta chemická, 2010. 60 s.
93. Surman, F. *Novel "green" catalysts for controlled ring-opening polymerization of lactide*. Brno: Brno University of Technology, Faculty of chemistry, 2010. 42 p.
94. KULOVANÁ, E. *Molecular modelling – structure and properties of carbene-based catalyst*. Brno: Vysoké učení technické v Brně, Fakulta chemická, 2012. 58 p.
95. ARDUENGO, A. J., et al. Electronic stabilization of nucleophilic carbenes. *Journal of the American Chemical Society*. 1992, 114, p. 5530–5534.
96. KASPERCZYK, J. Microstructural analysis of poly[(1,1-lactide)-co-(glycolide)] by ¹H and ¹³C n.m.r. spectroscopy. *Polymer*. 1996, vol. 37, issue 2, pp. 201-203. DOI: 10.1016/0032-3861(96)81088-3.
97. YU, L., ZHANG, Z., DING, J. Influence of LA and GA Sequence in the PLGA Block on the Properties of Thermogelling PLGA–PEG–PLGA Block Copolymers. *Biomacromolecules*. 2011-04-11, vol. 12, issue 4, pp. 1290-1297. DOI: 10.1021/bm101572j.

98. VOJTOVÁ, L., MRAVCOVÁ, L., VÁVROVÁ, M., CHYTIL, M., PEKAŘ, M., JANČÁŘ, J. Synthesis and Sol-gel Transition of Injectable Biodegradable Thermosensitive PLGA-PEG-PLGA Copolymers Modified by Itaconic Acid. *In Macro-2006*. Pune, India: National Chemical Laboratory, India, 2006, p. PHC-P1 (4 p.)
99. VOJTOVÁ, L., MRAVCOVÁ, L., VÁVROVÁ, M., CHYTIL, M., PEKAŘ, M., JANČÁŘ, J. Functionalization and Characterization of Thermoreversible Amphiphilic Hydrogels for Biomedical Applications. In: The 42nd IUPAC World Polymer Congress, Taipei, Taiwan: The Polymer Society, Taipei, 2008, pp. 191-192.
100. V VOJTOVÁ, L., MRAVCOVÁ, L., VÁVROVÁ, M., JANČÁŘ, J. *Injectable resorbable adhesives for bone repair application*. 1. Bratislava, Slovak Republic: Polymer Institute SAS, 2007, p. 83-83. ISBN 978-80-968433-4-3.
101. MICHLOVSKÁ, L., VOJTOVÁ, L., MRAVCOVÁ, L., HERMANOVÁ, S., KUČERÍK, J., JANČÁŘ, J. Functionalization Conditions of PLGA-PEG-PLGA Copolymer with Itaconic Anhydride. *Macromolecular Symposia*. 2010, vol. 295, no. 1, pp. 119-124. DOI: 10.1002/masy.200900071.
102. MICHLOVSKÁ, L., VOJTOVÁ, L., MRAVCOVÁ, L., JANČÁŘ, J. Novel biodegradable macromonomers based on PLGA-PEG-PLGA copolymer for regenerative medicine. In Studentská odborná konference chemie a společnost. Vysoké učení technické v Brně a Martin Weiter EDITOŘI LADISLAV OMELKA. *Sborník příspěvků*. Brno Vysoké učení technické v Brně, Fakulta chemická, 2010, pp. 167-172. ISBN 978-80-214-4212-2.
103. MICHLOVSKÁ, L., VOJTOVÁ, L., MRAVCOVÁ, L., JANČÁŘ, J. Thermogelling water solutions of multifunctional macromonomers based on PLGA-PEG-PLGA triblock copolymers. *Challenges of Modern Technology*. 2011, vol. 2, no. 1, pp. 12-15.
104. MICHLOVSKÁ, L. *Synthesis and Characterization of Multifunctionalized Biodegradable Copolymers*. Brno: Brno University of Technology, Faculty of Chemistry, 2014. 92 p.
105. MICHLOVSKÁ, L.: *Functionalization of biodegradable polymers by itaconic anhydride*. Brno: Brno University of Technology, Faculty of Chemistry, 2009. 59 p.

List of Abbreviations

β -PL	β -propiolactone
γ -BL	γ -butyrolactone
δ -VL	δ -valerolactone
ε -CL	ε -caprolactone
ATR-FTIR	attenuated total reflectance fourier transformed infrared spectroscopy
ABA	triblock copolymer with hydrophobic A end blocks and hydrophilic B blok
Bu	butyl
BUT	Brno University of Technology
BnOH	benzyl alcohol
C	catalysts
CGC	critical gel concentration
CGT	critical gel temperature
Cy	cyclohexyl
DBU	1,8-diaza[5.4.0]bicycloundec-7-ene
DMAP	4-(dimethylamino)pyridine
D-LA	D lactide
D, L-LA	D, L lactide
DMSO	dimethyl sulfoxide
DP	degree of polymerization
DSC	differential scanning calorimeter
EAM	enzyme activated monomer
Et	ethyl
FTIR	fourier transformed infrared
G'	storage modulus
GA	glycolide
GPC	gel permeation chromatography
^1H NMR	proton nuclear magnetic resonance
h	hours
I	initiator
IMes	1,3-bis(2,4,6-(trimethylphenyl)imidazol-2-ylidene
iPr	isopropyl
L-LA	L-lactide
Lip.	lipase
LSC	lyo screen control
M	monomer
Me	methyl
MeOH	methanol
MMD	multimodal distribution
Mn	number average molecular weight
MTBD	7-methyl-1,5,7-triazabicyclo[4.4.0]dec-5-ene
M_w/M_n	polydispersity index
NHC	N-heterocyclic carbenes
NHC- <i>t</i> Bu	1,3-di- <i>tert</i> -butylimidazol-2-ylidene
Nu	nucleophile
PBuOH	4-pyrene-1-butanol

PCL	polycaprolactone
PDLA	poly-D-lactide
PDLLA	poly-D,L-lactide
PDMAEMA	poly(N,N-dimethylaminoethyl methacrylate)
PEG	poly(ethylene glycol)
PGA	polyglycolide
Ph	phenyl
PLA	polylactide
PLGA	copolymer of lactide and glycolide
PLGA-PEG-PLGA	poly(D,L-lactic acid- <i>co</i> -glycolic acid)- <i>b</i> -poly(ethylene glycol)- <i>b</i> -poly(D,L-lactic acid- <i>co</i> -glycolic acid)
PLLA	poly-L-lactide
PMMA	poly(methyl methacrylate)
PPY	4-pyrrolidinopyridine
PS	polystyrene
Ref.	references
RI	refractive index
ROP	ring opening polymerization
s	second
S	solvent
SnOct ₂	tin(II)-2-ethylhexanoate
T	temperature
T _p	temperature of polymerization
t	time
t _p	time of polymerization
<i>t</i> -BuOK	potassium <i>tert</i> -butoxide
T _d	initial degradation temperature
T _{dm}	degradation temperature at max. rate
T _g	transition of temperature
T _m	melting point
TBD	1,5,7-triazabicyclo[4.4.0]dec-5-ene
TGA	thermogravimetric analysis
THF	tetrahydrofuran
TOF	turnover frequency
TTIM	test tube inverting method
UV	ultraviolet
UV-VIS	ultraviolet-visible
UPW	ultrapure water
ΔW^1	total weight loss of the end of first stage of degradation
ΔW^2	total weight loss of the end of second stage of degradation

List of Figures

- Figure 1. The order of locants on C atoms adjacent to carboxyl group in the hydroxy acid.
- Figure 2. Practical applications of the biodegradable polyesters [7, 9 – 13].
- Figure 3. Scheme of the ROP of ϵ -caprolactone to poly(ϵ -caprolactone).
- Figure 4. Scheme ROP of lactide to polylactide.
- Figure 5. Scheme ROP of glycolide to polyglycolide.
- Figure 6. A schematic representation of the polycondensation.
- Figure 7. ROP of lactones via anionic mechanism; (1) acyl-oxygen scission (2) alkyl-oxygen scission.
- Figure 8. Proposed pathway for cationic ROP of cyclic esters.
- Figure 9. ROP of lactones catalyzed by organometallic species [M] in presence of nucleophiles (Nu).
- Figure 10. ROP of lactones by the coordination-insertion mechanism.
- Figure 11. Scheme of intermolecular and intramolecular transesterification.
- Figure 12. Structures of (a) $\text{Sn}(\text{Oct})_2$ and (b) $\text{Al}(\text{iPr})_3$.
- Figure 13. Structure 4-(dimethylamino)pyridine DMAP and 4-pyrrolidinopyridine (PPY).
- Figure 14. Proposed mechanism for the ROP of LA using DMAP catalyst.
- Figure 15. Phosphine catalysts for the ROP of LA.
- Figure 16. Proposed mechanism for the ROP of LA using $\text{P}(\text{tert-Bu})_3$ catalyst.
- Figure 17. Proposed activation pathway for LA ROP using a bifunctional thiourea catalyst.
- Figure 18. Chemical structures DBU, TBD and MTB.
- Figure 19. Proposed dual activation of monomer and initiator for ROP of lactones.
- Figure 20. Proposed enzymatic ROP of cyclic esters.
- Figure 21. General formula of carbenes.
- Figure 22. Orbital presentation of carbenes.
- Figure 23. Structural diversity of *N*-heterocyclic carbenes.
- Figure 24. “In situ” generation of NHC using *t*-BuOK.
- Figure 25. Generation of the NHC catalyst from the ionic liquid reservoir.
- Figure 26. Generation of free carbene from silver(I) carbene complex.
- Figure 27. Generation of free carbene from stable chloroform and pentafluorobenzene adducts.
- Figure 28. Elimination of methanol from methoxyimidazolyl-2-ylidene.
- Figure 29. Proposed mechanism for the ring-opening polymerization of lactide in the presence of alcohol.
- Figure 30. Proposed zwitterionic polymerization of lactide to generate cyclic polylactide.
- Figure 31. Phase diagram of PLGA–PEG–PLGA copolymers in water [89].
- Figure 32. Schematic diagram of the micellar gelation mechanism for PLGA–PEG–PLGA copolymer in aqueous solution [89].
- Figure 33. Schematic diagram of a spontaneous thermogelling mechanism of PLGA–PEG–PLGA copolymers in water via a micelle network [88].
- Figure 34. Vacuum line-manifold for experiments under inert atmosphere in Polymer Synthesis Laboratory at Faculty of chemistry BUT.

- Figure 35. “In situ” generation of 1,3-di-*tert*-butylimidazol-2-ylidene free carbene using *t*-BuOK salt.
- Figure 36. Schematic illustration of imidazolium salt reaction with butyllithium at low temperature to gain 1,3-di-*tert*-butylimidazol-2-ylidene free carbene.
- Figure 37. Photos of a) Starting imidazolium salt, b) NHC-*t*Bu generated “In situ” in THF, c) NHC-*t*Bu generated according to Arduengo, d) NHC-*t*Bu generated according to Denk.
- Figure 38. Synthesis of P(L-LA)-*b*-PEG-*b*-P(L-LA) triblock copolymers using NHC-*t*Bu free carbene.
- Figure 39. The measured ¹H NMR spectrum of 1,3-di-*tert*-butylimidazol-2-ylidene free carbene in C₆D₆ under nitrogen atmosphere.
- Figure 40. FTIR spectrum of 1,3-di-*tert*-butylimidazol-2-ylidene.
- Figure 41. Obtained ¹H NMR spectra of P(L-LA)-*b*-PEG-*b*-P(L-LA) and P(D,L-LA)-*b*-PEG-*b*-P(D,L-LA) triblock copolymers prepared via ROP using NHC-*t*Bu at room temperature in 5 minutes in THF.
- Figure 42. Obtained ¹H NMR spectrum of PGA-*b*-PEG-*b*-PGA prepared via ROP using NHC-*t*Bu at room temperature in 5 minutes in THF.
- Figure 43. Obtained ¹H NMR spectrum of PCL-*b*-PEG-*b*-PCL prepared via ROP using NHC-*t*Bu at room temperature in 5 minutes in THF.
- Figure 44. ROP polymerization of PLGA-PEG-PLGA triblock copolymers using NHC-*t*Bu free carbene.
- Figure 45. GPC diagram of PLGA-PEG-PLGA copolymer.
- Figure 46. Obtained ¹H NMR spectrum of PLGA-PEG-PLGA copolymer prepared via ROP using NHC-*t*Bu at room temperature in THF.
- Figure 47. FTIR of PLGA-PEG-PLGA copolymer.
- Figure 48. Dependence of monomers conversion on the time of D,L-lactide and glycolide copolymerization using NHC/PEG catalytic system.
- Figure 49. Dependence of molecular weight and polydispersity index on polymerization time during copolymerization of D,L-lactide and glycolide.
- Figure 50. TGA of PLGA-PEG-PLGA copolymer.
- Figure 51. DSC of PLGA-PEG-PLGA copolymer.
- Figure 52. Inverting test tube method: a) the solution in phase sol b) the phase gel at 37 °C, c) the phase suspension.
- Figure 53. Phase diagram of PLGA-PEG-PLGA copolymer.
- Figure 54. Effect of polymer solution concentration (18 - 42 w/v %) on the storage modulus.
- Figure 55. ¹H NMR spectra of PLGA-PEG-PLGA copolymers from both sublimated and unsublimated monomers and detail in a range from 5.0 - 4.5 ppm.
- Figure 56. Rheological properties of PLGA-PEG-PLGA copolymers from either sublimated or unsublimated monomers (24 w/v % in ultrapure water).
- Figure 57. Detail in ¹H NMR spectra of PLGA-PEG-PLGA in a range from 5.00 - 4.50 ppm for ROP at different temperature.
- Figure 58. ¹H NMR spectra of poly[(lactide)-co-(glycolide)] obtained in the region of glycolide methylene protons [96].
- Figure 59. Influence of polymerization temperature on elastic modulus of the polymer solutions (concentration 42 w/v %).
- Figure 60. Detail in ¹H NMR spectrum in a range from 5.00 - 4.50 ppm for copolymers prepared in different medium.

- Figure 61. Influence of polymerization solvent on elastic modulus of the polymer solutions (concentration 42 w/v %).
- Figure 62. Detail in ^1H NMR spectrum in a range from 5.00 - 4.50 ppm for copolymers prepared with different solvent to monomer ratio.
- Figure 63. Influence of different solvent to monomer ratio on elastic modulus of the polymer solutions (concentration 42 w/v %).
- Figure 64. Detail in ^1H NMR spectrum in a range from 5.00 - 4.50 ppm for copolymers prepared with different initiator to catalyst ratio.
- Figure 65. Influence of different initiator to catalyst ratio on elastic modulus of the polymer solutions (concentration 42 w/v %).
- Figure 66. ^1H NMR spectra of copolymers prepared using SnOct_2 and NHC-*t*Bu.
- Figure 67. ^1H NMR spectra of copolymers prepared using SnOct_2 and NHC-*t*Bu detail in a range from 4.50 – 5.00 ppm.
- Figure 68. Phase diagrams of prepared copolymers.
- Figure 69. Elastic modulus of the polymer solutions (concentration 22 w/v %) prepared using SnOct_2 and NHC-*t*Bu.

List of Tables

- Table 1. Overview of the most common cyclic ester monomers.
- Table 2. N-heterocyclic carbene catalyzed ring-opening polymerization.
- Table 3. Properties of prepared polylactides.
- Table 4. Assignment of the absorption bands observed in the FTIR spectra of 1,3-di-*tert*-butylimidazol-2-ylidene (Nujol, KBr).
- Table 5. Properties of prepared triblock copolymers.
- Table 6. Properties of prepared PLGA–PEG–PLGA triblock copolymer.
- Table 7. Assignment of the absorption bands observed in the FTIR spectra of PLGA–PEG–PLGA copolymer.
- Table 8. Properties of prepared PLGA–PEG–PLGA copolymers.
- Table 9. Summary of the properties prepared copolymers PLGA–PEG–PLGA a different temperatures.
- Table 10. Sequences in the region of the glycolide methylene proton [96].
- Table 11. Influence of solvent on the properties of prepared PLGA–PEG–PLGA copolymers.
- Table 12. Properties of prepared copolymers PLGA–PEG–PLGA at different solvent to monomer ratio.
- Table 13. Properties of prepared copolymers PLGA–PEG–PLGA at different ratio catalyst to initiator.
- Table 14. Properties of PLGA–PEG–PLGA copolymers prepared using different catalysts.